From the Department of Internal Medicine I
of the University of Luebeck
Director: Prof. Dr. med. Dr. h.c. Hendrik Lehnert

Site-specific Modulation of Adipogenesis – Regulation by microRNAs miR-193a and miR-708

Dissertation
For Fulfillment of Requirements
For the Doctoral Degree
Of the University of Luebeck

-From the Department of Natural Sciences-

Submitted by
Mona Lisa Cherradi
From Hamburg

Luebeck 2018

First referee: Prof. Dr. med. Georg E. Brabant

Second referee: Prof. Dr. rer. nat. Henrik Oster

Date of oral examination: 11.07.2018

Approved for printing. Luebeck, 16.07.2018

Declaration/Erklärung

Hereby I declare that I have written the present dissertation without any assistance of third parties and have not used outside sources without declaration in the text. This dissertation has not been submitted in the same or similar version, not even in part, to any other authority for grading.

Ich versichere, dass ich die Dissertation ohne fremde Hilfe angefertigt und keine anderen als die angegebenen Hilfsmittel verwendet habe. Weder vorher noch gleichzeitig habe ich andernorts einen Zulassungsantrag gestellt oder diese Dissertation vorgelegt. Ich habe mich bisher noch keinem Promotionsverfahren unterzogen.

Luebeck, …16.07.2018…… …….

(Mona Lisa Cherradi)

بِسْمِ اللهِ الرَّحْمَنِ الرَّحِيمِ

الْحَمْدُ للهِ رَبِّ الْعَالَمِينَ

الرَّحْمنِ الرَّحِيمِ

مَلِكِ يَوْمِ الدِّينِ

إِيَّاكَ نَعْبُدُ وإِيَّاكَ نَسْتَعِينُ

اهدِنَا الصِّرَاطَ المُستَقِيمَ

صِرَاطَ الَّذِينَ أَنعَمتَ عَلَيهِمْ غَيرِ المَغضُوبِ عَلَيهِمْ وَلاَ الضَّالِّينَ

(Al-Fatiha)

Table of content

I Summary

Energy storage and supply is dominantly regulated by white adipose tissue (WAT). Due to its high plasticity WAT responds to metabolic stimuli by either hypertrophy and/or by adipogenesis. This regulation may vary depot specifically between the visceral and subcutaneous located depots. Fuel partitioning critically depends on the storage capacity of WAT whose impairment particularly of adipogenesis under pathophysiological conditions may contribute to many features of the metabolic syndrome. However, the underlying mechanisms governing general vs. differential regulation of the various WAT depots are currently far from clear even though a number of key genes involved in the differentiation and proliferation from preadipocytes to mature fat cells have been described. MicroRNAs have recently been established to critically be involved in the regulation of adipogenesis. The aim of the present study was therefore to systematically search for general and fat depot-specific microRNAs acting as regulators of adipogenesis in both visceral and subcutaneous WAT. Using a microRNA array approach we compared expression levels of microRNAs derived from primary *ex vivo* mouse and human, visceral and subcutaneous preadipocytes to their corresponding mature fat cells. Candidate microRNAs expression was validated in respective cell culture models. Subsequently the functional impact on adipogenesis was tested for selected microRNA candidates by a loss-of-function approach.

The unsupervised microRNA array approach identified nine candidate microRNAs, from which two, previously undescribed, microRNAs (miR-193a-3p, miR-708-5p) were further analyzed regarding their potential to regulate adipogenesis.

Due to its expression pattern in the cell culture models miR-708-5p showed potential as a general regulator of adipogenesis but this role could not conclusively been confirmed in the present study. Furthermore, when testing for adipocyte differentiation loss-of-function experiments for miR-708-5p showed no direct effect. In addition, lipolysis, glucose uptake and lipogenesis were not affected by miR-708-5p inhibition, suggesting no regulatory role for miR-708-5p characteristic lipid storage and lipid mobilization function of mature adipocytes. As adiponectin, leptin and IL-6 expression of adipocytes was not influenced by loss of miR-708-5p, key endocrine functions of adipocytes seemed not be altered by miR-708-5p. Finally, the results indicate that miR-708-5p expression might be regulated by androgens and may thus indirectly impact adipogenesis.

In contrast, present data support a role of miR-193a-3p in the negative regulation of epididymal adipogenesis under physiological conditions which may be mediated by WNT signaling as predicted by *in silico* target prediction.

In conclusion, the current work suggests a role for miR-708-5p in adipogenesis but only allows to exclude some distinct interactions without defining a clear target of action. For miR-193a-3p a regulatory role in the differentiation of epididymal adipocytes could be verified. Hence, this study could at least in part contribute to a better understanding of the fat depot-specific regulation of adipogenesis.

II Zusammenfassung

Weißes Fettgewebe spielt eine zentrale Rolle in der Speicherung und Mobilisierung von Energie in Form von Lipiden. Aufgrund seiner hohen Plastizität ist das weiße Fettgewebe in der Lage auf diverse metabolische Stimuli einerseits mit Fettzellvolumenerweiterung (Hypertrophie) oder andererseits mit Fettzellzahlerweiterung (Adipogenese) zu reagieren. Diese Regulation kann Depot-spezifisch variieren und sich zwischen viszeral oder subkutan lokalisierten Depots unterscheiden. Eine Störung der Adaption des Fettgewebes unter pathophysiologischen Bedingungen kann schwere metabolische Folgen wie ein metabolisches Syndrom nach sich ziehen. Allerdings sind die genauen Mechanismen, die der gemeinsamen aber auch unterschiedliche Steuerung in den verschiedenen Fettgeweben unterliegen, noch nicht vollständig aufgeklärt. Dies obwohl einige Schlüsselgene der Proliferation und Differenzierung von Präadipozyten und reifen Adipozyten bereits identifiziert wurden. Erst kürzlich wurde beschrieben, dass microRNAs die Adipogenese beeinflussen. Ziel dieser Arbeit war es daher systematisch microRNAs zu identifizieren, die eine generelle oder aber Fettgewebs-spezifische Rolle in diesem Prozess spielen. Dafür wurde ein microRNA-Array Ansatz gewählt, bei dem die Expression von microRNAs zwischen primären Präadipozyten und ihren korrespondierenden reifen Adipozyten sowohl aus murinem als auch humanem viszeralem und subkutanem Fettgewebe verglichen wurde. Die so identifizierten microRNAs wurden in entsprechenden Zellkulturmodellen verifiziert und anschließen ihr funktionaler Einfluss auf die Adipogenese mittels eines „loss-of-function“ Ansatzes getestet.

Insgesamt wurden durch den microRNA-Array Ansatz neun potentielle microRNAs identifiziert, von denen zwei bisher nicht in der Literatur beschrieben sind (miR-193a-3p und miR-708-5p). Diese wurden weiter charakterisiert und hinsichtlich ihres Einflusses auf die Adipogenese untersucht.

Aufgrund des Expressionsverlaufs im Zellkulturmodell konnte für miR-708-5p eine Funktion als genereller Regulator der Adipogenese angenommen werden. Allerdings konnte ihre Rolle im Rahmen der vorliegenden Arbeit nicht abschließend geklärt werden. Die spezifische Inhibierung von miR-708-5p zeigte weder einen direkten Einfluss auf die Adipozytendifferenzierung, noch konnten Effekte auf die Lipolyse, die Glukoseaufnahme sowie die Lipogenese nachgewiesen werden. MiR-708-5p scheint daher kein essentieller Regulator der Lipidspeicherung und –mobilisierung in reifen Adipozyten zu sein. Darüber hinaus konnten keine Effekte auf endokrine Funktionen der Adipozyten durch miR-708-5p

gezeigt werden. Die Expression von Adiponektin, Leptin und Interleukin-6 wurde nicht durch eine miR-708-5p Inhibierung beeinflusst. Interessanterweise gibt es aber Hinweise darauf, dass die Expression von miR-708-5p durch Androgene beeinflusst wird, was einen indirekten Einfluss von miR-708-5p auf die Adipogenese möglich erscheinen lässt.

Im Gegensatz hierzu konnte miR-193a-3p als negativer Regulator der epididymalen Adipogenese unter physiologischen Bedingungen identifiziert werden, wobei der WNT Signalweg ein mögliches Zielsystem darstellt, das in einem *in silico* Ansatz zur Vorhersage von Zielgenen identifiziert werden konnte.

Zusammenfassend lässt sich sagen, dass die zugrundeliegenden Arbeit einerseits eine Rolle der miR-708-5p in der Adipogenese vermuten lässt, dass aber, trotz des Ausschlusses diverser Komponenten, keine klare Funktion identifiziert werden konnte und andererseits ein negativer Einfluss der miR-193a-3p auf die epididymale Adipozytendifferenzierung gezeigt werden konnte. Somit konnte mit dieser Arbeit zumindest teilweise zu einem besseren Verständnis der Fettgewebs-spezifischen Regulation der Adipogenese beigetragen werden.

III Abbreviations

°C	Degree celcisus
µL	Microlitre
µm	Micrometre
µM	Micromolar
AdipoR	Adiponectin receptors
A-FABP	Fatty acid binding protein
AgRP	Agouti-related peptide
AKT	Protein kinase B
AMP	Adenosinmonophosphate
APC	Adenomatous polyposis coli
APS	Ammonium persulfate
AR	Androgen receptor
ARC	Arcuate nucleus of hypothalamus
ATGL	Adipose triglyceride lipase
ATP	Adenosintriphosphate
AUR	Amplex Ultra Red
BAT	Brown adipose tissue
BCA	Bicinchoninic acid
BMI	Body mass index
BMP	Bone morphogenic protein
BSA	Bovine serum albumine
C/EBP	CCAAT/enhancer-binding protein
cAMP	Cyclic adenosinmonophosphate
cDNA	Complementary deoxyribonucleic acid
CHOP10	C/EBP-homologous protein 10
CREB	cAMP response element binding protein
Ct	Threshold cycle
d	Day
DAB	3,3'-Diaminobenzidine
DAG	Diacylglycerol

DHAP	Dihydroxyacetone phosphate
DHT	5α-dihydrotestosterone
DKK2	Dickkopf-related protein 2
DM	Differentiation medium
DMEM	Dulbecco’s modified Eagle's medium
DNA	Deoxyribonucleic acid
DPM	Decay per minute
ECL	Enhanced chemiluminescence
EDTA	Ethylenediaminetetraacetic acid
EGF	Epidermal growth factor
EPI	Epididymal
ERK	Extracellular signal-regulated kinase
EtOH	Ethanol
FA	Fatty acid
FBS	Fetal bovine serum
Fbxw11/βTrCP2	Beta transducin repeat containing protein 2
FC	Fold change
FGF	Fibroblast growth factor
FGR	Free Glycerol Reagent
g	Gram
GADP	Glyceraldehydes-3-phosphate
GC	Glucocorticoid
GLUT4	Glucose transporter 4
GR	Glucocorticoid receptor
GSK3β	Glycogen synthase kinase-3β
h	Hour
H2O	Water
HEPES	4-(2-hydroxyethyl)-1-piperazineethanesulfonic acid
hMSC	Human mesenchymal stem cells
HPRT	Hypoxanthine phosphoribosyltransferase 1
HRP	Horseradish peroxidase
hsa	Homo sapiens/human
HSL	Hormone-sensitive lipase
IBMX	3-isobutyl-1-methylxanthine

ICC	Immunocytochemistry
IL-6	Interleukin-6
IM	Induction medium
ING	Inguinal
Ins	Insulin
IR	Insulin receptor
IRS	Insulin receptor substrate
ISO	Isoprenaline
kDa	Kilo Dalton
KEGG	Kyoto Encyclopedia of Genes and Genomes
KLF7	Kruppel-like factor 7
L	Litre
LEF	Lymphoid-enhancer-binding factor
LM	Lipolysis medium
logFC	Logarithmic fold change
Lowess	LOcally WEighted Scatterplot Smoothing
LRP5	Low-density lipoprotein-related protein 5
M	Molar
MAG	Monoacylglycerol
mat	Mature adipocyte
mg	Milligram
MGL	Monoacylglyceride lipase
min	Minute
miR/miRNA	Micro ribonucleic acid
miRISC	microRNA-containing RNA-induced silencing complex
mL	Millilitre
mM	Millimolar
mm	Millimetre
mmu	Mus musculus/mouse
mRNA	Messanger ribonucleic acid
ms	Milliseconds
MSC	Mesenchymal stem cells
NC	Negative control
n.d.	Not determined

NFκB	Nuclear factor kappa-light-chain-enhancer of activated B cells
ng	Nanogram
nM	Nanomolar
nm	Nanometre
NPY	Neuropeptide Y
nt	Nucleotides
OD	Optical density
PBS	Phosphate buffered saline
PCA	Principle component analysis
PCR	Polymerase chain reaction
Pen/Strep	Penicillin/Streptomycin
PM	Proliferation medium
pmol	Picomole
PMSF	Phenylmethanesulfonylfluoride
pol	Polymerase
POMC	Proopiomelanocortin
POPOP	1,4-bis(5-phenyloxazol-2-yl) benzene
PPARγ	Peroxisome proliferator-activated receptor γ
PPO	2,5-Diphenyloxazole
pre	Preadipocyte
PREF-1	Preadipocyte factor 1
PVDF	Polyvinylidene fluoride
RIPA	Radioimmunoprecipitation assay buffer
RNA	Ribonucleic acid
rpm	Rounds-per-minute
RT	Room temperature
RT-qPCR	Real-time quantitative polymerase chain reaction
RUNX2	Runt-related transcription factor 2
SDS	Sodium dodecylsulfate
sec	Seconds
SEM	Standard error of the mean
Serpina3	Serpin family A member 3
SV-40	Simian vacuolating virus-40
TCF	T-cell-specific transcription factor

TEMED	Tetramethylethylenediamine
TG	Triglycerides
TGFβ	Transforming growth factor β
TGFBR2	TGFβ receptor 2
TNFα	Tumor necrosis factor alpha
U	Units
UTR	Untranslated region
V	Volt
v	Volume
VE-H2O	Purified water
w	Weight
WAT	White adipose tissue
WB	Western Blot
WebGestalt	WEB-based GEne SeT AnaLysis Toolkit
WNT	Wingless-type MMTV integration site family member

1 Introduction

Adipose tissue is a metabolically active organ which is important for energy homeostasis. Obesity develops when food intake constantly exceeds energy expenditure, attributed to life style changes as determined by an overconsumption of energy and by decreased physical activity. As a consequence of exhausted adipose tissue storage capacity, obesity might lead to serious health consequences like the development of type 2 diabetes mellitus, cardiovascular complications and the development of certain types of cancer [1, 2].

The grade of obesity is defined by the body mass index (BMI = body weight (kg)/(body height)^2 (m^2)) and correlates to the body fat mass. The prevalence of obesity, defined as a body mass index (BMI) beyond 30 kg/m^2, has dramatically increased over recent years. For Germany a sharp rise in the prevalence has been observed particularly in male subjects when comparing the results of a national survey 1998 to 2011 [3]. This increase showed a gender difference with a much more prominent rise in men from 18.9% in 1998 to 23.3% in 2011. In women only an increase from 22.5% to 23.9% for the prevalence to develop obesity has been observed. Nevertheless, obesity remains a severe health problem in both genders.

1.1 Central regulation of food intake and obesity

Obesity develops as a result of an imbalance between food intake and energy expenditure. These two components are regulated by the central nervous system as well as feedback through peripheral signals [4, 5]. Key regions in the hypothalamus integrate these peripheral feedback signals and receive neuronal inputs both from the brain stem and the limbic system. The latter represents the most important centre to modulate hedonic eating [6]. The hypothalamus is a specific target for this endocrine feedback from the periphery. Among hypothalamic centres the arcuate nucleus of the hypothalamus (ARC) is one of the best characterized brain regions to control feeding behaviour. It is located close to the third ventricle and the median eminence and with this has a close proximity to the vasculature. This ensures specific blood supply allowing a more direct feedback through peripheral orexigenic or anorexigenic, endocrine signals like ghrelin, leptin (see 1.2.2.1) and insulin [7-9]. The ARC contains the anorexigenic (food intake decreasing) proopiomelanocortin (POMC) neurons as well as the orexigenic (food intake increasing) neuropeptide Y (NPY)/agouti-related peptide (AgRP) neurons [10-13]. Their activation leads to the respective release of anorexigenic or

orexigenic neuropeptides that further act centrally or in the periphery. Hence, anorexigenic signals lead to an inhibition of food intake and decreased appetite, whereby orexigenic signals lead to their increase [14, 15].

1.2 Adipose tissue function

Adipose tissue is a highly active metabolic organ that is able to store excess lipids effectively which may in turn be quickly mobilized to supply peripheral tissues on demand. By this it plays an important role in maintaining energy homeostasis with dominant actions for the fine tuning of glucose and lipid homeostasis but also for the regulation of insulin sensitivity [16]. Adipose tissue is also able to modulate an inflammatory response [17]. With the discovery of leptin in 1994 (see 1.2.2.1) [18], it was additionally regarded as an endocrine organ [19]. Adipose tissue is a highly heterogeneous organ and can be divided into white adipose tissue (WAT) and brown adipose tissue (BAT) whereby the latter one was just recently discovered in adult healthy humans [20]. Brown adipocytes differ from white adipocytes in morphology and function. While white adipocytes contain large lipid vacuoles for lipid storage, brown adipocytes contain many small lipid droplets and a large amount of mitochondria, giving them their characteristic brown color. In contrast to WAT, BAT is not important for lipid storage and for meeting the energy demands of peripheral tissues but rather to maintain body temperature, which is referred to as non-shivering thermogenesis. Thermogenesis can be induced by β3-adrenergic stimuli, e.g. cold exposure mediated by norepinephrine [21, 22]. Upon activation, BAT is able to take up high amounts of fatty acids (FA), triglyceride-rich lipoproteins and glucose [23] and enhances the cholesterol turnover by increased reverse cholesterol transport [24]. Hence, BAT activation can also contribute to systemic energy turnover and homeostasis. However, WAT remains the most important component to maintain the energy homeostasis which is preserved by key adipocyte functions like lipolysis, lipogenesis and glucose uptake (see 1.2.1). Additionally, the endocrine function of adipose tissue (see 1.2.2), the secretion of adipokines like leptin, adiponectin and interleukin 6 (IL-6), further links the adipose tissue to diverse biological processes, e.g. insulin signaling and glucose homeostasis [25, 26].

1.2.1 Adipocyte key functions – lipid storage and mobilization

1.2.1.1 Insulin-mediated glucose uptake and lipogenesis

In feeding/anabolic conditions insulin is secreted by the pancreatic β-cells to reduce plasma glucose levels. In adipocytes binding of insulin to the insulin receptor (IR) at the cell surface leads to an autophosphorylation of its tyrosine kinase activity [27]. Hence the insulin receptor substrates (IRS) 1 and 2 as well as other signaling molecules are able to bind to these phosphorylated sites of the IR leading to their phosphorylation and activation. The IRS molecules induce different signaling cascades resulting in genomic or non-genomic activities. The latter for example finally results in the translocation of the glucose transporter 4 (GLUT4) from cytosolic vesicles to the plasma membrane of the adipocyte [28-32]. This enables insulin-mediated glucose uptake into the adipocytes which is subsequently further processed.

The glucose molecule 2-Deoxy-D-glucose which has the 2-hydroxyl group replaced by hydrogen cannot further be processed in glycolysis and accumulates in the cell. When radioactively-labeled it can serve as a good marker for glucose uptake. However, under physiological conditions glucose is further processed in several steps to three-carbon sugars, dihydroxyacetone phosphate (DHAP) and glyceraldehydes-3-phosphate (GADP). GADP can further be processed to acetyl-CoA which serves as a substrate for *de novo* fatty acid synthesis. These FA (or dietary FA as well) are used for triglyceride (TG) synthesis, also referred to as lipogenesis, and stored in form of TGs in the lipid droplets of adipocytes. DHAP can be either converted to GADP and being used for *de novo* fatty acid synthesis as well or instead it can be converted to glycerol-3-phosphate which serves as the glycerol backbone for the TG synthesis. Step by step three FA are then added to the glycerol backbone [33-35]. By using radioactively-labeled glucose, the lipogenesis from this glucose precursor can be experimentally assessed in adipocytes.

Thus, lipogenesis is a precisely regulated biochemical pathway that is activated under anabolic conditions to safely store excess calories in form of triglycerides into the adipose tissue [36].

1.2.1.2 Lipolysis

Lipolysis is a biochemical pathway regulated in response to changing metabolic conditions. In anabolic conditions lipolysis is inactivated whereas energy deprivation leads to the hydrolysis

of the stored TGs thereby generating glycerol and FAs that are used by peripheral tissues as energy substrates for β-oxidation or ATP production [36].

Three enzymes are described to play important roles in the complete hydrolysis of TGs. First, the adipose triglyceride lipase (ATGL) hydrolyses the TG to a FA and diacylglycerol (DAG) and is thereby rate-limiting for this step [37, 38]. Second, the hormone-sensitive lipase (HSL) is the rate-limiting enzyme for the catabolism of DAG to another FA and monoacylglycerol (MAG) [39-41]. Third, MAG is hydrolyzed by the monoacylglyceride lipase (MGL) to the last FA and the glycerol backbone [42-45]. The FAs are then bound to adipose fatty acid binding proteins (A-FABP/FABP4/aP2) and released to the circulation to be provided to peripheral tissues to meet their energy demands [46]. Additionally, this is important to prevent the accumulation of toxic free FA in the adipocyte itself. Glycerol is released to the circulation via aquaporins and finally taken up by peripheral tissues [47].

1.2.2 Endocrine function - adipokines

WAT also maintains energy homeostasis by its endocrine function which includes the expression, secretion and response to adipokines. But adipokines are not only important under physiological conditions but are also implicated in long-term effects of obesity [26, 48-52].

1.2.2.1 Leptin

Leptin is a 16 kDa polypeptide, encoded by the *ob* gene and shares structural homology to cytokines [53]. The main site of expression is the adipose tissue, whereby it is predominantly expressed by the subcutaneous compared to visceral adipocytes. Furthermore, its expression is directly proportional to the body fat mass [54]. The main function of leptin is the regulation of energy homeostasis by controlling satiety, body weight and energy expenditure. This occurs via leptin-sensing neurons in the ARC. There, leptin leads to a decrease of orexigenic peptides like NPY and increases activity of anorexigenic POMC neurons (see 1.1) [7, 55, 56]. Furthermore, leptin exerts some roles in the regulation of insulin sensitivity [57-59]. Plasma leptin levels positively correlate to body fat mass, thus they are low in lean subjects and increase with increasing body fat mass, e.g. obesity [60]. Due to its anorexigenic function leptin was considered for an anti-obesity treatment strategy. However, studies of diet-induced obesity not based on a leptin mutation itself failed to achieve the expected reduction in body weight of obese people when using exogenous leptin administration. This cannot be explained by an insufficient leptin expression but rather by a defect in leptin action through its receptor leading to leptin resistance in conditions of hyperleptinemia [61, 62].

1.2.2.2 Adiponectin

Adiponectin is a 30 kDa protein and shares structural homology to the collagen superfamily [63, 64] and is exclusively secreted from the adipose tissue [54, 65]. Two adiponectin receptors exist, AdipoR1 and AdipoR2 [66]. By binding to these receptors adiponectin exerts its insulin-sensitizing effects on muscle (via AdipoR1) and liver (via AdipoR2). In muscle, adiponectin leads to increased glucose uptake and fatty acid oxidation, in liver to an increased fatty acid oxidation accompanied by decreased gluconeogenesis [67, 68]. In contrast to other adipokines, adiponectin plasma levels negatively correlate with fat mass, obesity and type 2 diabetes mellitus [69, 70]. Thus, weight loss increases adiponectin levels and is associated with improved insulin sensitivity [68, 71, 72]. In rodent models it was shown that adiponectin increases insulin sensitivity [73]. In addition to this main function of adiponectin, it also exerts anti-atherosclerosis effects [74]. Furthermore, adiponectin is considered to play a role in innate and adaptive immunity by showing anti-inflammatory properties [75].

1.2.2.3 Interleukin-6

Interleukin-6 (IL-6) is a 22- to 27 kDa protein and is secreted by immune cells, fibroblasts, endothelia cells, skeletal muscle and adipose tissue. Approximately 30% of the circulating IL-6 arises from adipose tissue in the non-inflammatory state, whereby visceral fat secretes more IL-6 compared to subcutaneous fat [76-78]. Plasma IL-6 levels are positively correlated with body weight, obesity and insulin resistance [76-78] and elevated IL-6 levels seem to be predictive for the development of type 2 diabetes mellitus [79]. Furthermore, IL-6 is described to impair the insulin signaling by targeting IRS-1 and suppressor of cytokine signaling 3 [80]. Additionally, expression of adiponectin is repressed by IL-6, undermining its beneficial effects on insulin sensitivity [81]. In contrast, weight loss decreases IL-6 levels in serum and adipose tissue again [82].

1.3 Body fat distribution and obesity

WAT is not homogenously distributed but accumulates in distinct WAT depots either viscerally or subcutaneously [83]. Preadipocytes of different WAT depots have been shown to exhibit distinct phenotypes. If derived from subcutaneous WAT they appear to be more proliferative, more resistant to tumor necrosis factor alpha (TNF-α)-induced apoptosis and to insulin resistance than if they originate from visceral WAT depots [84, 85]. The basis of these fat depot-specific differences in preadipocytes has been studied in more detail recently. These

studies indicate that adipocytes from subcutaneous depots differ to progenitors from other sources by their dependency on low-density lipoprotein-related protein 5 (LRP5) of the wingless-type MMTV integration site family member (WNT) signaling cascade (see 1.4.3.1). This could be confirmed in humans where a gain of function mutation in the LRP5 allele induced fat accumulation in the lower body associated with better metabolic health and reduced WAT inflammation. Knockdown of this pathway fat depot-specifically affected adipogenesis only in subcutaneous but not in visceral depots [86]. In contrast, an alteration in 14-3-3ζ selectively modulated the visceral depot. Visceral fat mass increased with 14-3-3ζ overexpression and a decreased with a knockdown [87, 88].These two mechanisms represent a number of further processes discussed to be involved in the changes observed in a depot specific regulation of WAT. However, these mechanisms have recently been reviewed in great detail without providing a generally accepted conclusion to date [83].

Sex steroids also seem to impact on adipose tissue distribution and local function. In men, low plasma androgen and sex hormone-binding globulin are associated to visceral obesity [89, 90]. In contrast, in women visceral obesity is associated with higher androgen plasma levels [91], as for example seen in women with polycystic ovary syndrome who exhibit insulin resistance, hyperandrogenism and abdominal obesity [92]. Furthermore, androgens seem to have local actions on different adipose tissue depots, whereby a higher sensitivity to androgens was more often observed in the epididymal/visceral fat depot [93-95].

1.3.1 Fat depot-specific regulation of WAT

In addition to the fat depot-specific differences of preadipocytes and impact of sex steroids also the response to overfeeding differs between fat depots. However, the molecular mechanisms important for WAT expansion in response to positive energy imbalance are far from clear. There are two possible mechanisms to store more energy in WAT in case of a positive energy balance. There is either hypertrophy of WAT with an increased filling of existing adipocytes and an increase in lipid droplet size (hypertrophic WAT growth) or an increase in the number of adipocytes induced by a stimulation of adipocyte precursor cells to differentiate into mature fat cells (hyperplastic WAT growth; also referred to as adipogenesis) [96, 97]. Hypertrophic cells are more prone to cell death, along with the recruitment of inflammatory macrophages [98-102] which in turn might lead to a loss of adipose tissue flexibility in storing and mobilizing lipids on demand. In contrast, hyperplasia may improve storage capacity and maintain the flexibility of adipose tissue for lipid storage and supply in certain forms of obesity [103-107]. Both mechanisms may as well occur in parallel. Currently,

it is still under debate which mechanisms are underlying both responses and which predominates under various exogenous conditions.

The visceral compartment appear to respond predominantly by adipocyte hypertrophy whereas subcutaneous depots rather increase their adipocyte number when challenged with the same stimulus [108] fitting to a metabolically more healthy phenotype of subcutaneous expansion in obesity. In humans an accumulation of visceral WAT and abdominal subcutaneous WAT is related to an increased mortality risk due to cardiovascular disease and type 2 diabetes mellitus. These adverse effects of obesity appear to depend on an enlargement of adipocytes (WAT hypertrophy) rather than on an increase of adipocyte proliferation [109]. This view was however recently challenged by data which suggests that an expansion of the number of adipocytes rather than their size in the visceral compartment determines the weight of the visceral fat [104].

Body fat distribution has been shown to impact on the risks associated with obesity. Obesity is strongly associated with an increase in free FA which is an important cofactor to hyperinsulinemia leading to insulin resistance [110]. Excess expansion of WAT in obesity stimulates the secretion of pro-inflammatory cytokines like IL-6 (see 1.2.2.3) and reduces adiponectin (see 1.2.2.2) [111]. The resulting low grade inflammation of WAT decreases the storing function of the fat cells and stimulates a release of non-esterified fatty acids which may cause ectopic lipid deposition and lipotoxicity in central metabolic organs like the liver and skeletal muscles and by this inducing insulin resistance [112-115].

However, a number of independent studies reported that not all obese subjects may be affected by insulin resistance but be metabolically healthy whereas some lean subjects exhibit a metabolically unfavourable “obese” phenotype including insulin resistance [116, 117]. The underlying pathophysiology is currently unclear. A difference in the distribution of fat in subcutaneous or visceral depots in both types of obesity may serve as one possible explanation. Nevertheless, the abdominal or central type of obesity was associated with a high risk for insulin resistance, type 2 diabetes, hyperlipidemia and atherosclerosis [118, 119]. The described fat depot-specific differences and their implications in obesity and its long-term consequences suggest that factors involved in fat depot-specific regulation may play an important role to determine these long-term effects. Thus, fat depot-specific hypertrophic or hyperplastic responses may differently change the WAT functions of lipid storage and mobilization as well as the adipokine expression profiles with a deregulation of factors facilitating these long-term effects.

1.4 Adipogenesis

Adipogenesis describes the underling mechanism of adipose tissue development and the hyperplastic processes in obesity. Adipogenesis can be divided into two parts: the adipogenic determination from pluripotent stem cells to preadipocytes as well as the terminal differentiation of preadipocytes to mature adipocytes. Both, commitment and termination, are well coordinated multi-step processes including several signaling pathways, transcription factor cascades and controlled gene expression that finally lead to adipocyte development. Thus, adipogenesis can be facilitated through essential endogenous factors but also exogenous signaling molecules and hormones influence adipogenesis.

Determination of adipocytes occurs from pluripotent mesenchymal stem cells (MSC) that are generally able to develop into chondrocytes, myocytes, osteocytes and (pre)adipocytes [120, 121]. Morphologically the preadipocytes cannot be distinguished from MSCs but they lost their ability to convert into the other cell types. This commitment is influenced by multiple signals whereby bone morphogenic protein (BMP) signaling as well as WNT signaling (see 1.4.3.1) seem to be most important for this process.

With the commitment to preadipocytes the early phase of adipogenesis is initiated. Thereby, preadipocyte factor 1 (PREF-1; see 1.4.2.1) is important to maintain the preadipocyte status of the cells. However, upon growth arrest, preadipocytes are able to reenter the cell cycle and undergo mitosis, a process referred to as mitotic clonal expansion. After this clonal expansion, the cells start to alter their cell shape from a fibroblastic morphology to the spherical shape of mature adipocytes. Furthermore, they start to accumulate lipids and gain the metabolic features of mature adipocytes. The mitotic clonal expansion can be induced *in vitro* as well. Therefore, cells are grown to confluence/growth arrest and are then induced to differentiation with a cocktail of inducers containing among other components dexamethasone (see 1.4.3.2) as well as a cAMP inducer e.g. isobutylmethylxanthine (IBMX). This leads to a synchronous reentry of preadipocytes into the cell cycle. Soon after induction of differentiation, CCAAT/enhancer-binding protein β (C/EBPβ; see 1.4.2.2) expression is induced, initiating the intermediate phase of adipocyte differentiation. C/EBPβ binds to the promoters of C/EBPα and peroxisome proliferator-activated receptor γ (PPARγ; see1.4.2.3) and activates their transcription. C/EBPα and PPARγ further cross activate each other as well as coordinately activate the transcription of many other genes involved in insulin sensitivity, lipogenesis and lipolysis leading to the mature adipocyte phenotype (Figure 1). Among these,

the genes encoding for GLUT4, A-FABP and Perilipin are transcribed which are characteristic markers for the late phase of adipogenesis (for review [122]).

1.4.1 Regulation of adipogenesis – endogenous and exogenous factors

1.4.2 Essential endogenous factors regulating adipogenesis

1.4.2.1 PREF-1

Preadipocyte factor 1 (PREF-1/DLK1) is usually highly expressed in preadipocytes, decreases with the progression of adipogenesis and is considered to exert anti-adipogenic properties. It is a transmembrane protein, ranging from 45-60 kDa due to post-translational N-linked glycosylation, and contains six tandem epidermal growth factor (EGF)-like repeats [123]. Additionally, multiple transcripts of PREF-1 exist which are generated by alternative splicing [124]. PREF-1 is activated by proteolytic cleavage at the extracellular domain whereby only the 50 kDa, but not the 25 kDa, soluble form is able to inhibit adipogenesis [125-127]. In 3T3-L1 cells it was shown that PREF-1 stable transfection lowered the degree of adipocyte differentiation. In contrast, PREF-1 inhibition in these cells enhanced adipocyte differentiation [128]. Its repressive role in adipogenesis is further indicated in mice studies showing that absence of PREF-1 leads to increased adiposity [129], whereby PREF-1 overexpression leads to adipose tissue lipoatrophy [130]. Thus, PREF-1 seems to play an important role in maintaining preadipocytes into proliferation and inhibiting their differentiation.

1.4.2.2 C/EBPs

The CCAAT/enhancer-binding protein (C/EBP) family includes several members like C/EBPα, C/EBPβ, C/EBPγ, C/EBPδ and C/EBP-homologous protein 10 (CHOP10) that are expressed in adipocytes. With the exception of CHOP10, the C/EBPs contain a DNA-binding domain and need to dimerize to gain their DNA-binding capacity. During adipogenesis they are temporally expressed, whereby the C/EBP cascade starts with the expression of C/EBPβ and C/EBPδ. Both promote adipogenesis, whereby C/EBPβ seems to be more important as indicated in studies with 3T3-L1 and NIH-3T3 cell lines [131]. However, C/EBPδ seems to be able to compensate for a loss of C/EBPβ as indicated in double-knockout mice which showed a more severe loss of adipose tissue mass compared to the C/EBPβ single knockout mice [132]. By binding to the promoters of C/EBPα and PPARγ, C/EBPβ and C/EBPδ activate their transcription and thereby further promoting adipogenesis [133, 134]. Once activated,

C/EBPα expression is maintained by autoactivation [133]. Many studies indicate an important role for C/EBPα in the development of adipose tissue in mice [135, 136] and the promotion of adipogenesis in cells [137, 138]. However, C/EBPα cannot efficiently function without PPARγ [139]. In contrast to its function in the promotion of adipogenesis, C/EBPα also exhibits an antimitotic function [140, 141]. It needs to be suppressed until preadipocytes went through the mitotic clonal expansion. The C/EBP member CHOP10 acts anti-adipogenic through heterodimerization with C/EBPβ thereby leading to its inactivation [142, 143]. Thus, the C/EBPs seem to regulate each others expression and function in a temporally defined manner thereby promoting adipocyte differentiation.

1.4.2.3 PPARy

The peroxisome proliferator-activated receptor γ (PPARγ) is expressed in three isoforms (PPARγ1, PPARγ2, PPARγ3) whereas in adipose tissue mainly the PPARγ2 isoform is expressed [144, 145]. To acquire DNA-binding activity, PPARγ needs to heterodimerize with the retinoid X receptor [146]. PPARγ promotes adipogenesis together with C/EBPα and is considered as the master regulator of adipogenesis. It was shown that exogenous expression of PPARγ in C/EBPα-lacking fibroblast can rescue adipogenesis, but C/EBPα is not able to rescue adipocyte differentiation in the absence of PPARγ [139]. In addition, no other factor has been discovered yet that can induce adipocyte differentiation in the absence of PPARγ. PPARγ is not only important for the promotion of adipogenesis but also for the maintenance of the differentiated state as indicated by an *in vivo* study where an inducible PPARγ knockout leads to the death of existing adipocytes [147]. Thus, as the master regulator of adipogenesis, PPARγ plays an important role in adipose tissue development and maintenance.

1.4.3 Exogenous factors regulating adipogenesis

1.4.3.1 WNT

The Wingless-type MMTV integration site family member (WNT) family of secreted glycoproteins mediate their autocrine and paracrine action through the frizzled receptors and the LRP 5/6 co-receptor [148-150]. In the canonical WNT pathway, cytosolic β-catenin is bound to the “destruction complex” comprising i. a. adenomatous polyposis coli (APC), axin and glycogen synthase kinase-3β (GSK3β). Without WNT stimulation (off-state), GSK3β phosphorylates β-catenin, thereby labeling it for ubiquitination that finally leads to its proteasomal degradation. In contrast, activation of WNT pathway, by binding of WNTs to the receptors (on-state), leads to a disassembly of the “destruction complex” and thereby the

accumulation of β-catenin in the cytoplasm and finally translocation to the nucleus. In the nucleus it binds to lymphoid-enhancer-binding factor/T-cell-specific transcription factor (LEF/TCF) activating the transcription of downstream genes (for review [151-154]). By this, WNT signaling has been described to promote myogenesis [155] and osteogenesis [156] while inhibiting adipogenesis [157]. Furthermore, WNT signaling is able to completely block the expression of C/EBPα and PPARγ [158] and thereby further differentiation of adipocytes. In contrast, WNT signaling inhibition in preadipocytes leads to their spontaneous differentiation [155]. In parallel to the canonical WNT signaling, β-catenin can also bind to the androgen receptor in response to testosterone stimulation leading to the inhibition of adipocyte differentiation [159]. Thus, WNT signaling and in particular β-catenin signaling plays an important role in the lineage commitment of MSCs as well as in the regulation of adipogenesis [151-154].

1.4.3.2 Glucocorticoids

Glucocorticoids (GCs) belong to the steroid hormones and bind to the glucocorticoid receptor (GR), a ligand-dependent transcription factor. The best known and physiological occurring glucocorticoids are cortisol (hydrocortisone) and cortisone. However, the synthetic glucocorticoid dexamethasone is commonly used for therapeutic treatment as well as in research due to its high potency to bind to the GR. GCs are known to have diverse effects on adipose tissue biology. In adipogenesis they are required for the full differentiation of adipocytes. Thereby they suppress PREF-1 and Runt-related transcription factor 2 (RUNX2) expression and inducing the expression of C/EBPβ, C/EBPδ and PPARγ [160-165]. Furthermore, they are also required for the maintenance of adipogenic genes that are involved in the TG homeostasis as well as in the inflammatory response [166, 167]. Their influence on adipocyte key functions like lipogenesis and lipolysis is controversially discussed, but it appears that GCs generally seem to play a role in lipid turnover [168]. However, chronic excess to GCs can result in fat accumulation and metabolic derangements. For example, hypercortisolism is associated with obesity and disturbances in fat distribution [169].

1.4.3.3 Androgens

Androgens belong to the steroid hormone superfamily and bind to the androgen receptor (AR), a ligand-dependent transcription factor. The best known and physiological occurring androgens are testosterone and 5-α-dihydrotestosteone (DHT), whereby DHT binds more potently to the AR compared to testosterone. DHT is often used in research to answer

scientific questions regarding androgen-specific actions because it cannot, unlike testosterone, be converted into estradiol. Controversial results have been obtained for androgen actions in adipose tissue biology probably due to the diversity of other factors that can influence androgen action (men vs. women, fat depot localization, local vs. systemic site of action). Androgens are considered to show rather inhibitory effects on adipogenesis. In several studies DHT negatively regulated adipogenic differentiation of human mesenchymal stem cells (hMSC) as well as in human primary cells of abdominal subcutaneous, mesenteric and omental fat depots in males [170], of abdominal subcutaneous adipose-derived stem cells in women [171] and in abdominal subcutaneous and omental primary human cell cultures in both sexes [172]. Also in 3T3-L1 [159] and C3H10T1/2 [173] cell lines DHT exerted inhibitory effects on adipocyte differentiation resulting in decreased expression of C/EBPα and PPARγ in both cell lines. Singh *et al*. also suggest a role of androgens for lineage commitment towards a myogenic phenotype and not to the adipogenic lineage [173].

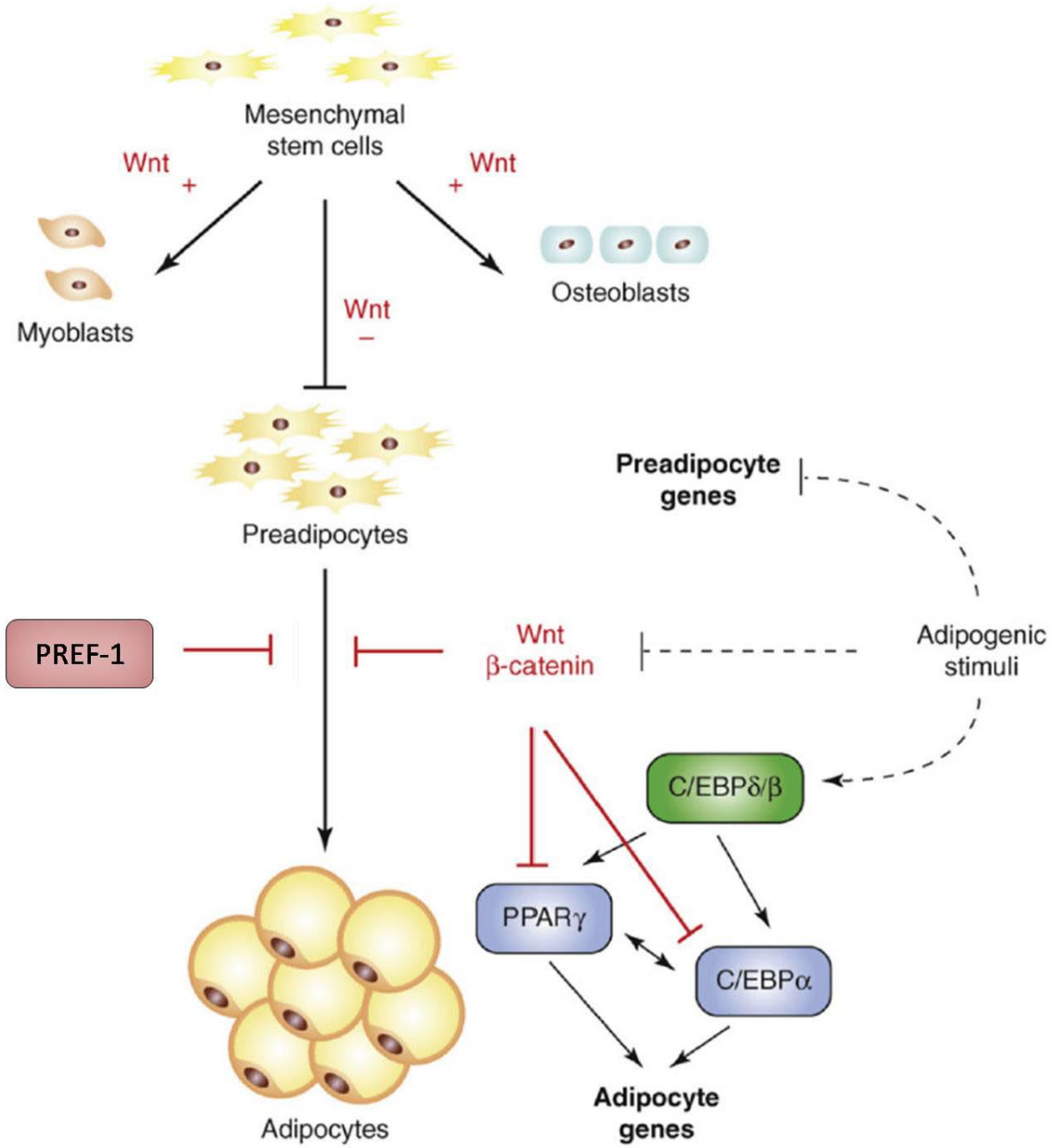

Figure 1 – Schematically depicted model of adipogenesis: from commitment to termination. Inactivation of WNT signaling leads to the commitment of mesenchymal stem cells (MSC) to preadipocytes. Preadipocyte status is maintained by PREF-1 and activated WNT signaling (= early phase of adipogenesis). However, adipogenic stimuli (dexamethasone, IBMX) induce the adipocyte differentiation. First C/EBPβ and C/EBPδ are expressed (= intermediate phase of adipogenesis) which subsequently activate the expression of the master regulators C/EBPα and PPARγ. C/EBPα and PPARγ coordinately activate the transcription of adipogenic genes (e.g. GLUT4, A-FABP, Perilipin) involved in insulin sensitivity, lipogenesis and lipolysis leading to the mature adipocyte phenotype (=late phase of adipogenesis). For details see text (1.3); modified from Christodoulides *et al*. (2009) [151].

So far, adipose tissue development and function underlies many fine-tuned regulatory mechanisms. But adipogenesis can also be regulated by non-coding RNAs, adding another level of regulation to the complexity of adipocyte differentiation.

1.5 MicroRNAs

The first microRNA (miRNA/miR), lin-4, was discovered in 1993 [174, 175] and since then research on microRNAs regulation and function constantly increased. MicroRNAs are small 19-25 nt long non-protein-coding RNAs that regulate post-transcriptionally the gene expression [176]. They bind to their target mRNA which results in decreased mRNA levels [177] and subsequently less translation to protein.

MicroRNAs are transcribed as long primary transcripts, so-called pri-miRNAs [178], in most cases by RNA polymerase pol II [179, 180] and only in the minority by polymerase pol III [181]. The majority of microRNAs are transcribed from intergenic locations, away from annotated genes, using their own promoter [179, 180]. Furthermore, they are often found in close proximity to other microRNAs and are transcribed as microRNA clusters [178]. However, some microRNAs can also be transcribed from intronic regions of known genes, either in sense- or antisense orientation [182-184]. The pri-miRNA transcripts contain a hairpin structure which is recognized by the nuclear RNase III Drosha. The stem-loop is cleaved by Drosha and releases the 60-80 nt microRNA precursor [178, 185], the pre-miRNA, containing a 5’ phosphate and a 2 nt 3’ overhang [186, 187]. The pre-miRNA is then exported to the cytoplasm by Ran-GTP and Exportin 5 active transport [188, 189]. In the cytoplasm the pre-miRNA is further processed to the 19-25 nt microRNA duplex by the cytoplasmic RNase III Dicer [190-194]. The mature microRNA is in one of the strands. Usually the strand with less stable pairing at its 5’ end determines the mature microRNA [195, 196] and is loaded into the effector complex microRNA-containing RNA-induced silencing complex (miRISC). Core component of the miRISC complex are members of the argonaute protein family, which seem to facilitate the binding of the mature microRNA [190, 197]. Once assembled to the miRISC complex, the mature microRNA will either lead to cleavage or translational repression of the target mRNA. MiRISC usually binds to the 3’ UTR of the target mRNA, facilitated by the heptameric seed region from nucleotides 2-8 of the microRNA [198]. When complementarity is sufficient enough the mRNA will be cleaved. Otherwise it comes to translational repression of the target mRNA. As in mammals microRNA and mRNA lack sufficient complementarity in most cases, translational repression is more prevalent (Figure 2)

[199]. There is also knowledge increasing that translational repression can occur at different stages of translation [200-204]. By these mechanisms, microRNAs are able to target several mRNAs and mRNAs can be targeted by several microRNAs [205].

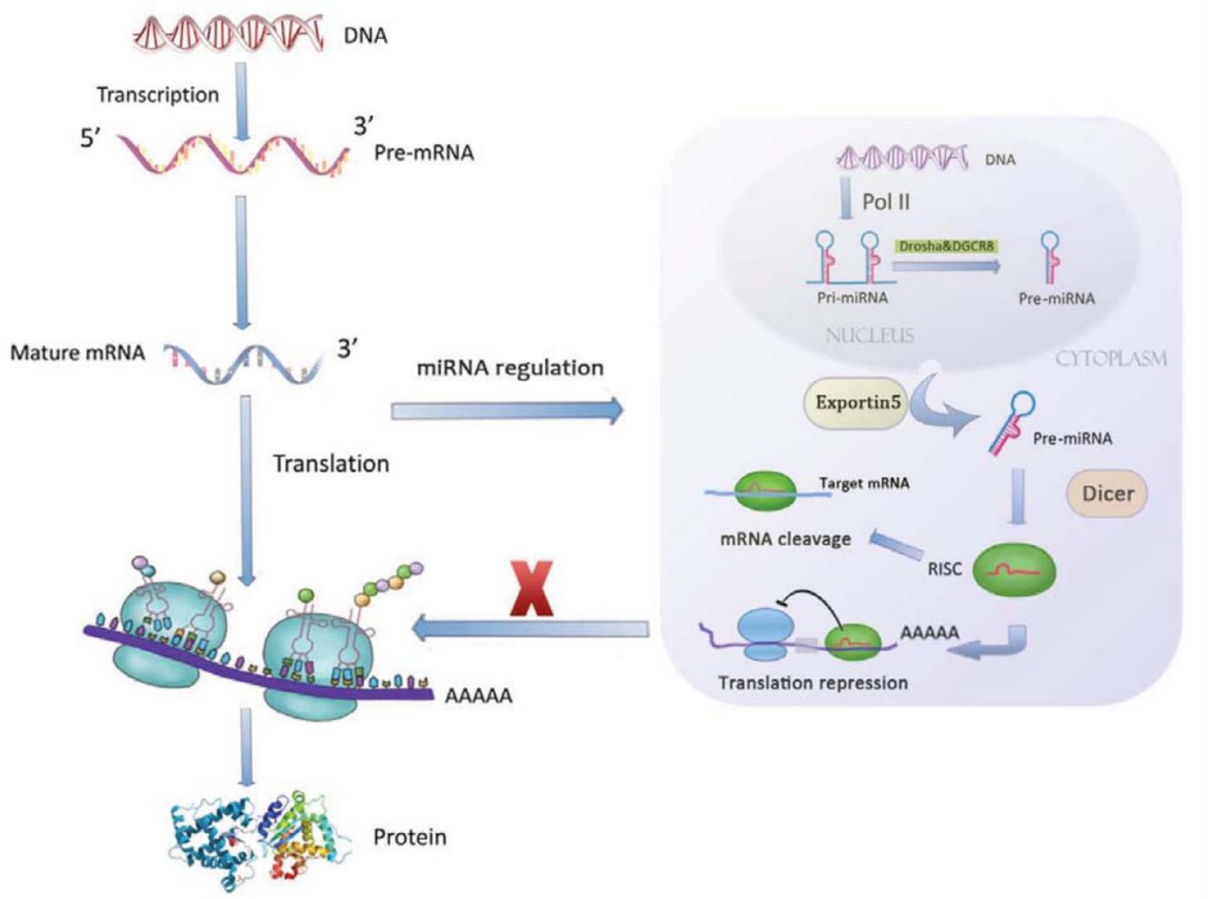

Figure 2 - Model for microRNA biogenesis and activity. MicroRNAs are transcribed by polymerase pol II to the long pri-miRNA transcript. Nuclear RNAse III Drosha cleaves the pri-miRNA to the 60-80 kDa pre-miRNA precursor. The pre-miRNA is exported to the cytoplasm by Exportin 5. Cytoplasmatic RNAse III Dicer further processes the pre-miRNA to the final mature miRNA. The mature miRNA is introduced into the effector complex RISC. The miRNA-RISC assembly (miRISC) is able to bind mRNA. Binding of miRNA to the mRNA leads to either cleavage (sufficient complementarity) or translational repression of the mRNA and subsequently to less functional protein. For details see text (1.5); modified from Chen *et al.* (2014) [206].

The microRNA effects can further be enhanced or reduced by feed-forward or feedback loops [207] of microRNA actions as well as by synergistically acting microRNAs [208-210]. Furthermore, microRNAs can be transported through the circulation and influence regulatory processes in peripheral organs and target cells [211-213]. Circulating microRNAs can also be

associated to obesity [214, 215], type 2 diabetes mellitus [216, 217] and the metabolic syndrome [218, 219]. Hence, microRNAs started to come into focus for disease treatment strategies, either as a biomarker [220-222] or as part of a treatment strategy using antagomirs that inhibit target microRNA [223-226].

Thus, microRNAs can regulate diverse biological processes in health and disease, e.g. developmental timing, apoptosis, cell proliferation and cell differentiation. As the studies of circulating microRNA in obesity already indicate, microRNAs were found to play a role in fat cell metabolism and adipogenesis.

1.5.1 MicroRNAs in adipogenesis

Knowledge is increasing that microRNAs regulate diverse biological processes including fat cell metabolism and adipogenesis [227-234]. In hMSCs it was shown that adipocyte differentiation is inhibited when microRNA biogenesis enzymes like Dicer and Drosha are inhibited, indicating a role for microRNAs early in adipogenesis [235]. Most studies focused on individual microRNAs and showed that microRNAs regulate adipocyte differentiation by modulating signaling pathways in different stages of adipogenesis. Thus, microRNAs were identified playing a role in the lineage commitment of MSCs. Commitment to preadipocytes, for example, is supported by miR-17 and miR-106a by targeting BMP2 [236] and miR-204 and miR-211 by targeting RUNX2 [237]. In contrast, miR-27a seems to promote osteogenesis rather than adipogenesis [238]. Also clonal expansion of preadipocytes appears to be in part regulated by microRNAs. Thus, the miR-17-92 cluster promotes clonal expansion by targeting retinoblastoma-like 2 [239]. In contrast, targeting of E3F3 by miR-363 leads to an inhibition of clonal expansion and impaired adipocyte differentiation [240]. During the termination phase from preadipocytes to mature adipocytes, microRNAs are described to exert anti-adipogenic as well as pro-adipogenic properties. Hence, miR-31 expression leads to a downregulation of C/EBPα (see 1.4.2.2) thereby inhibiting adipogenesis [241, 242]. Furthermore, the master regulator of adipogenesis, PPARγ (see 1.4.2.3), is a direct target of miR-27a/b [243-245] and miR-130 [246] leading to impaired adipocyte differentiation. Also the important transcription factors cAMP response element-binding protein (CREB) and C/EBPβ (see 1.4.2.2) are targets of miR-155 [247]. In contrast, miR-375 seems to act pro-adipogenic by modulating the ERK-PPARγ-AFABP pathway [248]. By targeting TGF-β receptor 2 (TGFBR2), which is involved in anti-adipogenic TGF-β signaling, miR-21 promotes adipogenesis [249].

But not only adipogenesis processes are targeted by microRNAs. Also adipocyte key functions can be influenced by microRNA expression. Thus, miR-224-5p was found to regulate fatty acid metabolism by targeting acyl-CoA synthetase long chain family member 4 [250]. In addition, A-FABP targeted by miR-369 leads to a disruption in fatty acid trafficking [251]. Also glucose uptake and insulin sensitivity can be affected by microRNA function [252-254]. Moreover, miR-378 was described in two independent studies to exert lipolytic and lipogenic properties [255, 256]. These studies indicate that microRNAs can influence adipogenesis not only on a developmental but also on a functional level in mature adipocytes.

In addition, there is good evidence that microRNAs act in a fat depot-specific manner. MiR-146b positively affects adipogenesis by inhibiting the proliferation in human visceral preadipocytes targeting Kruppel-like factor 7 (KLF7) mRNA [257]. MiR-378 [258, 259] and miR-365 [260, 261] specifically interact in BAT formation.

Thus, there are multiple examples for a specific involvement of individual microRNAs in adipogenesis but most studies focus on the impact of single microRNAs in circumscriptive human or animal cell culture models. Whether specific microRNAs play a general role in the regulation of WAT differentiation independent of the species and the fat depot localization is currently elusive.

2 Aim of the study

WAT may expand under a nutritional challenge by hypertrophy and/or hyperplasia. This appears to be differently regulated in the different WAT depots located either in the visceral or in the subcutaneous compartment. However, currently the underlying mechanisms governing general vs. differential regulation of the various WAT depots are far from clear even though a number of key genes involved in the differentiation and proliferation from preadipocytes to mature fat cells have been described.

MicroRNAs are new and promising players important in adipogenesis. Therefore, the aim of the present study was to systematically search for fat depot-specific and general microRNAs acting as regulators of adipogenesis in both visceral and subcutaneous WAT. For this, an unsupervised microRNA array approach was used to identify differently expressed microRNAs between preadipocytes and mature adipocytes not only in mouse but as well in human *ex vivo* visceral and subcutaneous WAT samples. Candidate microRNAs expression was validated in respective cell culture models. Subsequently the functional impact on adipogenesis was tested for selected microRNA candidates by a loss-of-function approach (Figure 3).

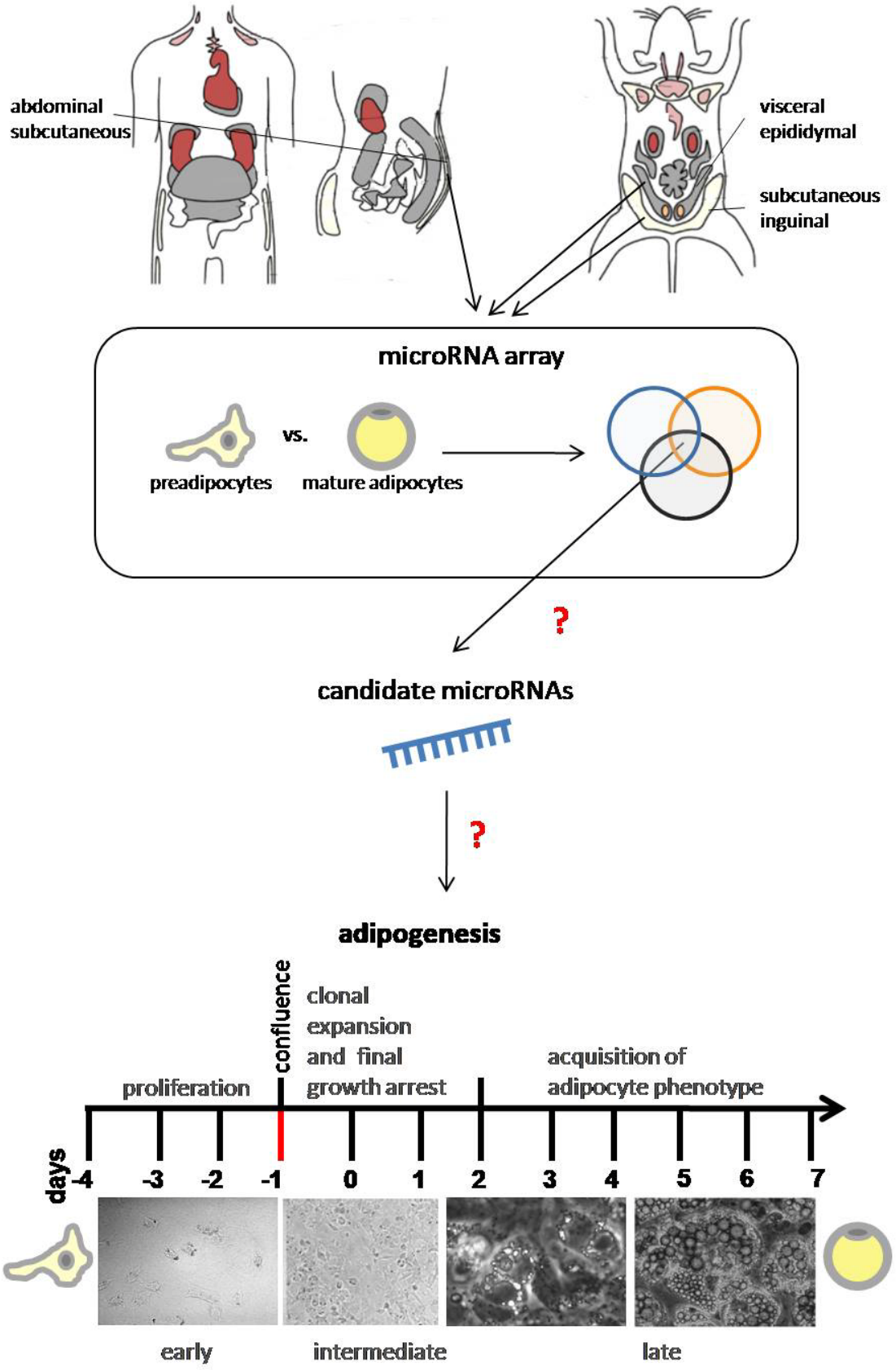

Figure 3 - Schematically depicted aim of the study and overview about key experimental approaches to answer the underlying question. Human and mouse fat distribution modified from Choe *et al.* 2016 [262].

3 Materials and Methods

3.1 Materials

3.1.1 Chemicals

Sigama Aldrich, Steinheim, Germany

Sodium chloride (NaCl), glycerin, sodium dodecyl sulfate (SDS), Tween 20, glycerol, bromphenol blue, NP-40, Na-Deoxycholat, ethylenediaminetetraacetic acid (EDTA), sodium orthovarnadate (Na_3VO_4), sodium fluoride (NaF), phenylmethylsulfonyl fluoride (PMSF), triiodothyronine (T_3), insulin, indomethacine, dexamethasone, bicinchoninic acid (BCA) solution, rosiglitazone, transferrin, fibroblast growth factor 2 (FGF2), ammonium persulfate (APS), N,N,N′,N′-Tetramethylethane-1,2-diamine (TEMED), β-mercaptoethanol, Oil Red O, formalin, Free Glycerol Reagent, Glycerol Standard Solution, Triton-X-100, sodium bicarbonate ($NaHCO_3$), biotin, D-panthithenate, toluene, PPO (2,5-Diphenyloxazole), POPOP (1,4-bis(5-phenyloxazol-2-yl) benzene).

Merck, Darmstadt, Germany

Porassium chloride (KCl), calcium chloride ($CaCl_2*2H_2O$), hydrogen chloride (HCl), monopotassium phosphate (KH_2PO_4), di-sodium hydrogen phosphate ($Na_2HPO_4*2\ H_2O$), ammonium cholride (NH_4Cl), potassium hydrogen carbonat ($KHCO_3$), ascorbic acid, copper(II)sulfate ($CuSO_4$), sodium azide (NaN_3).

Roth, Karlsruhe, Germany

Glucose, methanol, skim milk, isopropanol, hemalum solution, ethanol.

Biomol, Hamburg, Germany

4-(2-hydroxyethyl)-1-piperazineethanesulfonic acid (HEPES), bovine serum albumin (BSA), tris, 3-isobutyl-1-methylxanthine (IBMX).

Gibco, Life Technologies, Paisley, UK

Penicillin/Streptomycin, Dulbecco's modified Eagle's medium (DMEM) high glucose, fetal bovine serum (FBS), trypsin/EDTA 1X, DPBS, DMEM (phenol-red free; 4.5 g/L glucose; + glutamine; - pyruvat), Ham´s F12, DMEM/F12 (phenol-red free).

Other companies

DMEM w/o glucose (Biochrome AG, Berlin, Germany), Clarity Max™ Western ECL reagent (Bio-Rad Laboratories GmbH, Munich, Germany), Dako REAL peroxidase blocking solution (Dako, Hamburg, Germany), goat serum (Dako, Hamburg, Germany), Dharmacon siRNA buffer 5X (Dharmacon, Lafayette, CO, USA), Optiphase HiPhase scint solution (Fisons Chemicals, Loughborough Leics, UK), FBS (for hMSCs; Hyclone, Thermo Scientific, Cramlington, UK), l-glutamine (for hMSCs; Hyclone, Thermo Scientific, Cramlington, UK), HEPES (for hMSCs; Hyclone, Thermo Scientific, Cramlington, UK), Amplex Ultra Red (Invitrogen, Eugene, Oregon), Lipofectamine 2000 (Invitrogen, Schwerte, Germany), DMEM low glucose (Lonza, Verviers, Belgium), mounting solution Medite Pertex (Medite GmbH, Burgdorf, Germany), 2-deoxy-D[^{3}H]glucose (Perkin Elmer-Cetus, Norwalk, CT USA), ^{3}H-glucose (Perkin Elmer-Cetus, Norwalk, CT USA), Qiazol Reagent (Qiagen, Hilden, Germany), cell proliferation reagent WST-1 (Roche, Mannheim, Germany), Acrylamide/Bis solution 29:1 (Serva, Heidelberg, Germany), 5X PrimeScript™ RT Master Mix (Perfect Real Time) (Takara Bio USA, Mountain View, CA, USA).

3.1.2 Consumables

Sarstedt, Nümbrecht, Germany

Biosphere Filter Tips (20 µL, 100 µL, 200 µL, 1000 µL), cell scraper, microtest plate 96-well F, PCR plate clear flat caps, PCR-Plate, 96-well, half skirt, pipette tips (10 µL, 200 µL, 1000 µL), reaction tubes (1.5 mL, 2.0 mL, 15 mL, 50 mL), save-seal reaction tube (1.5 mL, 2.0 mL), scintillation counting tubes Mini-Vial GmL, serological pipette (5 mL, 10 mL, 25 mL, 50 mL), TC dish standard (100 mm, 150 mm), TC-plate standard F (6-well, 12-well, 24-well, 96-well).

Greiner Bio-One, Kremsmünster, Austria

T175 flask, T75 flask, microplate, 96-well black, EASY strainer 100 µm

Bio-Rad Laboratories Ltd, Watford, UK

Hard Shell PCR plates 96-well clear, microseal "B" seal, Mini PROTEAN Spacer plates, Mini PROTEAN Short plates.

Other companies

Non-stick Rnase-Free Microfuge Tubes (0.5 mL, 1.5 mL) (Ambion, Thermo Fisher Scientific, Waltham, MA USA), TC-plates (12-well, 24-well, 48-well) (Costar, Thermo Fisher Scientific, Waltham, MA, USA), miRCURY LNA™ microRNA Array 7th Gen (Exiqon,Vedbeak, Denmark), Affymetrix Gene Chip Mouse Gene 1.0 ST Arrays (Thermo Fisher Scientific, Waltham, MA, USA), Immobilon-P Transfer Membrane type PVDF (Millipore, Darmstadt, Germany), coverslips 16-18 mm (Roth, Karlsruhe, Germany), microscope slide (Roth, Karlsruhe, Germany).

Kits

Amaxa Nucleofector Kit V (Lonza, Basal, Switzerland), Cell proliferation reagent WST-1 (Roche, Mannheim, Germany), EnVision+Dual link System HRP (DAB+) Kit (Dako, Hamburg, Germany), GeneChip® WT PLUS Reagent Kit (Thermo Fisher Scientific, Waltham, MA USA), MemCode Reversible Protein Stain Kit (Thermo Fisher Scientific, Waltham, MA USA), miRCURY LNA™ microRNA Hi-Power Labeling Kit, Hy3™/Hy5™ (Exiqon, Vedbeak, Denmark), miRCURY LNA™ Universal RT microRNA PCR Universal cDNA Synthesis Kit II (Exiqon, Vedbeak, Denmark), Neon™ Transfection System 100µL Kit (Thermo Fisher Scientific, Waltham, MA, USA), NucleoSpin miRNA kit (Macherey-Nagel, Düren, Germany), TGX Stain-free FastCast acrylamide gel system (Bio-Rad Laboratories GmbH, Munich, Germany).

Enzymes

Collagenase A(Roche, Mannheim, Germany), cOmplete ULTRA Tablets Mini EASYpack (Roche, Mannheim, Germany), miRCURY LNA™ Universal RT microRNA PCR ExiLENT SYBR® Green master mix (Exiqon, Vedbeak, Denmark), 2X SYBR® Premix Ex Taq™ (Tli RNaseH Plus) and 5X PrimeScript™ RT Master Mix (Perfect Real Time) (Takara Bio USA, Mountain View, CA, USA).

Standards

PageRuler Plus Prestained Protein Ladder (Thermo Fisher Scientific, Waltham, MA, USA)

3.1.3 Devices

Centrifuges

Eppendorf 5810R, Eppendorf 5424 and miniSpin Plus (Eppendorf GmbH, Hamburg, Germany), Biofuge primo, Multifuge 3 S-R and Biofuge fresco (Heraeus Holding GmbH, Hanau, Germany), Mikro 2.2 R (Hettich Zentrifugen, Tuttlingen, Germany).

Weighing balances

Mettler AJ100 (Mettler-Toledo GmbH, Gießen, Germany), Kern 440-47N (Kern & Sohn GmbH, Balingen-Frommern, Germany), Atilon (Acculab GmbH, Göttingen, Germany).

Microscopes

Evos Auto FL (Thermo Fisher Scientific, Waltham, MA, USA), Nikon TMS and Nikon ECLIPSE TE300 (Nikon, Amsterdam, Netherlands), Axiovert 40 CFL (Zeiss, Jena, Germany).

Refrigerator, freezer and cryo tank

Liebherr 4 °C and -20 °C (Liebherr GmbH, Biberach an der Riß, Germany), Locator JR cryo tank, Hera freeze (-80°C) and Hera freeze HFU B Series (-80°C) (Thermo Fisher Scientific, Waltham, MA, USA).

Clean bench

Holten LaminAir and Safe 2020 (Thermo Fisher Scientific, Waltham, MA, USA), ScanLaf Mars Safty Class 2 (LaboGene ApS, Lynge, Denmark).

Incubators

Forma Steri-Cycle CO2 Incubator (Thermo Fisher Scientific, Waltham, MA, USA), Hera Cell (Heraeus Holding GmbH, Hanau, Germany).

Thermal cyclers

Cyclone gradient (Peqlab, Erlangen, Germany), Thermal cycler PTC-100 (MJ Research Inc., St. Bruno, Canada), realplex2 mastercycler epgradient S (Eppendorf GmbH, Hamburg), Germany), C1000Touch Thermal Cycler with CFX96 Real-Time system (Bio-Rad Laboratories GmbH, Munich, Germany).

Spectrophotometer

Nanodrop ND-1000, ND-2000 and ND-8000 Spectrophotometer (Thermo Fisher Scientific, Waltham, MA, USA), SPECTROstar Nano (BMG Labtech GmbH, Ortenberg, Germany), Tecan Infinite M200 (Tecan, Groedig, Austria).

Western blot devices

Mini PROTEAN electrophoresis/blotting chamber and Mini PROTEAN gel casting stands (Bio-Rad Laboratories GmbH, Munich, Germany), ChemiDocTMTouch Imaging System (Bio-Rad Laboratories GmbH, Munich, Germany), Sonorex Ultrasound (Bandelin, Berlin, Germany), Power supply Power Pack P25 T(Biometra GmbH, Göttingen, Germany), RCT basic safety control magnetic stirrer (IKA-Werke GmbH, Staufen, Germany), Thermomixer compact (Eppendorf GmbH, Hamburg, Germany).

Other devices

Tecan HS4800™ hybridization station (Tecan, Groedig, Austria), Agilent G2565BA Microarray Scanner System and Agilent 2100 Bioanalyzer (Agilent Technologies, Santa Clara, CA, USA), Amaxa Nucleofector 2b Device (Lonza, Basal, Switzerland), Neon™ Transfection System (Thermo Fisher Scientific, Waltham, MA, USA), CanonScan 4400F scanner (Canon, Hamburg, Germany), β-counter LS6500 (Beckman Coulter Inc, Fullerton, CA USA), Vortex Genie 2 (Scientific Industries Inc, Bohemia, NY, USA),

pH meter PB-11 (Sartorius AG, Göttingen, Germany), Pipettes – Research (Eppendorf GmbH, Hamburg, Germany), Pipetus red dot (Hirschmann Laborgeräte, Eberstadt, Germany), Scala fume hood (Waldner, Wangen, Germany), water bath OLS 200 (Grant Instruments, Cambridge, UK), VX-65 autoclave (Systec GmbH, Linden, Germany).

3.1.4 Antibodies

Primary antibodies:

Target	**Dilution**	**Species**	**for**	**Cat.-No.**	**Company**
C/EBP-β	1:1000	rabbit	WB	sc-150	Santa Cruz, Heidelberg, Germany
PREF-1	1:1000	rabbit	WB	AB3511	Chemicon, Darmstadt, Germany
A-FABP	1:5000	goat	WB	sc-18661	Santa Cruz, Heidelberg, Germany
AR	1:1000	rabbit	WB	sc-816	Santa Cruz, Heidelberg, Germany
AR	1:100	rabbit	ICC	DLN-12143	Dianova GmbH, Hamburg, Germany
Lamin A	1:100	rabbit	ICC	sc-20680	Santa Cruz, Heidelberg, Germany

Secondary antibodies:

Species	**Dilution**	**Company**
Polyclonal Goat Anti-Rabbit Immunglobulin HRP	1:10000	Dako, Hamburg, Germany
Polyclonal Goat Anti-Mouse Immunglobulin HRP	1:10000	Dako, Hamburg, Germany
Polyclonal Rabbit Anti-Goat Immunglobulin HRP	1:10000	Dako, Hamburg, Germany

3.1.5 Primers and Inhibitors

Gene primer

All primers were synthesized by Biometra (Göttingen, Germany).

Name	**Sequence**
HPRT (mouse)	CACAGGACTAGAACACCTGC *(forward)* GTTGGATACAGGCCAGACTTTGT *(reverse)*
HPRT (human)	GAAAAGGACCCCACGAAGTGT *(forward)* TGGCGATGTCAATAGGACTCC *(reverse)*
Adiponectin (mouse)	CTTAATCCTGCCCAGTCATGC *(forward)* CCATCCAACCTGCACAAGTTC *(reverse)*
Adiponectin (human)	AAGGACAAGGCTATGCTCTTC *(forward)* TGAGTTAGTGGTGATCAGTTGG *(reverse)*
Leptin (mouse)	GTG CCT ATC CAG AAA GTC CAG GAT G *(forward)* CTG GTG AGG ACC TGT TGA TAG AC *(reverse)*
Leptin (human)	CCAAGCAAGGCCAAAATTACC *(forward)* CCACCCACTGTGTGTGATAGCAA *(reverse)*
IL-6 (mouse)	AGCCAGAGTCCTTCAGA *(forward)* GGTCCTTAGCCACTCCT *(reverse)*
IL-6 (human)	CAATAACCACCCCTGACCCAA *(forward)* TGACCAGAAGAAGGAATGCCC *(reverse)*

MicroRNA primer

All primers are miRCURY LNA™ Universal RT microRNA PCR LNA™ PCR primer sets (Exiqon, Vedbeak, Denmark).

Name	**Sequence**
hsa-let-7e-5p	5’-UGAGGUAGGAGGUUGUAUAGUU-3’
hsa-miR-142-3p	5’-UGUAGUGUUUCCUACUUUAUGGA-3’
hsa-miR-146b-5p	5’-UGAGAACUGAAUUCCAUAGGCU-3’
hsa-miR-191-5p	5’-CAACGGAAUCCCAAAAGCAGCUG-3’
hsa-miR-193a-5p	5’-AACUGGCCUACAAAGUCCCAGU-3’
hsa-miR-223-3p	5’-UGUCAGUUUGUCAAAUACCCCA-3’
hsa-miR-365a-3p	5’-UAAUGCCCCUAAAAAUCCUUAU-3’
hsa-miR-378a-3p	5’-ACUGGACUUGGAGUCAGAAGGC-3’
mmu-miR-378a-3p	5’-ACUGGACUUGGAGUCAGAAGG-3’
hsa-miR-708-5p	5’-AAGGAGCUUACAAUCUAGCUGGG-3’

Inhibitors

Name	Sequence	Company
miRIDIAN microRNA Hairpin Inhibitor Negative Control #1	UCACAACCUCCUAGAAAGAGUAGA	Dharmacon, Lafayette, CO USA
miRIDIAN microRNA Human hsa-miR-708-5p inhibitor	AAGGAGCUUACAAUCUAGCUGGG	Dharmacon, Lafayette, CO USA
miRCURY LNA Power Inhibitor Negative Control A	TAACACGTCTATACGCCCA	Exiqon, Vedbeak, Denmark
miRCURY LNA Power Inhibitor hsa-miR-708-5p	CCAGCTAGATTGTAAGCTCCT	Exiqon, Vedbeak, Denmark
miRCURY LNA Power Inhibitor hsa-miR-193a-3p	TGGGACTTTGTAGGCCAGT	Exiqon, Vedbeak, Denmark

3.1.6 Software

ImaGene® 9 miRCURY LNA™ microRNA Array Analysis Software (Exiqon, Vedbeak, Denmark), ImageLab Version 5.2.1 software (Bio-Rad Laboratories GmbH, Munich, Germany), web tool "miRWalk", web tool "WebGestalt", GraphPad Prism 5 software (GraphPad Software, Inc., La Jolla, CA, USA), Microsoft Excel (Microsoft Corporation, Redmond, WA USA), Rosetta Resolver® software system (Rosetta Bio software, Seattle, WA, USA).

3.2 Methods

3.2.1 Ethics

All animal procedures were approved by the Ministerium für Energiewende, Landwirtschaft, Umwelt, Natur und Digitalisierung (University of Luebeck) and according to their forms and regulations. Mice were housed in the animal facility of the University of Luebeck at 22°C with a day and night cycle of 12 hours. The human studies were approved by the Regional Ethics committee at Huddinge University Hospital and by the Regional Ethics committee of the University of Luebeck. A written informed consent was obtained from all donors.

3.2.2 *Ex vivo* fat cell isolation and erythrocyte lysis

Epididymal and inguinal WAT depots were taken from C57BL/6J male mice and human abdominal subcutaneous WAT from one female and one male participant (62 ±9 years old). To separate the stroma-vascular fraction (containing the preadipocytes) from mature adipocytes, adipose tissues were directly digested with 1 mg collagenase A per 1 mL isolation buffer for 45 min at 37 °C and then filtered through a 100 µm nylon mesh. As a first step mature adipocytes were allowed to separate from the stroma-vascular cells by floating to the surface due to their fat content. Hence mature adipocytes were collected from the surface and transferred to another tube. They were washed once with isolation buffer and centrifuged at 200g for 5 min. The isolation buffer was removed and mature adipocytes were resuspended in 800 µL QIAzol reagent for RNA isolation (see 3.2.12.1). The stroma-vascular cells were collected by centrifugation for 5 min at 200g. The pellet was washed once with isolation buffer and after another centrifugation step the isolation buffer was removed. To remove the erythrocytes, the pellet was resuspended in 5-10 mL erythrocyte lysis buffer, incubated for 10 min at room temperature (RT) and then centrifuged for 5 min at 200g. The erythrocyte lysis buffer was removed and cells were washed once again with isolation buffer before the

preadipocyte pellet was resuspended in 800 µL QIAzol reagent for RNA isolation (see 3.2.12.1).

Isolation Buffer	
NaCl	123 mM
KCl	5 mM
$CaCl_2$*2 H_2O	1.3 mM
Glucose	5 mM
HEPES	100 mM
Pen/Strep	100 U/mL
BSA	4% (w/v)
in VE-H_2O	
sterile filtered	

Erythrocyte Lysis Buffer	
NH_4Cl	154 mM
$KHCO_3$	10 mM
EDTA	0.1 mM
in VE-H_2O	

3.2.3 MicroRNA Array

All microRNA array experiments were conducted at Exiqon Services, Vedbeak, Denmark. The quality of the total RNA was verified by an Agilent 2100 Bioanalyzer profile. 250 ng (human) and 400 ng (mouse) total RNA from *ex vivo* samples (preadipocytes and mature adipocytes) and reference was labeled with Hy3™ and Hy5™ fluorescent label, respectively, using the miRCURY LNA™ microRNA Hi-Power Labeling Kit, Hy3™/Hy5™ following the procedure described by the manufacturer. The Hy3™-labeled samples and a Hy5™-labeled reference RNA sample were mixed pair-wise and hybridized to the miRCURY LNA™ microRNA Array 7th Gen, which contains capture probes targeting all microRNAs for human, mouse or rat registered in the miRBASE 18.0. The hybridization was performed according to the miRCURY LNA™ microRNA Array Instruction manual using a Tecan HS4800™ hybridization station. After hybridization the microarray slides were scanned and stored in an ozone free environment (ozone level below 2.0 ppb) in order to prevent potential bleaching of the fluorescent dyes. The miRCURY LNA™ microRNA Array slides were scanned using the Agilent G2565BA Microarray Scanner System (Agilent Technologies, Inc., USA) and the image analysis was carried out using the ImaGene® 9 miRCURY LNA™

microRNA Array Analysis Software. The quantified signals were background corrected (Normexp with offset value 10, [263]) and normalized using the global LOcally WEighted Scatterplot Smoothing (Lowess) regression algorithm. Differently expressed microRNAs between preadipocytes and mature adipocytes with fold change ±2 were considered for further analysis.

3.2.4 Cell culture

All cell culture experiments were conducted under sterile conditions. All necessary consumables, buffers, solutions and media were sterilized by filtration or autoclaving. All media were warmed up to 37°C in a water bath before usage. All cells were cultured in incubators at 37°C and 5% CO_2.

3.2.4.1 Mouse EPI and ING cell lines

Immortalized cells from the epididymal (EPI) and inguinal (ING) WAT from male C57BL/6J wild type mice were generated as described previously [264], kindly provided by Prof. Klein (University of Luebeck, Germany) and used for murine cell culture experiments.

Preadipocytes that should be passaged but not differentiated were cultured in basic medium in 150 mm dishes. To maintain their differentiation potential, preadipocytes were only allowed to reach 70-80% confluence to avoid cell accumulation because this can lead to spontaneous fat incorporation which might lead to a loss of proliferation and differentiation capacity.

For controlled differentiation, preadipocytes were seeded to 100 mm dishes or well-plates of different sizes depending on the experimental set up. Therefore, the 150 mm dishes were washed twice with DPBS before trypsination with trypsin/EDTA for 3 min at 37°C. Detached cells were resuspended in basic medium whereby 1/10 of the cell suspension remained on the 150 mm dish for further cultivation of preadipocytes. The remaining cell suspension was equally distributed to the 100 mm dishes or well-plates and cells were cultured in differentiation medium (mDM) until 100% confluence. Confluent cells (day -1) were induced to differentiate with induction medium containing dexamethasone, indomethacine and IBMX for 24 hours. These additives are important to switch the cell status from proliferation towards differentiation. Following induction (day 0), cells were further differentiated in mDM and lipid droplet formation was microscopically controlled. After 6-7 days cells were fully differentiated to mature adipocytes. The medium needed to be changed ever 1-2 days due to the increasing metabolism of the differentiating cells.

Basic Medium (mouse)	
FBS	20% (v/v)
Penicillin	100 U/mL
Streptomycin	100 µg/mL
in DMEM	
(4.5 g/L glucose; + glutamine; - pyruvat)	

Differentiation Medium (mDM) (mouse)	
FBS	20% (v/v)
T3	1 nM
Insulin	20 nM
in DMEM	
(4.5 g/L glucose; + glutamine; - pyruvat)	

Induction Medium (IM) (mouse)	
Isobutylmethylxanthine	500 µM
Indomethacine	250 µM
Dexamethasone	2 µg/mL
in Differentiation Medium	

3.2.4.2 Human mesenchymal stem cells (hMSCs)

Human cell culture experiments were performed with hMSCs isolated from male subcutaneous WAT (16 years old, BMI 24 kg/m^2) as described before [265] and kindly provided by Prof. Mikeal Rydén and Prof. Peter Arner (Unit of Endocrinology and Diabetes at the Karolinska University Hospital, Stockholm, Sweden). Furthermore, all hMSC cell culture experiments were conducted at their lab during my research stay.

Cells that should be passaged but not differentiated were cultured in proliferation medium (PM) in T175 flasks. To maintain their differentiation potential cells were only allowed to reach 80-90% confluence to avoid cell accumulation because this can lead to spontaneous fat incorporation which might lead to a loss of proliferation and differentiation capacity.

For controlled differentiation, cells were seeded to T175, T75 flasks or well-plates of different sizes depending on the later experimental set up. Therefore, the T175 flasks were washed once with PBS before trypsination with 4 mL trypsin/EDTA for 3 min at 37°C. Detached cells were resuspended in 8 mL PM and transferred to a 50 mL tube. The flask was rinsed with another 10 mL PM which was added to the same tube afterwards. Cells were centrifuged at 200 g for 10 min. Supernatant was removed and the pellet resuspended in 1 mL PM

(for 1 T175 flask). Cells were counted in a Bürker cell counting chamber by counting four large squares. Cell number was calculated as followed: $Cells_{total}$= $Mean_{(cells/large\ square)}$ x $10_{(dilution)}$ x $10.000_{(chamber\ factor)}$ x mL $PM_{(used/flask)}$ followed by $v_{condition}$=($Cells_{required}$/$Cells_{total}$) x mL $PM_{(used/flask)}$. For further hMSC cultivation in T175 flask, 750.000 cells were returned. For controlled differentiation the remaining cells were equally distributed to the T175, T75 flask or well-plates with defined cell numbers (see below) and cultured in PM for three days until 100% confluence. Then fibroblast growth factor 2 (FGF2) was removed from the PM and cells were incubated without FGF2 for 24 hours. Following this cells were washed twice with PBS and the differentiation medium (hDM) was added (day d-3). The additives (IBMX, dexamethasone, rosiglitazone) are important to switch the cell status from proliferation towards differentiation signals and by this promoting the incorporation of lipids into the lipid droplets. After 3 days IBMX and dexamethasone were removed (=day 0), after 10 days rosiglitazone was removed (day 7). After 10 days cells were fully differentiated. The medium was changed every 2-3 days.

Proliferation Medium (PM) (human)	
FBS (heat-inactivated)	10% (v/v)
L-Glutamine	2 mM
HEPES buffer	0.5 M
Penicillin	50 U/mL
Streptomycin	50 mg/mL
FGF2	2.5 ng/mL
in DMEM	
(- glucose; - glutamine; - pyruvat)	

Differentiation Medium (hDM) (human)	
Proliferation medium	1 part
(*without FBS and FGF)*	
Ham´s F12	1 part
> mix the 2 media 50/50	
Insulin	860 nM
T3	0.2 nM
Transferrin	10 µg/mL
Rosiglitazone *(until d7)*	1 µM
IBMX *(d-3 – d0)*	100 µM
Dexamethasone *(d-3 – d0)*	1 µM

Cell numbers for hMSC differentiation

T175 flask:	T75 flask:	6-well plate:	12-well plate:	24-well plate:	48-well plate:
3.5×10^6 cells	1.5×10^6 cells	500.000 cells/well	250.000 cells/well	125.000 cells/well	65.000 cells/well

3.2.5 DHT stimulation

The 5α-dihydrotestosterone (DHT) was kindly provided by Dr. Ralf Werner (Department of Paediatric and Adolescent Medicine, University of Luebeck, Germany). All DHT stimulation studies were performed with a final DHT concentration of 10 nM. As control ethanol (EtOH) was used in equal volume. For chronic DHT stimulation studies medium was changed every day in the mouse cell lines, every second day in the hMSCs. For acute DHT stimulation studies cells were stimulated for 1 hour and 8 hours with 10 nM DHT.

3.2.6 Transfection

3.2.6.1 Lipofectamine reverse transfection (for mouse EPI and ING cell lines)

All steps of transfection were performed under sterile conditions. Cells were seeded in 100 mm dishes and were allowed to grow to 90-100% confluence. At day of transfection (day -2, which is one day before induction of differentiation) cells were washed twice with PBS and trypzinised with 1 mL trypsin/EDTA for 3 min at 37 °C. Detached cells were resuspended in 5 mL differentiation medium (mDM), transferred to a 50 mL tube and centrifuged at 200 g for 10 min. Supernatant was removed and the pellet resuspended in 1 mL mDM (per 100 mm dish). Cells were counted in a Neubauer cell counting chamber by counting four large squares. Cell number was calculated as followed: $Cells_{total} = Mean_{(cells/large\ square)} \times 10_{(dilution)} \times 10.000_{(chamber\ factor)} \times mL\ mDM_{(used/dish)}$ followed by $v_{condition} = (Cells_{required}/Cells_{total}) \times mL\ mDM_{(used/dish)}$. Subsequently a cell suspension with $2.5\text{-}3.0 * 10^5$ cells/well was prepared in serum-free DMEM to ensure a confluent cell layer after 24 hours. Meanwhile the transfection solution with 1 µL Lipofectamine2000/well and 25 pmol/well of specific miRCURY LNA Power Inhibitor or scrambled negative control (NC) was prepared according to the manufactures instructions.

Culture vessel	Vol. of plating medium	Vol. of dilution medium	RNA (Inhibitors)	Lipofectamine 2000
24-well	500 µL	2x 50µL	25 pmol	1 µL

For the reverse transfection the wells were first filled with the respective transfection solution followed by cell suspension. After 24 hours the medium was changed and the differentiation protocol was started beginning with the induction of differentiation (day -1) (see 3.2.4.1).

3.2.6.2 Electroporation: Amaxa Transfection (for mouse EPI and ING cell lines)

All steps of transfection were performed under sterile conditions. Transfection occurred with the Amaxa Nucleofector™ 2b Device and the Amaxa Nucleofector™ Kit V. According to the manufactures instructions the Nucleofector™ solution was prepared by mixing 0.5 mL Supplement-1 with 2.25 mL Nucleofector™.

Mouse cells were seeded in 100 mm dishes and were differentiated until day 3 (see 3.2.4.1). At day of transfection (day 3) cells were washed twice with PBS and trypzinised with 1 mL trypsin/EDTA for 3-4 min at 37 °C. Detached cells were resuspended in 5 mL differentiation medium (mDM), transferred to a 50 mL tube and centrifuged at 200g for 10 min. Supernatant was removed and the pellet resuspended in 1 mL PBS (per 100 mm dish). Cells were counted in a Neubauer cell counting chamber by counting four large squares. Cell number was calculated as described above (see 3.2.6.1). For transfection $1.5*10^6$ cells/cuvette were used.

The calculated cell volume was transferred to a 1.5 mL tube and ~500 µL PBS was added. Cells were centrifuged at RT for 5 min at 200g and the supernatant was just removed before transfection. For transfection the cell pellet was resuspended in 100 µL Nucleofector™ solution containing 50 pmol (for EPI cells) or 25 pmol (for ING cells) of miRCURY LNA Power Inhibitor or scrambled negative control (NC) inhibitor. 100 µL transfection solution (cells + inhibitors) was carefully transferred to the transfection cuvette to avoid air bubbles. For transfection of mature adipocytes special program recommended by the manufacturer (T-033) was used. Afterwards, cells were gently rinsed with 0.5 mL mDM, transferred to pre-warmed mDM (5.5 mL for $1.5*10^6$ cells) using the Amaxa-pipette and were allowed to rest. For seeding, cells were mixed carefully trying to avoid repeated aspiration and then seeded with 250.000 cells/well (= 1 mL/well) to a 24-well plate. Medium was changed after 24 hours and cells were used 72 hours (day 6) after transfection for experiments, e.g. lipolysis (see 3.2.7).

3.2.6.3 Electroporation: Neon™ Transfection (for hMSCs)

All steps of transfection were performed under sterile conditions and transfection occurred with the Neon™ Transfection System using the 100µL Neon™Tip with buffer E2.

The required number of hMSCs were cultivated in T175 flask and differentiated until day 5 (see 3.2.4.2) before used for transfection. At day of transfection (day 5) the T175 flasks were washed once with PBS before trypsination with 4 mL trypsin/EDTA for 3 min at 37°C. Detached cells were resuspended in 8 mL differentiation medium (hDM) and transferred to a 50 mL tube. The flask was rinsed with another 10 mL DM which was added to the same tube afterwards. Cells were centrifuged at 200g for 10 min. Supernatant was removed and the pellet resuspended in 1 mL PBS (for 1 T175 flask). Cells were counted in a Bürker cell counting chamber by counting four large squares. Cell number was calculated as described above (see 3.2.4.2). For transfection of $1*10^6$ cells/Neon™Tip$_{100µL}$ were used.

The calculated cell volume was transferred to a 15 mL tube and ~9 mL PBS was added. Cells were centrifuged at RT for 10 min at 200g, the supernatant was removed and cells were resuspended in R-Buffer provided by the Neon™ Transfection Kit. $1*10^6$ cells were suspended in 90 µL R-Buffer and 50 pmol (in 10µL) of miRIDIAN Hairpin-Inhibitor or scrambled negative control (NC) inhibitor was added and then mixed carefully. For transfection the Neon™Tube was filled with 3 mL buffer E2 and placed into the Neon™Pipette station. The Neon™Pipette with the Neon™Tip$_{100µL}$ was used to slowly aspirate the transfection solution (cells + inhibitors) to avoid air bubbles. Then the Neon™Pipette with the 100 µL sample was inserted into the Neon™Tube containing the E2-Buffer. Cells were transfected with 1300 V for 20 ms in 2 pulses. Following this, cells were transferred to the appropriate volume of pre-warmed hDM with supplements but without antibiotics. For seeding cells were mixed carefully trying to avoid repeated aspiration and then seeded as described above (see 3.2.4.2). Medium was changed after 24 hours and cells were used at day 9 or day 10 of differentiation for experiments, e.g. lipolysis (see 3.2.7), lipogenesis (see 3.2.9) and glucose uptake (see 3.2.8).

3.2.7 Lipolysis and glycerol measurement

3.2.7.1 Mouse EPI and ING cell lines

Lipolysis capacity was determined in fully differentiated cells. Cells were washed twice with DMEM (phenol-red free; 4.5 g/L glucose; + glutamine; - pyruvat) before all medium was completely removed. For stimulated lipolysis cells were treated with 200 µL/well of 500 nM

isoprenaline (ISO) in lipolysis medium (mLM) whereas plain mLM (basal) was used as control. Subsequently cells were incubated for 3 hours at 37 °C. Afterwards cells were put on ice and the conditioned mLM was collected for glycerol measurement. For normalization, cells were lysed in 75 µL/well lysis buffer (see 3.2.13.1), purified and the protein concentration determined.

The glycerol concentration in the conditioned mLM was determined in a 96well plate format. Therefore 40 µL sample or blank (plain mLM) were mixed with 60 µL Free Glycerol Reagent and 5 µL Glycerol Standard Solution (0.26 mg glycerol/mL) was mixed with 95 µL Free Glycerol Reagent. The plate was incubated for 15 min at room temperature in the dark and subsequently the optical density (OD) was measured at 540 nm wave lengths in a photometer. Total glycerol per total protein was calculated as followed:

1. cGlycerol [mg/mL] = ($OD_{sample}/OD_{standard}$)*0.26 and then divided by the dilution factor (40 µL sample/5 µL standard) > cGlycerol [mg/mL]/8

2. Glycerol concentration was converted from mg/mL to µg/mL ((cGlycerol [mg/mL]/8)*1000) which was then adjusted to the 200 µL mLM used for stimulation cGlycerol [µg/mL]*0.2 = **$cGlycerol_{total}$**

3. Total protein concentration was determined by cProtein [mg/mL]*$0.075_{(Lysis\ buffer\ used)}$ = **$cProtein_{total}$**

4. The total glycerol concentration was then normalized to the total protein concentration **$cGlycerol_{total}$ [µg]/$cProtein_{total}$ [mg]**

3.2.7.2 Human mesenchymal stem cells (hMSCs)

Lipolysis capacity was determined in fully differentiated cells (day 9). Cells were washed twice with DMEM/F12 (phenol-red free) before all medium was completely removed. For stimulated lipolysis cells were treated with 200 µL/well of 500 nM isoprenaline in lipolysis medium (hLM) whereas plain hLM (basal) was used as control. Subsequently cells were incubated for 3 hours at 37 °C. Afterwards cells were put on ice and the conditioned hLM was collected for glycerol measurement. For normalization, cells were lysed in 75 µL/well lysis buffer (see 3.2.13.1), purified and the protein concentration determined.

For the determination of the total glycerol concentration in the conditioned hLM a standard curve (300, 250, 200, 150, 100, 50, 25, 12.5, 6.25, 3.125, 1.56 and 0 [µM]) was prepared with

the Glycerol Standard Solution (0.26 mg glycerol/mL; 2823 µM). Next the Free Glyerol Reagent was diluted 1:100 with Amplex Ultra Red (AUR; 10 mM stock), e.g 990 µL FGR + 10 µL AUR, and wrapped in aluminium foil to protect the solution from light. For measurement, 20 µL/well of glycerol standard curve and conditioned hLM (sample) was filled into a black 96-well plate before 100 µL/well FGR-AUR solution was added. The plate was incubated for 15 min at room temperature in the dark and subsequently the fluorescence was measured at Extinction/Emission 530/590 nm wave length in a fluorescence reader. Total glycerol [µM] and protein [µg/mL] concentrations were calculated from their standard curves by linear regression analysis before the total glycerol concentration was then normalized to the protein concentration.

PBS (10X)	
NaCl	1,37 M
KCl	0.027 M
KH_2PO_4	0.018 M
Na_2HPO_4	0.1 M
in VE-H_2O	

Lipolysis Medium (mLM) (mouse)	
BSA	2% (w/v)
ascorbic acid	knife point
adjust to pH 7.35-7.45	
in DMEM - Phenol-red free	
(4.5 g/L glucose; - glutamine; - pyruvat)	

Lipolysis Medium (hLM) (human)	
BSA	2% (w/v)
ascorbic acid	knife point
adjust to pH 7.35-7.45	
in DMEM/F12 - Phenol-red free	

3.2.8 Glucose uptake / Insulin sensitivity

To assess the insulin sensitivity of the cells, glucose uptake was determined with non-metabolisable radioactive-labeled glucose. Here, hMSCs which were transfected at day 5 of transfection by Neon™ Transfection (see 3.2.6.3) were used and seeded into 48-well plates.

Glucose uptake was then determined at day 10 of differentiation. Prior to glucose uptake measurements, cells were starved for 24 hours with hDM without insulin. Then cells were washed 3x with 250 µL/well medium A before 125 µL/well medium B was added and cells were incubated for 3 hours at 37 °C. Subsequently cells were incubated in presence or absence (=control) of insulin. Therefore, 2.5 µL/well insulin (diluted in medium B; final concentration $1*10^{-8}$ M) were added to ½ of the wells, the plate was rocked gently and incubated for 15 min at 37 °C. Following this, 2.5 µL/well 2-deoxy-D[^{3}H]glucose (diluted 1:20 in medium B) were added to every well, gently swirled after each addition and incubated for 20 min at 37 °C. Afterwards, cells were put on ice, washed 3x with 0.5 mL cold PBS before 100 µL/well of lysis buffer containing 0.1% SDS were added for cell lysis. 10µL lysates/sample was taken to determine protein concentration for normalization (see 3.2.13.1). To measure radioactive glucose uptake, 80 µL lysates/sample, positive control (2.5 µL 2-deoxy-D[^{3}H]glucose dilution in 100 µL lysis buffer/0.1% SDS) and negative control (lysis buffer/0.1% SDS only) were transferred to scintillation tubes, 3 mL of Optiphase HiPhase scint solution were added and gently mixed before each sample was counted for 5 min in a β-counter.

Medium A (glucose uptake & lipogenesis)

DMEM w/o glucose

Medium B (glucose uptake)

Medium A	1 part
Ham´s F12	1 part
> mix the 2 media 1:1	
add to 1 litre: *adjust to final pH 7.4*	
$NaHCO_3$	2.4 g
Biotin	16 mg
D-panthithenate	8 mg
HEPES	7.14 g

3.2.9 Lipogenesis

To assess the lipogenesis capacity of the cells, formation of triglycerides was determined with radioactive-labeled glucose. Therefore, hMSCs which were transfected at day 5 of

transfection by Neon™ Transfection (see 3.2.6.3) were used and seeded into 48-well plates. Lipogenesis was then determined at day 10 of differentiation. Prior to lipogenesis determination, cells were starved for 24 hours with hDM without insulin. Then cells were washed 3x with 250 µL/well medium A (see 3.2.8) before 250 µL/well medium C was added and cells were incubated for 3 hours at 37 °C. Meanwhile insulin was diluted in medium D to $1*10^{-7}$ M final concentration = medium D+Ins). Following the 3 hours incubation, 125 µL/well of either medium D+Ins or medim D only (=control) were added each to ½ of the wells, the plate was rocked gently and incubated for 120 min at 37 °C. Following this, cells were put on ice, washed 3x with 0.5 mL cold PBS before 100 µL/well of lysis buffer containing 0.1% SDS were added for cell lysis. 10µL lysates/sample was taken to determine protein concentration for normalization (see 3.2.13.1). To determine the incorporation of radioactive glucose 80 µL lysates/sample, positive control (2.5 µL ^{3}H-glucose diluted in 100 µL lysis buffer/0.1% SDS) and negative control (lysis buffer/0.1% SDS only) were transferred to scintillation tubes. 4 mL of Optiphase HiPhase scint solution was added to the controls and 4 mL Toluene containing scintillation liquid was added to the samples. They were mixed gently and allowed to rest over night for phase separation before each sample was counted for 5 min in a β-counter.

Medium C (lipogenesis)		**Medium D** (lipogenesis)		**Toluene containing scintillation liquid**	
Glucose	1 µM	Medium C	1 mL	PPO	12.5 g
in DMEM w/o glucose		^{3}H-glucose	1 µL	POPOP	0.75 g
				in Toluene	2.5 L

3.2.10 Cell proliferation assay (WST-1 assay)

Preadipocytes were seeded at a density of $1*10^{4}$ cells/well into 4x 96-well plates, to follow proliferation of preadipocytes over 4 days. Treatment with 10 nM DHT or equal volume EtOH (control) was started immediately after seeding and refreshed every 24 hours. Cells were cultured in 100 µL/well mDM. Cell proliferation rate was determined at 24, 48, 72 and 96 hours after seeding according to the manufactures instructions by adding 10 µL cell

proliferation reagent WST-1 (final dilution 1:10). After 1 hour OD was measured at 450 nm wave lengths in a photometer.

3.2.11 Immunocytochemistry

Immunocytochemistry (ICC) is a technique to visualize the location of a protein of interest within cells. Therefore a primary antibody is used which binds specifically to the target protein. The primary antibody can then be detected by a horseradish peroxidase (HRP)-labeled secondary antibody. The target protein is then indirectly visualized when the peroxidase substrate 3,3'-Diaminobenzidine (DAB) is added. The oxidation of DAB will lead to a brown appearance of the target protein. By this also the sub-cellular localization (nucleus or cytoplasm) of the target protein can be detected.

Preadipocytes were seeded at a density of $2*10^4$ cells/well into 12-well plates, each well equipped with coverslips. Mature adipocytes were differentiated in 6-well plates until day 5 of differentiation, washed twice with PBS and trypzinised with 0.5 mL trypsin/EDTA for 3 min at 37 °C. Detached cells were resuspended in 2 mL differentiation medium (mDM), transferred to a 50 mL tube and centrifuged at 200 g for 10 min. Cells were counted and seeded at a density of $4*10^4$ cells/well into 12-well plates containing coverslips. Cells (preadipocytes and mature adipocytes) were allowed to attach to the coverslips for 24 hours before treating cell with 10 nM DHT or equal volume EtOH (control) for 24 hours. After 24 hours cells were washed twice with PBS and then fixed with 10% formalin. Fixed cells were stored at 4 °C until immunocytochemical staining.

For immunocytochemical staining, cells were washed once with PBS and then incubated for 10 min at RT with 0.2% Triton-X-100 in PBS to permeabilize the nucleus for antibody staining. Following this, cells were blocked for 15 min at RT with peroxidase blocking followed by 60 min blocking with blocking solution containing goat serum at RT. Subsequently cells were probed with first antibody to androgen receptor, lamin A (positive control) or without antibody (negative control) in a wet chamber at 4 °C over night. Afterwards cells were washed 3x with PBS containing 0.05% Tween 20 before incubated with the secondary antibody (EnVision+Dual link System HRP (DAB+) Kit) for 3 min at RT in a wet chamber. Hence, cells were washed 3x with PBS/0.05% Tween 20 followed by 2x washing with PBS. In a wet chamber specific antibody binding was stained with DAB+ (EnVision+Dual link System HRP (DAB+) Kit) for 10 min at RT. The surplus DAB+ was removed by washing cells 2x with VE-H_2O before cells were counter stained with hemalum solution for 10 min at RT. Surplus hemalum solution was removed by washing cells several

times with tap water followed by 2x washing with VE-H_2O. Before mounting cells were quickly dehydrated with increasing alcohol concentrations (75%-90%-100%). Pictures of stained cells were taken with EVOS Auto FL microscope. For quantification only cells with positive cytosol staining as well as clearly visible nucleus were included. From these, cells were distinguished between “nucleus negative” and “nucleus positive” stained cells. Cells were considered “nucleus negative” when bluish counter staining predominated and “nucleus positive” when brownish ICC staining was dominant.

Blocking solution (immunocytochemistry)

BSA	1% (w/v)
goat serum	5% (v/v)
NaN_3	0.1% (w/v)
in PBS	

3.2.12 RNA isolation, cDNA synthesis and RT-qPCR

Preliminary to the quantitative real-time polymerase chain reaction (RT-qPCR) the purified single-stranded RNA needs to be reverse transcribed to a double-stranded nucleic acid, cDNA. Thereby non-sequence-specific primers are used to amplify all potential target transcripts. With the quantitative PCR technique the transcription rate of a specific gene (mRNA) or microRNA of interest can be determined by using sequence-specific primer sets. The basic principle in the real-time PCR is to use a fluorescent dye that intercalate with double-stranded DNA whereby the emitted fluorescence signal can be measured after every amplification step. Thus the fluorescence intensity is directly proportional to the specific amplification of the target gene/microRNA. Correlating the logarithmic increase of the fluorescence intensity with the threshold cycle (Ct) the quantitative amount of the target gene/microRNA can be determined. The quantification can be semi-quantitative when comparing the transcription rate of the target to the transcription rate of a housekeeping gene or absolute when using a standard curve.

3.2.12.1 RNA purification

Prior to the RNA isolation, all cells (independent of origin or culture dish/well size) from former experiments were washed twice with PBS and then resuspended in 800 µL QIAzol

reagent. The RNA was isolated using the NucleoSpin miRNA Kit to the manufactures instructions of protocol 6.3 'RNA purification in combination with TRIzol® lysis: small and large RNA in one fraction' with following minor changes: After the third washing in step 10 the flow through was removed and columns were centrifuged another time at 11.000g for 30 sec to dry the silica membrane. Furthermore, in the last step, the eluated RNA (35 µL) was again transferred to the column, incubated for 5 min and was than eluated again by centrifugation (11.000g for 30 sec). To protect the RNA from degaradation, it was immediately stored at -80 °C. RNA concentration and purity was determined using a Nanodrop ND-1000 or ND-2000 spectrophotometer.

3.2.12.2 cDNA synthesis of microRNAs

For cDNA synthesis total RNA (containing the microRNAs) was adjusted to 5 ng/µL RNA by using nuclease-free water. Using the miRCURY LNA™ Universal RT microRNA PCR Universal cDNA Synthesis Kit II the reverse transcription reaction mixture/well was prepared as followed:

Reagent	**Volume [µL]**
5X Reaction buffer	2
Nuclease-free water	4.5
Enzyme mix	1
Synthetic RNA spike-ins or nuclease-free water	0.5
Template total RNA (5 ng/µL)	2
Total volume	*10*

The 10 µL reaction mixture was reverse transcribed in a thermocycler for 60 min at 42 °C followed by 5 min at 95 °C for heat-inactivation of the reverse transcriptase. The cDNA was stored at -80 °C. The cDNA was diluted 1:50 when used in the RT-qPCR.

3.2.12.3 cDNA synthesis of mRNA

For cDNA synthesis 1 µg RNA was adjusted with nuclease-free water to a total volume of 16 µL before 4 µL 5X PrimeScript™ RT Master Mix were added. The 20 µL reaction mixture was reverse transcribed in a thermocycler for 15 min at 37 °C followed by 5 sec at 85 °C for

heat-inactivation of the reverse transcriptase. The cDNA was stored at -80 °C. The cDNA was diluted 1:10 or 1:50 (for mouse adiponectin and leptin) when used in the RT-qPCR.

3.2.12.4 Quantitative real-time PCR for microRNAs

The quantification of specific microRNAs was determined with a quantitative real-time PCR and normalized to a housekeeping microRNA that is equally expressed in all compared samples and not influenced by the experimental procedure/treatment/etc. All samples were measured in duplicates and the reaction mixture/well was prepared with 5 µL miRCURY LNA™ Universal RT microRNA PCR ExiLENT SYBR® Green master mix and 1 µL miRCURY LNA™ Universal RT microRNA PCR LNA™ PCR primer set. The 6 µL reaction mixture was filled into each well before 4 µL diluted cDNA was added. The closed 96-well plate was centrifuged at 2500 rpm for 3 min. For all primer sets following PCR program was applied:

microRNA RT-qPCR

95 °C	10 min	
95 °C	10 sec	repeat 40x
60 °C	60 sec	
ramp-rate 1.6 °C/sec		

Hsa-miR-191-3p and hsa-let-7e-5p were used as internal control for normalization for mouse and human cell lines, respectively. RT-qPCR was performed with a realplex^2 mastercycler epgradient S and with a C1000Touch Thermal Cycler with CFX96 Real-Time system. Depicted are (2^-ΔCt)*10000 values.

3.2.12.5 Quantitative real-time PCR for mRNA

The quantification of specific target genes was determined with a quantitative real-time PCR and normalized to a housekeeping gene that is equally expressed in all compared samples and not influenced by the experimental procedure/treatment/etc. All samples were measured in duplicates and the reaction mixture/well was prepared as followed:

Reagent	Volume [µL]
2X SYBR® Premix Ex Taq™ (Tli RNaseH Plus)	5
Nuclease-free water	3
Primer forward	1
Primer reverse	1
Total volume	*10*

The 10 µL reaction mixture was filled into each well before 2 µL diluted cDNA was added. The closed 96-well plate was centrifuged at 2500 rpm for 3 min. RT-qPCR was performed with a realplex^2 mastercycler epgradient S. The PCR program was adjusted to the primer sets used. For mouse adiponectin, IL-6 and hypoxanthine phosphoribosyltransferase (HPRT) as well as human adiponection, IL-6, leptin and HPRT the 2-step PCR program was used. For mouse leptin the 3-step PCR program was applied.

2-step RT-qPCR			3-step RT-qPCR		
95 °C	120 sec		95 °C	120 sec	
95 °C	20 sec	repeat 40x	95 °C	30 sec	
60 °C	30 sec		55 °C	60 sec	repeat 40x
			72 °C	120 sec	

Target gene expression was normalized to the housekeeping gene (here HPRT) expression and quantified by the ΔΔCt method, calculated as followed:

$\Delta Ct = (Av.\ Ct_{gene} - Av.\ Ct_{housekeeper})$

$\Delta\Delta Ct = (\Delta Ct_{treatment} - \Delta Ct_{control})$

3.2.13 Protein analysis, Electrophoresis and Western Blot

3.2.13.1 Protein purification and BCA assay

Cells from previous cell culture experiments were washed twice with ice-cold PBS before cold lysis buffer was added. The amount of lysis buffer used increased depending on the

amount and status (preadipocyte or mature adipocyte) of the cells to avoid too low or too high protein concentrations. Subsequently cells were scraped from the surface and transferred to a 1.5 mL tube. For cell lysis, cells were incubated for 30 min on ice with several times of vortexing for 15 sec. For complete lysis, cells were transferred to a cold ultrasound water bath for 1 min before centrifugation at 13.000 rpm for 10 min at 4 °C. After centrifugation the aqueous phase, containing the proteins, was transferred to another tube and stored at -20 °C.

The protein concentration was determined using the bicinchoninic Acid (BCA) assay principle which primarily relies on two reactions. First, the Cu^{2+} ions from the copper(II)sulfate solution are reduced to Cu^{+} by the peptide bonds in the proteins whereby this reduction is proportional to the protein amount in the sample. Second, each Cu^{+} ion forms a chelate complex with two molecules of BCA thereby appearing purple-colored. This complex absorbs light at 562 nm.

To determine the protein concentration, a standard curve (25, 12.5, 6.25, 3.125, 1.56, 0.78 and 0 [mg/mL]) was prepared with BSA in RIPA buffer. Next the BCA solution was mixed 1:50 with the copper(II)sulfate solution, e.g. 1000 µL BCA + 20 µL copper(II)sulfate. For measurement, 5 µL/well sample or standard was filled into a 96-well plate before 100 µL BCA-Cu^{2+} reagent was added. The plate was incubated for 30 min at 37 °C, followed by 15 min incubation at 4 °C to stop the reaction. Subsequently the OD was measured at 562 nm wave lengths in a photometer. Protein concentration was calculated from the standard curve by linear regression analysis.

RIPA Buffer (100 mL)	
Tris/HCl pH 7.4	50 mM
NaCl	150 mM
NP-40	1% (v/v)
Na-Deoxycholate	0.25%
EDTA	1 mM
in VE-H_2O	

Lysis Buffer (10 mL)	
RIPA Buffer	10 mL
cOmplete ULTRA Tablets, Mini, EASYpack	1
Na_3VO_4 (activated)	1 mM
NaF	1 mM
PMSF *(add just before use)*	1 mM

3.2.13.2 SDS-polyacrylamide gel electrophoresis

The SDS-polyacrylamide gel electrophoresis is a technique to separate proteins according to their molecular weight independent of their structure and charge. Therefore, proteins get concentrated in the stacking gel before they enter (all at once) the separating gel. The percentage of polyacrylamide determines the density of the separating gel and can be adapted to the size of the proteins which should be determined. For the DHT experiments self-made 12% polyacrylamid separating gels were used, for the microRNA experiments 12% TGX Stain-free FastCast acrylamide were used for protein separation.

The solution for the separating gel was carefully filled into the gel casting stand and then overlayed with methanol to avoid polymerization delay by air oxygen. After approx. 30 min the gel was completely polymerized and the stacking gel could be added on top. Therefore the methanol was removed and the stacking gel solution carefully filled onto the separating gel. A gel comb was immediately inserted to form the wells and define the lanes where samples and protein ladder will be placed.

Separating gel (12%) (self-made)	
VE-H_2O	7.5 mL
1.5 M Tris pH 8.8	6 mL
Acrylamid/Bis (30%)	9.6 mL
10% SDS	500 µL
10% APS	96 µL
TEMED	48 µL

Stacking gel (4%) (self-made)	
VE-H_2O	6.9 mL
0.5 M Tris pH 6.8	3 mL
Acrylamid/Bis (30%)	2 mL
10% SDS	100 µL
10% APS	48 µL
TEMED	24 µL

Protein samples were mixed with loading buffer and adjusted with lysis buffer to equal protein concentrations per sample. Prior to separation, proteins were denaturated at 98 °C for 10 min. For electrophoresis the gel comb was removed and samples and a protein ladder, to determine the approx. molecular weight, were loaded onto the gel and separated at 100 V in

the electrophoresis chamber filled with running buffer (1X) until maximum separation capacity was reached.

Loading Buffer (4X)	
Glycerol	50% (v/v)
SDS	10% (w/v)
Tris/HCl pH 6.8	312,5 mM
Bromphenol blue	knife point
β-mercaptoethanol	20% (v/v)
(add just before use)	
in VE-H_2O	

Running Buffer (10X)	
Tris	0.25 M
Glycin	1,92 M
SDS	1% (w/v)
in VE-H_2O	

3.2.13.3 Western Blot

The western blot is a technique for the transfer and immobilization of electrophoretic separated proteins to a membrane, whereby the protein separation pattern is preserved. Furthermore, the western blot technique allows a quantitative as well as qualitative determination and identification of specific proteins from a protein mixture. The proteins on the membrane are accessible for antibodies which bind specifically to their target proteins, so-called immunoblotting. The attached antibody can then be detected either directly when itself is labeled or indirectly by a labeled secondary antibody. Commonly used secondary antibodies are labeled with horseradish peroxidase (HRP) which can be detected by enhanced chemiluminescence (ECL) substrate.

After the SDS-polyacrylamid gel electrophoresis the proteins were transferred to a polyvinylidene fluoride (PVDF) membrane in blotting buffer (1X) at 100 V for 60 min. The membrane was then blocked with 5% skim milk or 5% BSA (depending on the antibody) in TBS-T buffer for 1 hour at RT to prevent unspecific binding of the antibody. Subsequently the membrane was probed with the specific primary antibodies for the proteins of interest (see 3.1.4) over night at 4 °C with gently shaking. To remove the unbound primary antibody the membrane was washed with TBS-T buffer for 1 hour changing buffer every 10 minutes.

Following this the membrane was incubated with respective HRP-conjugated secondary antibodies 1:10000 in 5% skim milk in TBS-T for 1 hour at RT (see 3.1.4). Afterwards the membrane was washed again with TBS-T buffer for 1 hour changing buffer every 10 minutes. Finally proteins were visualized by using Clarity Max™ Western ECL reagent that leads to a chemiluminiscence signal generated by the HRP conjugated to the secondary antibody and detected with the ChemiDoc^{TM}Touch Imaging System. Signals were normalized to total protein on the membrane detected with the TGX Stain-free FastCast acrylamide gel system or MemCode Reversible Protein Stain Kit for the self-made gels and analyzed with ImageLab Version 5.2.1 software. Thereby is the intensity of the signal proportional to the protein amount.

Blotting Buffer (10X)	
Tris	0.25 M
Glycin	1.92 M
in VE-H_2O	

Blotting Buffer (1X)	
VE-H_2O	700 mL
Blotting Buffer 10X	100 mL
Methanol	20% (v/v)

TBS pH 7.4 (10X)	
Tris	100 mM
NaCl	1.5 M
in VE-H_2O	

TBS-T pH 7.4 (1X)	
TBS 10X	100 mL
VE-H_2O	900 mL
Tween20	0.1% (v/v)

3.2.14 Oil Red O staining

Adipocyte differentiation is characterized by the formation of lipid droplets and the constant increase of lipid content. The lipid content can be visualized by Oil Red O staining leading to a red appearance of the lipids. Therefore, cells were washed twice with PBS and fixed with 10% formalin for at least 24 hours at 4°C. Afterwards the formalin was removed and cells were stained with freshly prepared Oil Red O working solution for at least 1h at RT. After staining, the cells were washed several times with H_2O until all surplus staining solution was removed. Pictures of stained cells were taken with CanonScan 4400F scanner. For

quantification, the Oil Red O staining was dissolved out with isopropanol for 20 min. Optical density was determined at 500 nm wave lengths in a photometer.

Oil Red O stock solution	
Oil Red O	0.5 g
Isopropanol	100 mL

Oil Red O working solution	
Oil Red O stock solution	60%
VE-H_2O	40%
freshly prepared	

3.2.15 Transcriptomics

For transcriptome analysis, preadipocytes from both murine fat depots were treated 24 hours with 10 nM DHT or EtOH control. Following stimulation cells were resuspended in QIAzol reagent and snap frozen in liquid nitrogen. The samples were sent on dry ice to the Ernst-Moritz-Arndt-University Greifswald, Interfaculty Institute for Genetics and Functional Genomics, Department of Functional Genomics where the transcriptome analysis was conducted in collaboration with Prof. Uwe Völker and Dr. Georg Homuth. There, the microarray-based transcriptome analysis was performed as described by Lietzow et al. [266]. In brief, the total RNA was extracted from cells with a modified TRIzol reagent-based phenol extraction method [267], followed by further column purification. RNA quality and integrity were controlled with a ND-8000 spectrophotometer and by means of lab-on-a-chip capillary electrophoresis technology using an Agilent 2100 Bioanalyzer, respectively. Subsequently, transcriptome analysis of individual samples was performed by using Affymetrix Gene Chip Mouse Gene 1.0 ST Arrays and GeneChip® WT PLUS Reagent Kit according to the manufacturer's instructions. Rosetta Resolver® software system was used for microarray data analysis. Significantly different mRNA levels were defined using the following criteria: one-way ANOVA with Benjamini and Hochberg FDR ($p \leq 0.05$), signal correction statistics (Ratio Builder software; $p \leq 0.05$), and an expression value ratio between the different conditions ≥ 2.0-fold.

3.2.16 MicroRNA target prediction and pathway analysis

For target prediction of the selected mouse microRNAs the web tool miRWalk was used on default settings. For more reliable prediction five additional algorithms (Targetscan, miRanda, miRDB, RNA22 and RNAhybrid) were added to the analysis, each one premises different properties among miRNA-mRNA targeting. Predicted mouse microRNA targets from at least

four algorithms were used for pathway analysis using the web tool WebGestalt (WEB-based GEne SeT AnaLysis Toolkit). The enrichment analysis for Kyoto Encyclopedia of Genes and Genomes (KEGG) pathways was performed on default settings with *mus musculus* genome selected as reference set.

3.2.17 Statistical analysis

Statistical analyses were performed with GraphPad Prism 5 software and Microsoft Excel if not indicated otherwise. Results are presented as mean values ± SEM. Statistical significance was determined using the unpaired, two-tailed Student's t-test. P-values ≤ 0.05 (*) were considered significant.

4 Results

4.1 MicroRNA expression in adipogenesis

4.1.1 MicroRNA array: Differential expression of microRNAs

To identify microRNAs that might play a leading role in the modulation and progression of adipogenesis a microRNA array was performed. The focus of interest was to identify microRNAs that could play a general, species independent role of adipogenesis in both the visceral and subcutaneous fat depot. Therefore, *ex vivo* epididymal (EPI) and inguinal (ING) WAT from mice as well as *ex vivo* subcutaneous WAT from male and female humans were used. From these tissues preadipocytes and mature adipocytes were separated and used for the microRNA array analysis.

When comparing preadipocytes and mature adipocytes in all three analyzed tissues, nine microRNAs (Figure 4a) shared differential expression under all conditions. Three of these microRNAs, miR-199a-5p, miR-199-3p and miR-652-3p, were excluded from further analysis because they were regulated in opposite directions in mouse and human tissue samples (Figure 4b), arguing against a general and species independent role in adipogenesis. Of the six remaining microRNAs consistently regulated between mouse and human samples microRNAs miR-146b-5p, miR-142-3p and miR-223-3p were higher expressed in preadipocytes than in mature adipocytes whereas the expression of microRNAs miR-193a-3p, miR-365-3p and miR-708-5p was higher in mature adipocytes (Figure 4b) compared to preadipocytes. These microRNAs were further validated and characterized regarding a potential causal role in the progression of adipogenesis.

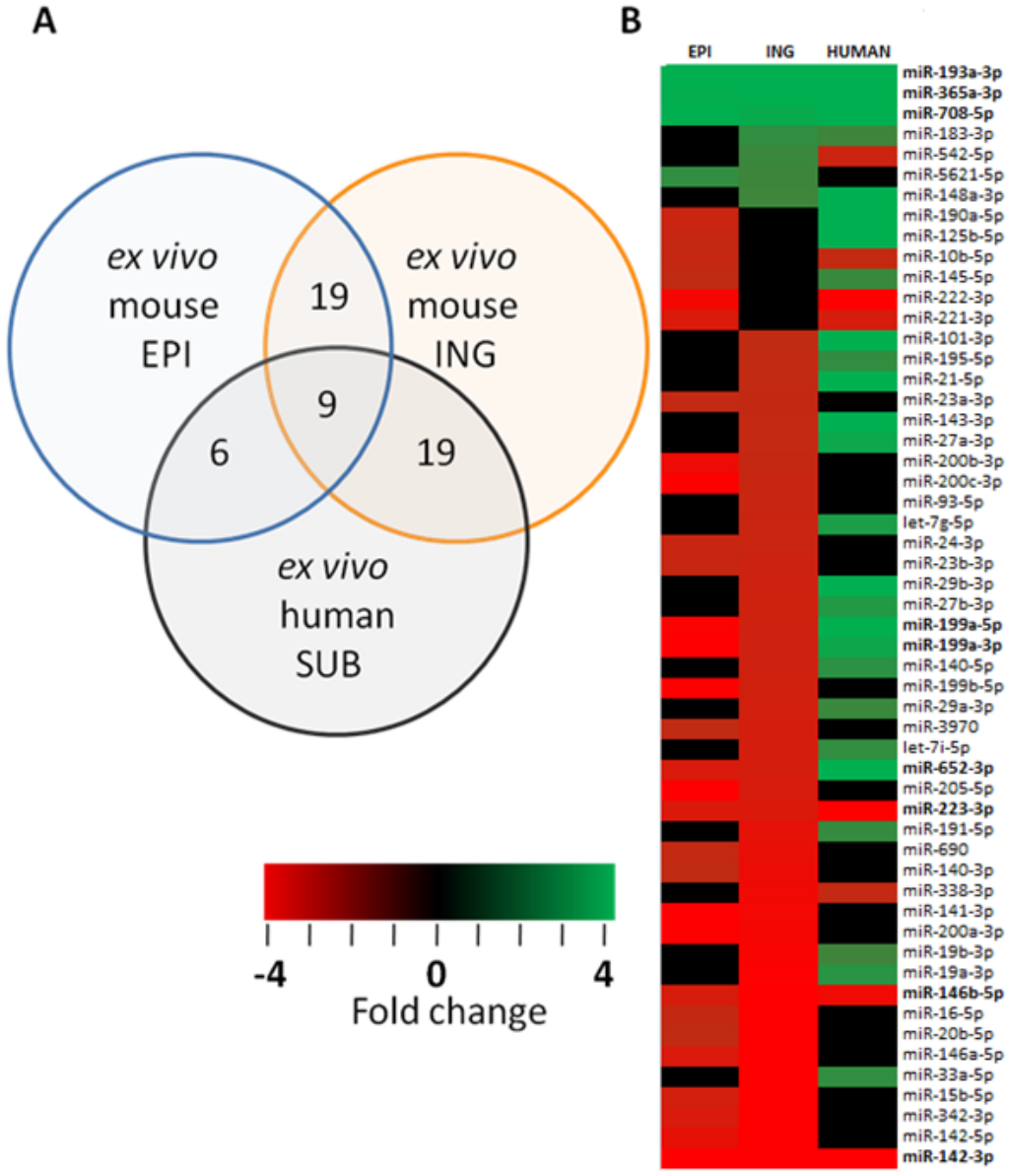

Figure 4 - MicroRNA array from mouse EPI and ING as well as human subcutaneous *ex vivo* white adipose tissues. (A) Venn diagram representing differential expressed microRNAs between preadipocytes and mature adipocytes of *ex vivo* mouse EPI and ING as well as human subcutaneous white adipose tissue. (B) Heatmap showing up- and downregulated microRNAs in *ex vivo* mouse EPI and ING as well as human subcutaneous WAT. Boldface microRNAs are differently expressed between preadipocytes and mature adipocytes in all three analyzed tissue samples; (n=1-2/group).

As the microRNA expression from the tissue samples might give rather steady state information compared to the dynamic information of a cell culture system, the six identified microRNAs (miR-142-3p, miR-223-3p, miR-146b-5p, miR-193a-3p, miR-708-5p, miR-365a-3p) were further analyzed regarding their dynamic expression during adipogenesis.

4.1.2 MicroRNA expression profiles during adipocyte differentiation

To analyze dynamic microRNA expression during adipogenesis, immortalized, well characterized mouse EPI and ING WAT cell lines as well as human subcutaneous adipose-derived mesenchymal stem cells (hMSCs) were used. These cell lines are able to differentiate *in vitro* from preadipocytes to mature adipocytes.

To further confirm the validity of the cell culture models miR-378a-3p expression was analyzed as an internal control. MiR-378a is well described to play an important role in adipogenesis of cells from different origins [256, 258, 259, 268-270] and is expressed in human adipocytes as well [255, 271, 272]. MiR-378a-3p was also expressed in the tissue samples used for the microRNA array but was under the threshold initially set in the murine tissue samples (see Table S1-4). It was therefore not represented in the underlying array analysis. However, a low expression of miR-378a-3p in preadipocytes which increased with induction of differentiation (day 0) could be confirmed in both the mouse and human cell lines (Figure 5a). But whereas miR-378a-3p expression reached a plateau in the mouse cell lines, its expression was constantly increasing in the hMSCs (Figure 5a).

In none of the three cell lines the expression of miR-142-3p and miR-223-3p could be verified (data not shown). Therefore, these microRNAs were excluded from further analysis. In contrast to the microRNA array results, miR-146b-5p expression was upregulated in parallel to adipogenesis progression in the mouse EPI and ING cell lines but showed a very low expression in the preadipocytes and mature adipocytes derived from the hMSCs (Figure 5b). According to the microRNA array results, the expression pattern for microRNAs miR-193a-3p, miR-708-5p and miR-365a-3p could be confirmed in all three cell lines (Figure 5c-e). For miR-146b-5p, miR-365-3p, miR-708-5p and miR-193a-3p similar expression pattern were detectable in the mouse EPI and ING fat depots, with low expression in preadipocytes which was increasing when differentiation was induced (day 0) and mature adipocytes were formed (Figure 5b-e). The hMSCs showed a similar expression pattern of the candidate microRNAs (Figure 5c-e) except for miR-146b-5p (Figure 5b). Only the magnitude of expression seemed to differ between the fat depots when semi-quantitatively assessed by RT-qPCR. Hence, miR-708-5p was characterized by a very low expression in preadipocytes (in some samples even under the detection limit of RT-qPCR) which was immediately increasing after induction of differentiation (day 0) in mouse and human cell lines (Figure 5d). In contrast, miR-193a-3p expression was already detectable in preadipocytes (day -2 – day 0) before it was further increasing in mature adipocytes, especially in the ING depot (Figure 5e).

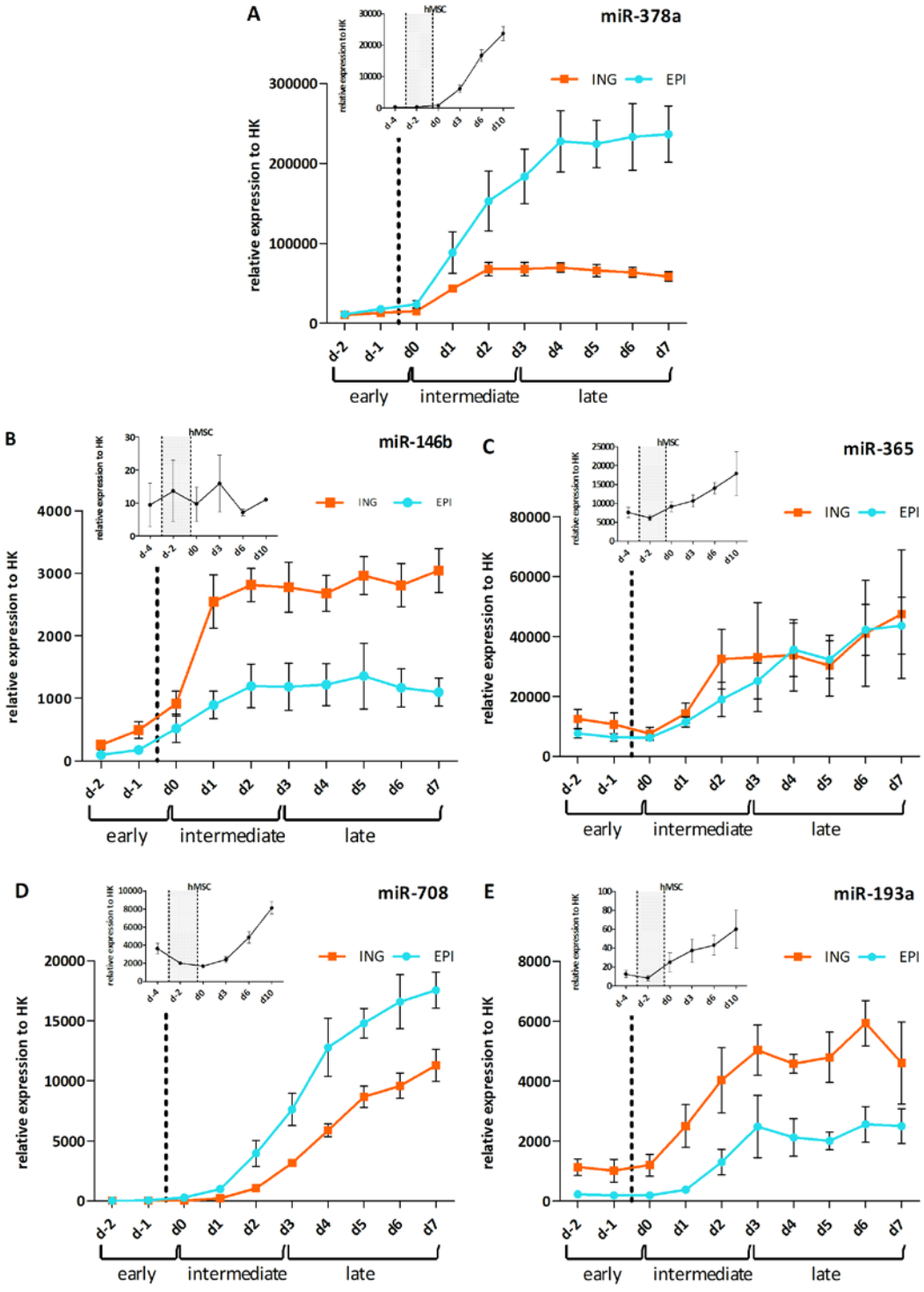

Figure 5 - MicroRNA expression profiles in mouse EPI and ING as well as hMSCs. MicroRNA expression profiles in murine EPI and ING cell lines as well as in hMSC of (A) miR-378a-3p, (B) miR-146b-5p, (C) miR-365a-3p, (D) miR-708-5p and (E) miR-193a-3p. Dotted line/grey box indicates induction of differentiation, n=4-6/group. Early phase: day-2 to day 0 in mouse and day -4 to day 0 in hMSCs; intermediate phase: day 0 to day 3 in mouse and day 0 to day 4 in hMSCs; late phase: day 3 to day 7 in mouse and day 4 to day 10 in hMSCs.

For all analyzed microRNAs an increasing expression was detectable after induction of differentiation, leading to the assumption that these microRNAs could play an active role in adipogenesis and might be effective regulators of adipocyte differentiation.

4.2 Functional analysis of miR-193a and miR-708

After characterization of the candidate microRNAs expression profiles during adipocyte differentiation the question remains whether these microRNAs are effectors of adipogenesis or simply a byproduct. The microRNAs miR-146b and miR-365a have been previously characterized in fat development and adipogenesis. MiR-365 was described as an important regulator of BAT development and WAT browning [260, 261] and miR-146b in the promotion of WAT adipogenesis [257, 273-275]. Therefore, these microRNAs were excluded from further analysis. Thus, further analysis was concentrated on a potentially causal role of miR-708-5p and miR-193a-3p in adipogenesis as both microRNAs have not yet been described in the context of adipocyte differentiation.

4.2.1 MiR-193a and miR-708 inhibition and knock-down verification

To analyze microRNA function during adipogenesis, mouse EPI and ING cells were either transfected with specific microRNA inhibitors (antagomirs) of the respective microRNA (anti-193a-3p or anti-708-5p) or negative controls (NC). Successful inhibition was determined by RT-qPCR.

Both microRNAs miR-193a-3p and miR-708-5p were 80-90% downregulated by antagomir transfection (anti-193a, anti-708) in EPI (Figure 6a) and ING (Figure 6b) fat depots compared to the control transfected cells. This leads to the assumption that the antagomir approach is suitable to study miR-193a and miR-708 effects on adipogenesis.

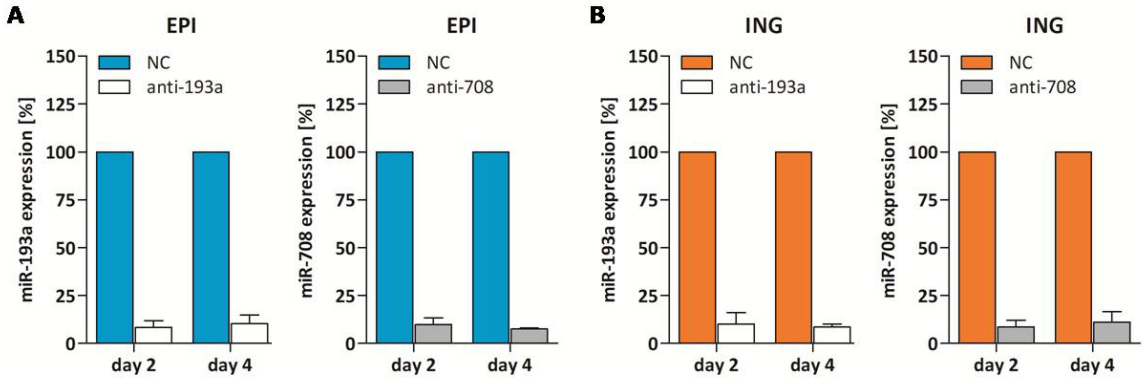

Figure 6 - Knock-down verification after miR-193a-3p and miR-708-5p inhibition in EPI and ING cells. Quantification of miR-193a-3p inhibition (anti-193a) and miR-708-5p inhibition (anti-708) relative to negative control (NC) transfected cell by RT-qPCR in (A) EPI and (B) ING murine cell lines, n=3-4/group.

4.2.2 Mir-193a and miR-708 effects on lipid content

Adipocyte differentiation is characterized by the formation of lipid droplets and the constant increase of lipid content. The lipid content can be visualized by Oil Red O staining leading to a red appearance of the lipids.

Following transfection with the miR-708-5p inhibitor no effects on lipid content could be observed neither for the EPI (Figure 7a) nor the ING (Figure 7b) fat depot. Similarly, Oil Red O staining in the anti-193a transfected cell from the ING depot was unchanged (Figure 7b), whereas in the EPI fat depot the Oil Red O staining revealed a higher lipid content in anti-193a transfected cells compared to controls (Figure 7a). These effects were already visible at day 4 of differentiation and were even more pronounced at day 6 when cells are fully differentiated (Figure 7a), indicating an accelerated differentiation of the anti-193a transfected cells compared to controls in the EPI depot.

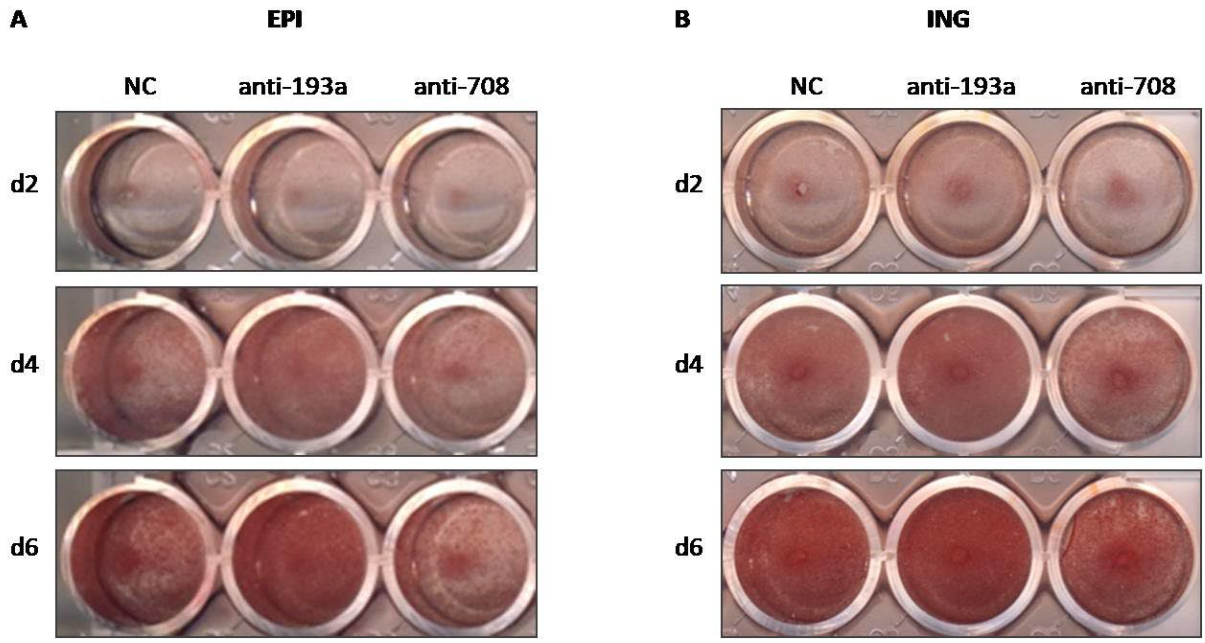

Figure 7 – Effects of miR-193a-3p and miR-708-5p inhibition on lipid content in EPI and ING cells. Representative Oil Red O staining for negative control (NC), anti-193a and anti-708 transfected cells at days 2, 4, and 6 of adipocyte differentiation in (A) EPI and (B) ING cell lines, n=6/group.

4.2.3 MiR-193a and miR-708 effects on adipogenesis marker proteins

Adipogenesis can be differentiated into three parts, the so called early, intermediate and late differentiation phase. Each phase is characterized by the expression of specific proteins. These proteins can be determined by western blot analysis and thereby giving an idea of the developmental status of the cells during adipocyte differentiation. C/EBPβ was used as a marker for the intermediate phase and A-FABP as a late phase marker.

The C/EBPβ protein levels were significantly reduced at day 6 in the anti-193a transfected cells compared to controls in the EPI compartment (Figure 8a), indicating an altered adipocyte differentiation in these cells. For the ING depot no differences between anti-193a transfected cells and controls are detectable for C/EBPβ (Figure 8b). However, anti-708 transfected cells showed significantly higher C/EBPβ protein concentrations at day 2 and day 4 in the ING depot (Figure 8b), but were not altered in the EPI depot (Figure 8a), which might indicate a shift in adipogenesis in the ING depot.

However, in the anti-708 transfected cells no alterations in the late phase marker A-FABP were detectable in both adipose tissues (Figure 8c, d). In parallel, no changes in A-FABP protein levels were detectable in the ING depot when transfected with miR-193a inhibitor (Figure 8d), indicating that adipocyte differentiation is not affected in the ING fat depot

neither by miR-708-5p nor miR-193a-3p. In contrast, in the EPI compartment a significantly higher A-FABP concentration was detectable at day 6 in the anti-193a transfected cells compared to controls (Figure 8c), leading to the assumption that anti-193a transfected cells differentiate faster than the controls.

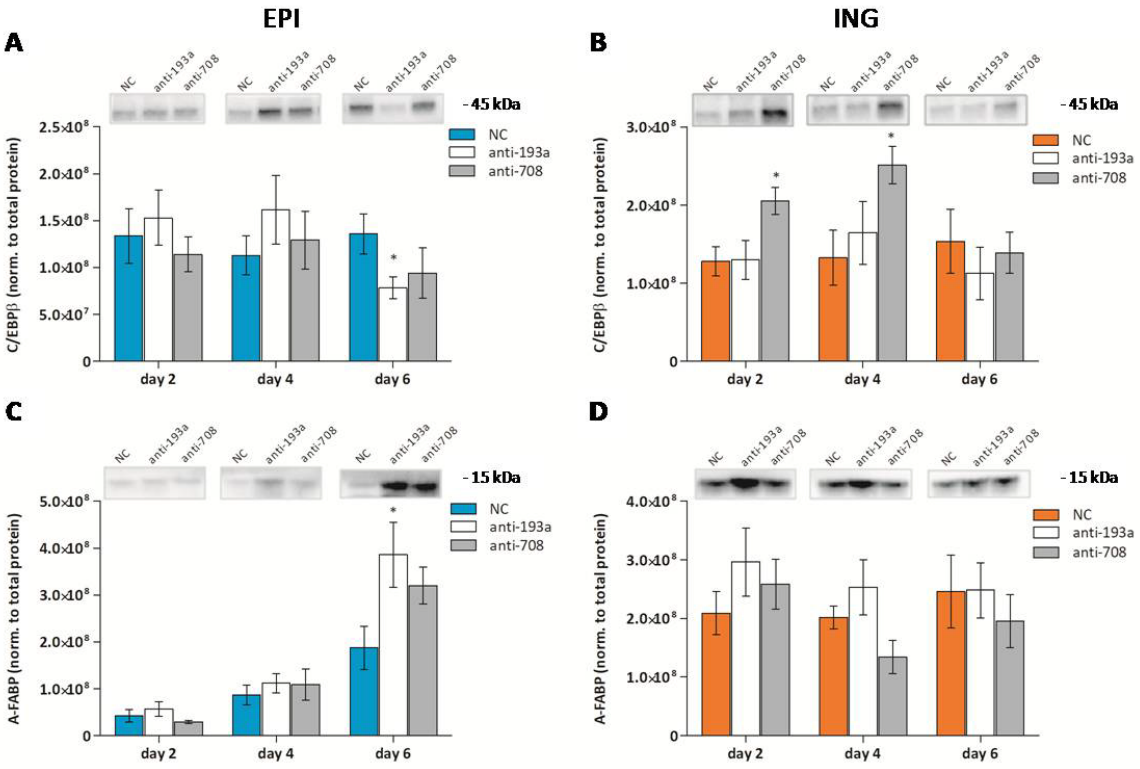

Figure 8 – Effects of miR-193a-3p and miR-708-5p inhibition on adipogenesis markers in EPI and ING cells. Quantification and representative western blot for (A, B) C/EBPβ (C, D) A-FABP protein levels in negative controls (NC), anti-193a and anti-708 inhibitor transfected cells in murine (A, C) EPI and (B, D) ING cell lines at days 2, 4 and 6 of adipocyte differentiation, n=5/group. *= $p<0.05$ with student´s t-test. Total protein blots for normalization see supplementary Figure S1.

In summary, the functional analysis indicated that miR-708-5p did not affect adipocyte differentiation in both fat depots whereas miR-193a-3p seemed to negatively affect EPI adipogenesis as determined by western blot and Oil Red O staining.

4.3 Target prediction for miR-193a

Since the functional analysis of miR-193a-3p revealed that this microRNA alters EPI adipogenesis, the question arises which target genes and signaling pathways might be involved in the action of miR-193a-3p. For a microRNA target prediction the web tool

miRWalk with additional algorithms (Targetscan, miRanda, miRDB, RNA22, RNAhybrid) was used. The predicted targets were further analyzed regarding their occurrence in diverse signaling pathways by applying the web tool WebGestalt for a KEGG pathway enrichment analysis. The top 10 determined KEGG pathways for miR-193a target genes (Table 1a) included the WNT signaling pathway. Matching to the WNT signaling pathway some of the predicted targets for miR-193a included proteins that are part of the β-catenin destruction complex (e.g APC2, Dickkopf-related protein 2 (DKK2)) or those which interact with the destruction complex leading to ubiquitination (e.g beta-transducin repeat containing protein 2 (βTrCP2/Fbxw11), SIAH1a, SIAH1b) of β-catenin (Table 1b).

Table 1 - MiR-193a-3p target prediction and subsequent KEGG pathway enrichment analysis. (A) Top 10 predicted KEGG pathways for miR-193a-3p predicted target genes determined with the web tool WebGestalt. (B) MiR-193a-3p target genes that match to the WNT signaling pathway from the KEGG pathway enrichment analysis. Displayed are the gene symbols.

A

Top 10 predicted KEGG pathways for miR-193a-3p predicted target genes
Pathways in Cancer
Endocytosis
Wnt signaling pathway
MAPK signaling pathway
ErbB signaling pathway
Metabolic pathways
Focal adhesion
Renal cell carcinoma
Pancreatic cancer
Hepatitis C

B

MiR-193a-3p predicted target genes matching to the WNT signaling pathway	
Apc2	Mapk8
Btrc	Ppp2r5c
Camk2b	Prkca
Ccnd3	Rock2
Csnk1e	**Siah1a**
Cxxc4	**Siah1b**
Daam2	Smad2
Dkk2	Smad3
Fbxw11	Smad4
Fzd3	Tbl1xr1
Fzd5	Trp53
Gsk3b	Wnt4
Mapk10	Wnt5a

4.4 MiR-708 impact on adipocyte key functions and adipokine expression

Since no effects of miR-708-5p on adipocyte differentiation could be determined it was speculated that miR-708-5p may have an impact on adipocyte key functions and/or adipokines expression rather than on differentiation *per se*. Therefore, the impact of miR-708-5p inhibition on lipolysis, glucose uptake and lipogenesis as well as on adiponectin, leptin and IL-6 expression was determined.

4.4.1 MiR-708 inhibition and knock-down verification

To analyze miR-708-5p function in the regulation of key functions and adipokines expression, mouse EPI and ING cells as well as hMSCs were either transfected with specific miR-708-5p inhibitor (anti-708) or negative control during the intermediate phase of adipocyte differentiation. Successful inhibition was determined by RT-qPCR.

In both mouse cell lines miR-708-5p expression was 80-90% downregulated by antagomir transfection compared to controls (Figure 9a, b). In the hMSCs a miR-708-5p downregulation to 60-70% could be detected (Figure 9c). This leads to the assumption that the achieved miR-708-5p inhibition is suitable to study miR-708 effects on adipocyte key functions and adipokine expression.

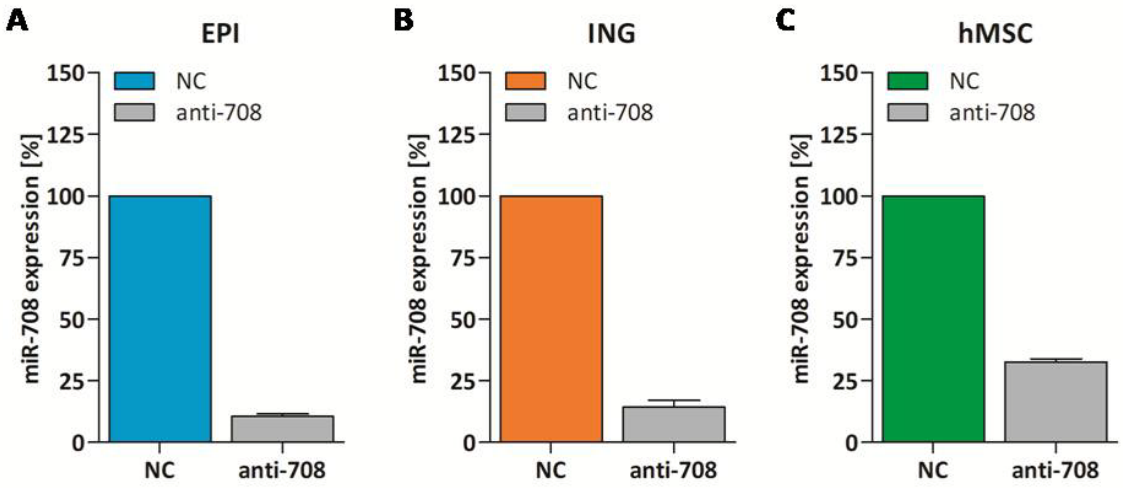

Figure 9 - Knock-down verification after miR-708-5p inhibition in EPI, ING and hMSC cells. Quantification of miR-708-5p inhibition (anti-708) relative to negative control (NC) transfected cell by RT-qPCR in (A) EPI and (B) ING murine cell lines as well as (C) hMSCs, n=3-4/group.

4.4.2 MiR-708 effects on lipolysis

During lipolysis the stored triglycerides are broken down to free fatty acids and the glycerol backbone which are then released to the circulation for the energy supply of peripheral tissues. Lipolysis can be induced by stimulation with isoprenaline (ISO) which specifically binds to the beta-adrenergic receptor. To determine the lipolysis rate the secreted glycerol was measured.

Compared to controls, transfection with miR-708-5p inhibitor revealed no changes in glycerol concentration neither in basal nor in 500 nM ISO stimulated lipolysis in all three cell lines (Figure 10). This indicates that the hydrolysis of stored lipids is not regulated by miR-708-5p.

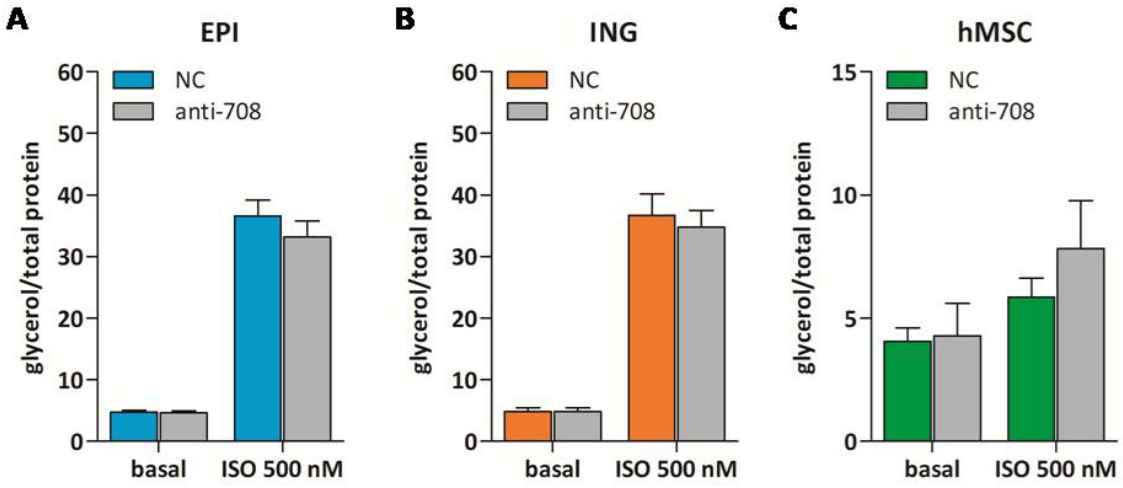

Figure 10 – Effects of miR-708-5p inhibition on lipolysis in EPI, ING and hMSCs. Glycerol release in anti-708 transfected cells (anti-708) compared to controls (NC) under basal and stimulated (500 nM isoprenaline) lipolysis conditions in (A) EPI and (B) ING murine cell lines as well as (C) hMSCs, n=3-6/group.

4.4.3 MiR-708 effects on glucose uptake and lipogenesis

In the catabolic state adipocyte mobilize stored lipids (lipolysis) for the energy demand of peripheral tissues. In contrast, under anabolic conditions lipids and glucose can be stored in form of triglycerides following insulin-dependent stimulation of glucose uptake into adipocytes. To measure this, glucose uptake of non-metabolisable radioactive 2-deoxy-D[^{3}H]glucose into mature adipocytes as well as the (indirect) incorporation of radioactive ^{3}H-glucose into triglycerides (lipogenesis) was determined.

No changes in glucose uptake could be determined in the absence (-Insulin) or presence (+Insulin) of insulin in anti-708-5p transfected cells compared to controls of hMSCs (Figure

11a). In parallel, ^{3}H-glucose incorporation during lipogenesis was not changed under the same conditions in hMSCs (Figure 11b). This leads to the assumption that neither glucose uptake nor lipogenesis were affected by miR-708-5p inhibition in the differentiated hMSCs.

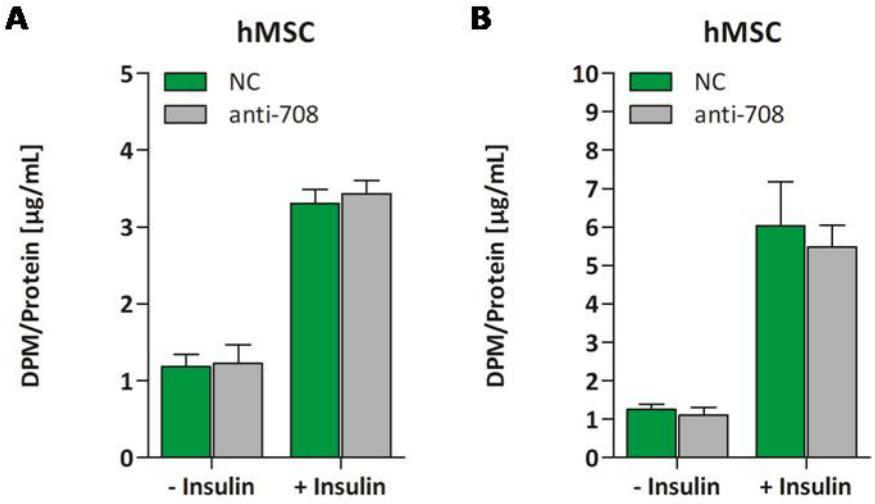

Figure 11 –Effects of miR-708-5p inhibition on glucose uptake and lipogenesis in differentiated hMSCs. ^{3}H-radioactivity in anti-708 transfected cells (anti-708) compared to controls (NC) under non-insulin (-Insulin) and insulin (+Insulin) stimulated conditions in hMSCs in (A) glucose uptake and (B) lipogenesis, n=4-6/group.

4.4.4 MiR-708 effects on adiponectin, leptin and IL-6 expression

Adipokines are secreted by the adipose tissue in response to metabolic changes. Their controlled regulation and release is important to maintain the body homeostasis. Therefore, it was analyzed whether the expression of adiponectin, leptin and IL-6 is regulated by miR-708-5p. Adipokine expression was assessed by RT-qPCR.

All three analyzed adipokines (adiponectin, leptin and IL-6) were expressed in control cells of all three cell lines but their expression was not changed by miR-708-5p inhibition (Figure 12). This indicates that miR-708-5p seems not to play a role in these adipokines regulation.

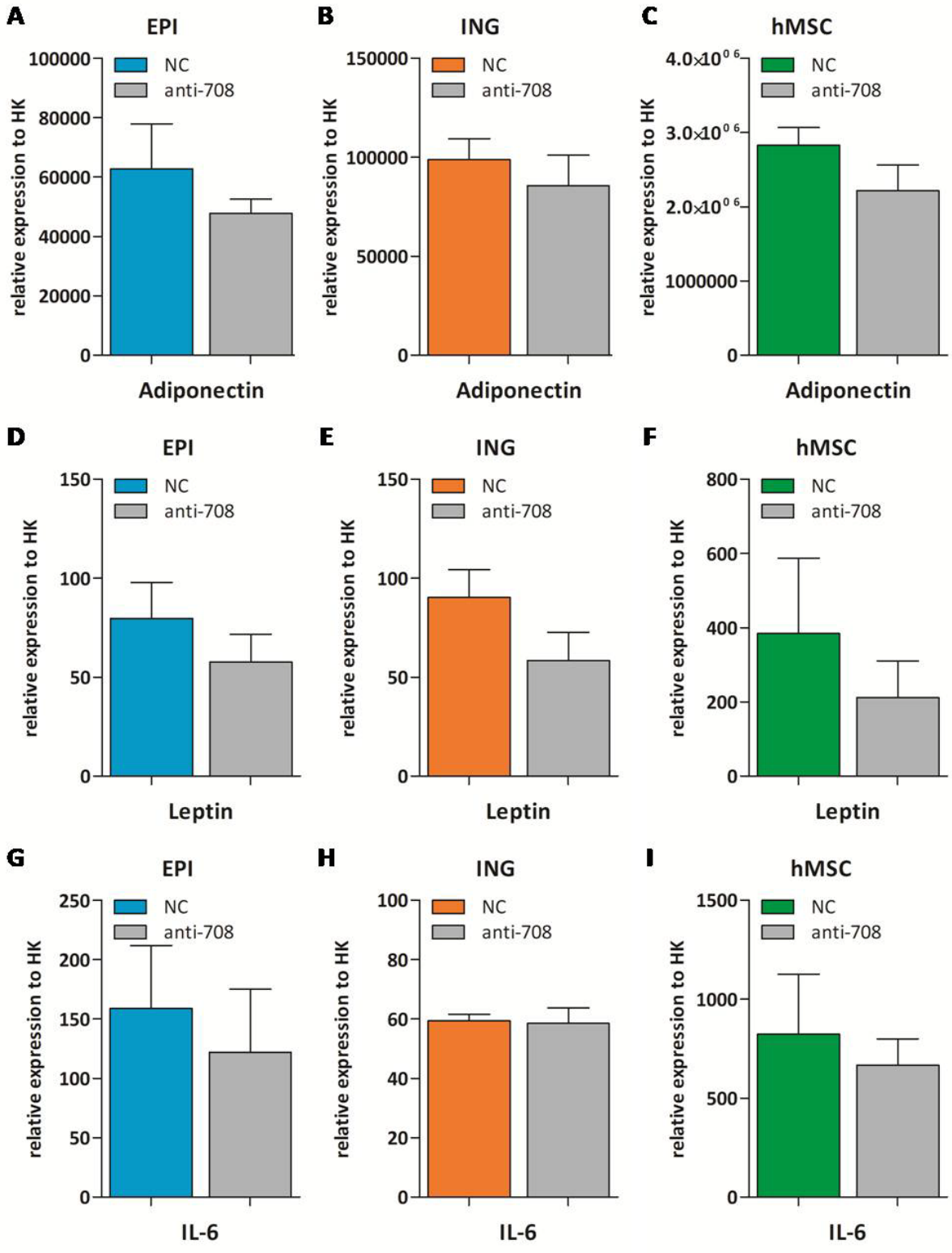

Figure 12 –Effects of miR-708-5p inhibition on adiponectin, leptin and IL-6 expression in EPI, ING and hMSCs. (A, B, C) Adiponectin, (D, E, F) leptin and (G, H, I) IL-6 expression in anti-708 transfected cells (anti-708) compared to controls (NC) in (A, D, G) EPI and (B, E, H) ING murine cell lines as well as (C, F, I) hMSCs, n=3-5/group.

MiR-193a-3p could be identified as a regulator of epididymal adipocyte differentiation. However, miR-708-5p functions still seems to be elusive since it was demonstrated that it plays neither a causal role in adipocyte differentiation nor in the regulation of adipocyte key functions and adipokine expression. Nevertheless, the microRNA array data and the expression profile of miR-708-5p indicated a relation of this microRNA to adipocyte development.

Since sex-steroids are described to have a regulatory role on adipogenesis further analysis was concentrated on whether miR-708-5p might be regulated by androgens and by this maybe exhibit an indirect role on adipocyte function via androgen-mediated pathways.

4.5 MiR-708 and androgens

Androgens are known to show a regulatory role on adipogenesis. In addition, they are also able to regulate microRNA expression [276, 277]. Thus, to assess whether androgens influence miR-708-5p expression, cells were chronically or acutely stimulated with 10 nM DHT and expression was determined by RT-qPCR.

4.5.1 Effects of acute DHT treatment on miR-708 expression

MicroRNA expression and turnover can be changed within several hours [278], thus the changes in miR-708-5p expression after 1 hour and 8 hours DHT treatment in mature adipocytes were assessed.

Acute DHT stimulation did not change the miR-708-5p expression at any of the indicated time points in the EPI depot (Figure 13a) as well as in the ING depot (Figure 13b).

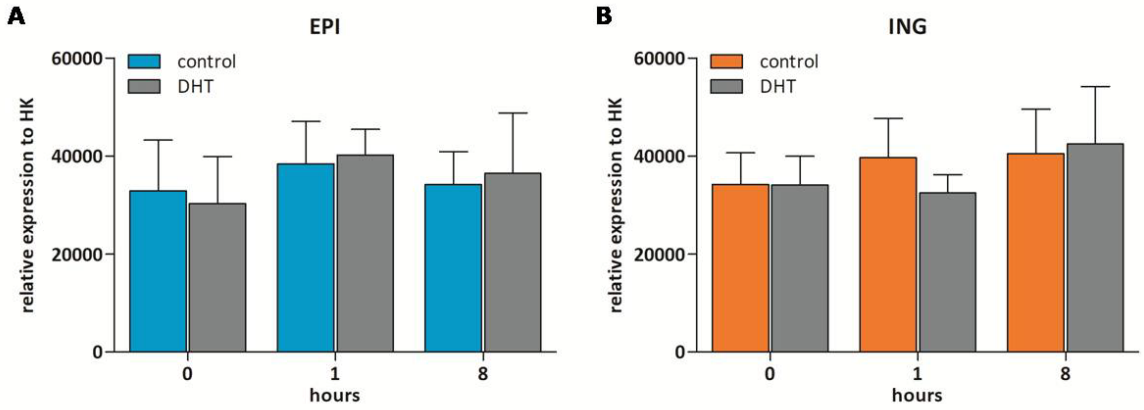

Figure 13 – Expression of miR-708-5p after acute DHT stimulation in EPI and ING cells. MiR-708-5p expression in 10 nM DHT treated mature adipocytes compared to controls in (A) EPI and (B) ING cells. n=3/group.

4.5.2 Effects of chronic DHT treatment on miR-708 expression

Since the half life and turnover of microRNAs ranges from 1 hour to several hours [278], also the chronic effects of DHT stimulation were determined to ensure that a potential DHT effect on miR-708-5p expression can be uncovered. Therefore, cells were treated from day -3 on with 10 nM DHT or mock control (EtOH) until full differentiation.

Chronic DHT treatment revealed a decreased expression of miR-708-5p compared to controls in both tissues, which is significant at day 2 and day 5 in the EPI cells (Figure 14a) and from day 1 to day 4 in the ING cells (Figure 14b) compared to controls, indicating a potential regulatory role of DHT on miR-708-5p expression.

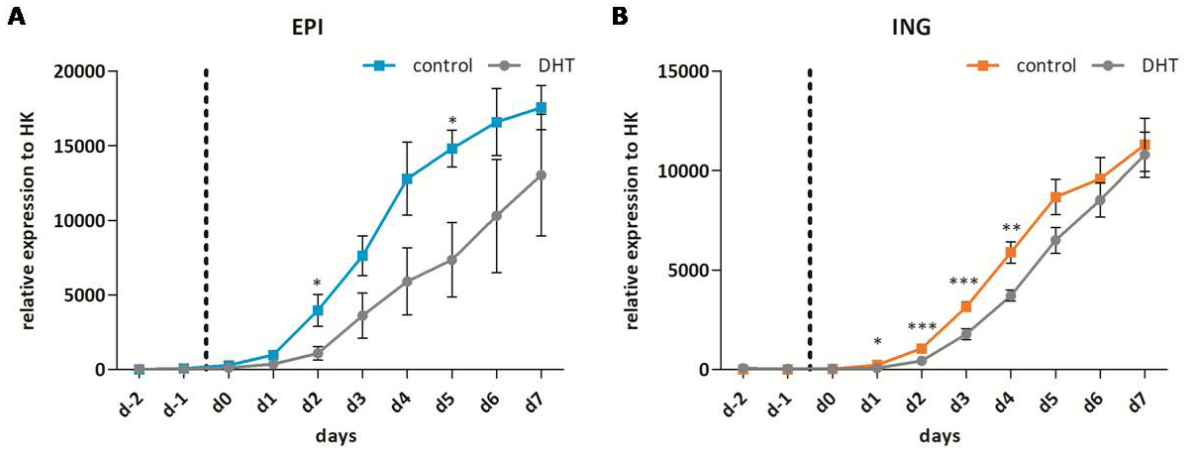

Figure 14 - Expression of miR-708-5p after chronic DHT stimulation in EPI and ING cells. MiR-708-5p expression during differentiation when chronically stimulated with 10 nM DHT or control conditions in (A) EPI and (B) ING cells. n=6/group; *= p<0.05, **=p<0.01, ***=p<0.005 with student´s t-test.

The data on chronic DHT stimulation indicates that miR-708-5p expression might be regulated by androgens. In contrast, the results of the acute stimulation for 1 h and 8 h do not support such conclusion. Thus, the question arises whether the effects detected in the chronic DHT set up might be an indirect effect of DHT on adipogenesis leading to an altered miR-708-5p expression rather than a direct effect of DHT on miR-708-5p expression *per se*.

To elucidate this, the effects of chronic DHT treatment on fat depot-specific adipocyte differentiation were further analyzed.

4.6 DHT effects on fat depot-specific adipocyte differentiation

4.6.1 DHT effects on proliferation

First, the effects of DHT on preadipocytes and thereby its impact on proliferation were tested by determining their proliferation rate during chronic DHT treatment.

The proliferation assay revealed that the proliferation of preadipocytes is not affected by DHT compared to controls in both the EPI (Figure 15a) and ING cells (Figure 15b).

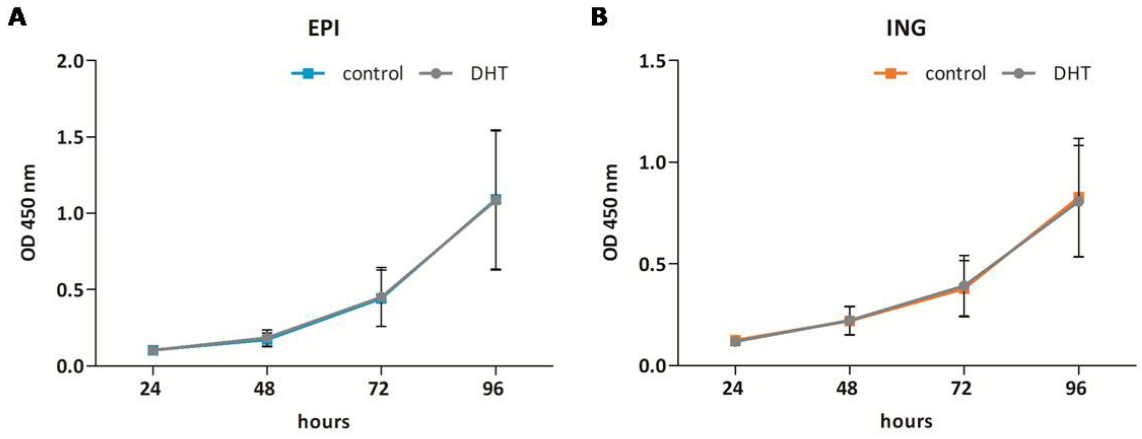

Figure 15 – Effects of chronic DHT stimulation on preadipocyte proliferation in EPI and ING cells. Proliferation of preadipocytes when chronically stimulated with 10 nM DHT or control conditions in (A) EPI and (B) ING cells; n=4/group.

4.6.2 DHT effects on preadipocyte transcriptome

Although the proliferation of preadipocytes was not altered by DHT the transcriptome of 24 hours DHT treated preadipocytes was determined to evaluate whether other pathways are affected by DHT treatment. Preadipocytes were used to ensure the best possible comparability between the ING and EPI fat depots.

The principle component analysis (PCA; Figure 16a) indicated only minor differences between DHT treated cells and controls in both fat depots. However, EPI and ING preadipocyte controls seem to differ in their transcriptome (Figure 16a). The transcriptome analysis identified no significantly altered gene transcripts in EPI preadipocytes treated with DHT compared to controls (Figure 16b). In ING cells only one gene, Serpina3c, was significantly altered and 2.41-fold higher expressed in the DHT treated cells compared to controls (Figure 16c). However, comparing the transcriptome of EPI and ING control cells, 1977 genes were significantly altered. From these, 406 genes were ≥ 2.0-fold higher expressed in EPI controls compared to ING controls, and 69 genes were ≥ 2.0-fold higher in INGs compared to EPI controls (Figure 16d).

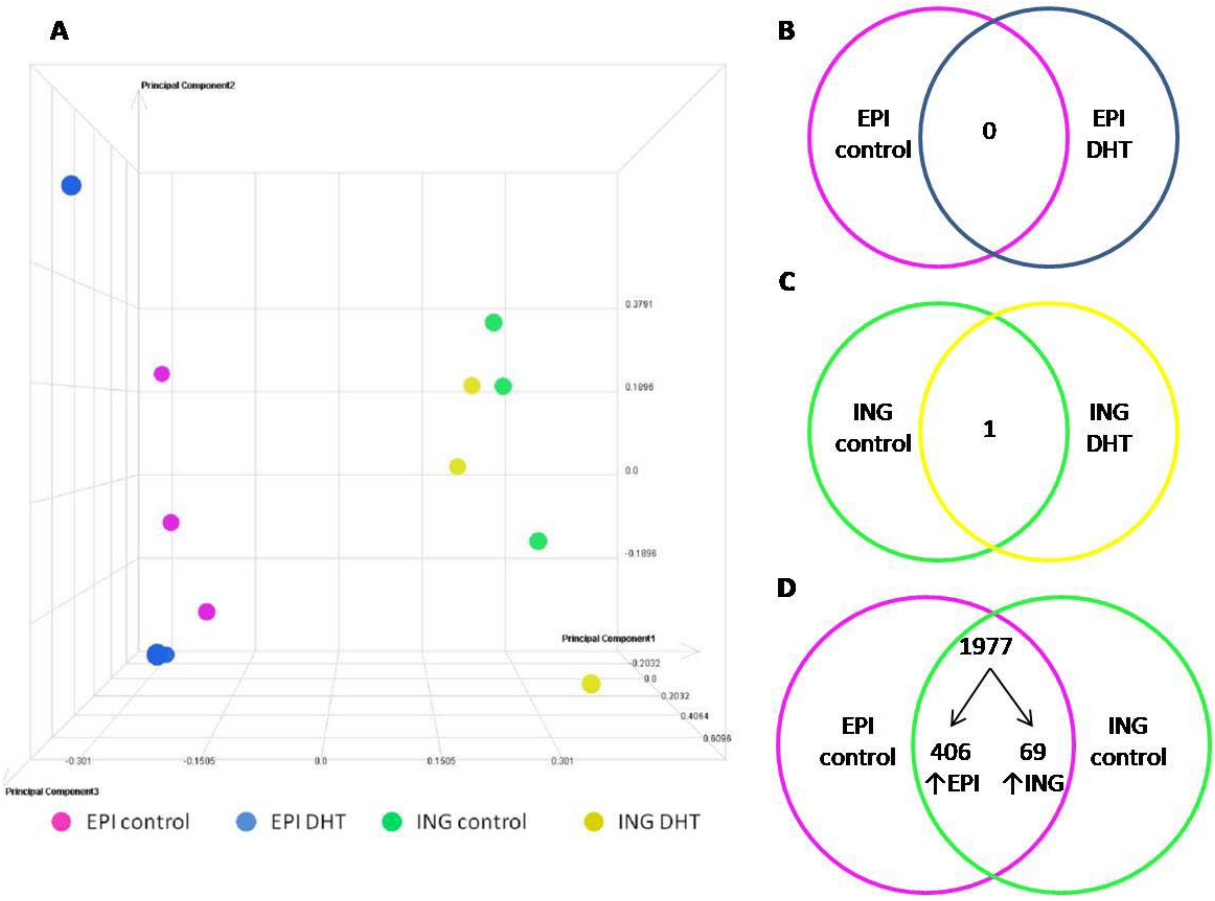

Figure 16 - Effects of 24 hours DHT stimulation on preadipocyte transcriptome in EPI and ING cells. (A) Principle component analysis of EPI and ING preadipocytes, treated for 24 hours with DHT or EtOH control. Venn diagrams representing the transcriptome analysis for (B) EPI control vs. EPI DHT, (C) ING control vs. ING DHT and (D) EPI control vs. ING control preadipocytes. Genes were included when fulfilled following three criteria: $p \leq 0.05$ one-way ANOVA with Benjamini and Hochberg FDR, $p \leq 0.05$ signal correction statistics, and an expression value ratio between the different conditions ≥ 2.0-fold; n=3/group.

The transcriptome analysis, together with the proliferation assay, indicates that DHT has no effect on preadipocytes. Therefore, the DHT effects on adipocyte differentiation were further assessed.

4.6.3 DHT effects on lipid content

Next, effects of chronic DHT stimulation on adipocyte differentiation were determined. Therefore, the degree of adipocyte differentiation was analyzed by visualizing the lipid content of formed mature adipocytes with an Oil Red O staining.

For the ING depot no changes in lipid content were detectable in the DHT treated cells compared to controls (Figure 17c, d). DHT treatment in the EPI cells seemed to decrease lipid content at day 6 (Figure 17a) although quantification was not significant (Figure 17b).

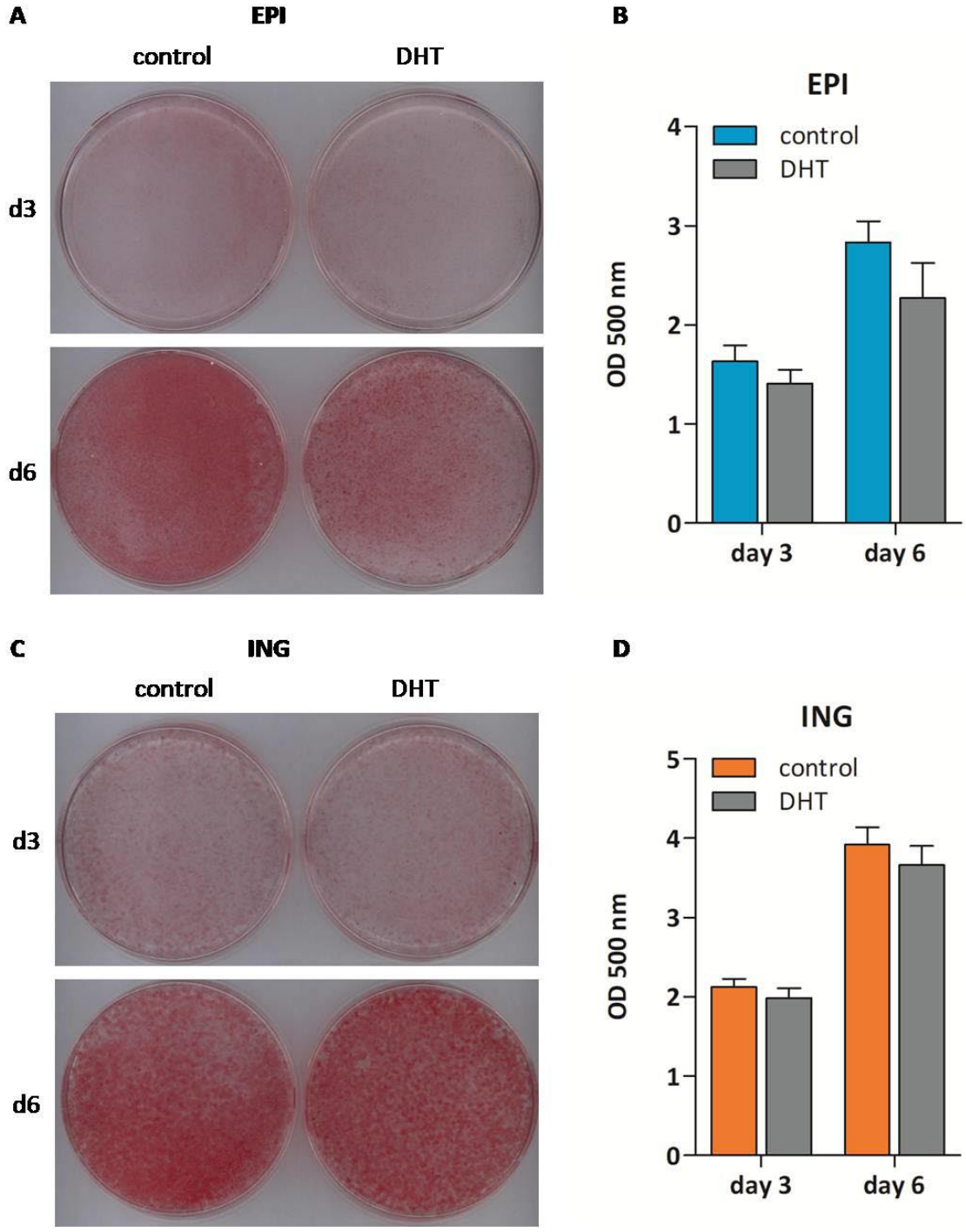

Figure 17 – Effects of chronic DHT stimulation on lipid content in EPI and ING adipocytes. (A,C) Representative Oil Red O staining and (B,D) quantification for control and 10 nM DHT treated cells at days 3 and 6 of adipocyte differentiation in (A, B) EPI and (C, D) ING cell lines, n=6/group.

4.6.4 DHT effects on adipogenesis marker proteins

Following Oil Red O staining, the degree of adipocyte differentiation was specified by analyzing characteristic protein markers for the different phases of adipogenesis to determine the developmental status of the cells during adipocyte differentiation. PREF-1 was used as an early phase marker, C/EBPβ as a marker for the intermediate phase and A-FABP as a late phase marker.

Western blot analysis of PREF-1 showed the expected decline of PREF-1 levels during adipogenesis in both cell lines. In the ING cells no differences between DHT treated cells and controls were detectable (Figure 18b). In EPI cells, western blots indicated a higher PREF-1 protein concentration in the DHT treated cells compared to the controls in particular at day 4 and day 6 (Figure 18a).

The C/EBPβ protein levels showed the expected peak in the intermediate phase of adipogenesis in both fat depots. In the ING cells, no differences between DHT treated cells and controls were detectable (Figure 18d), whereas in the EPI cells C/EBPβ protein levels seemed to be decreased in the DHT treated cells at day 0 and day 2 (Figure 18c).

As expected, the protein levels of A-FABP increased during adipocyte differentiation in both fat depots. Nevertheless, A-FAPB protein levels were not affected by DHT treatment compared to controls in the ING cell lines (Figure 18f). In the EPI cells, A-FABP protein concentration tended to be lower in DHT treated cells compared to the controls at day 4 and day 6 (Figure 18e).

PREF-1, C/EBPβ and A-FABP protein levels showed a trend to be altered by DHT treatment in EPI cells and together indicating a decelerated adipocyte differentiation under these conditions. However, statistical analysis revealed no significant alterations.

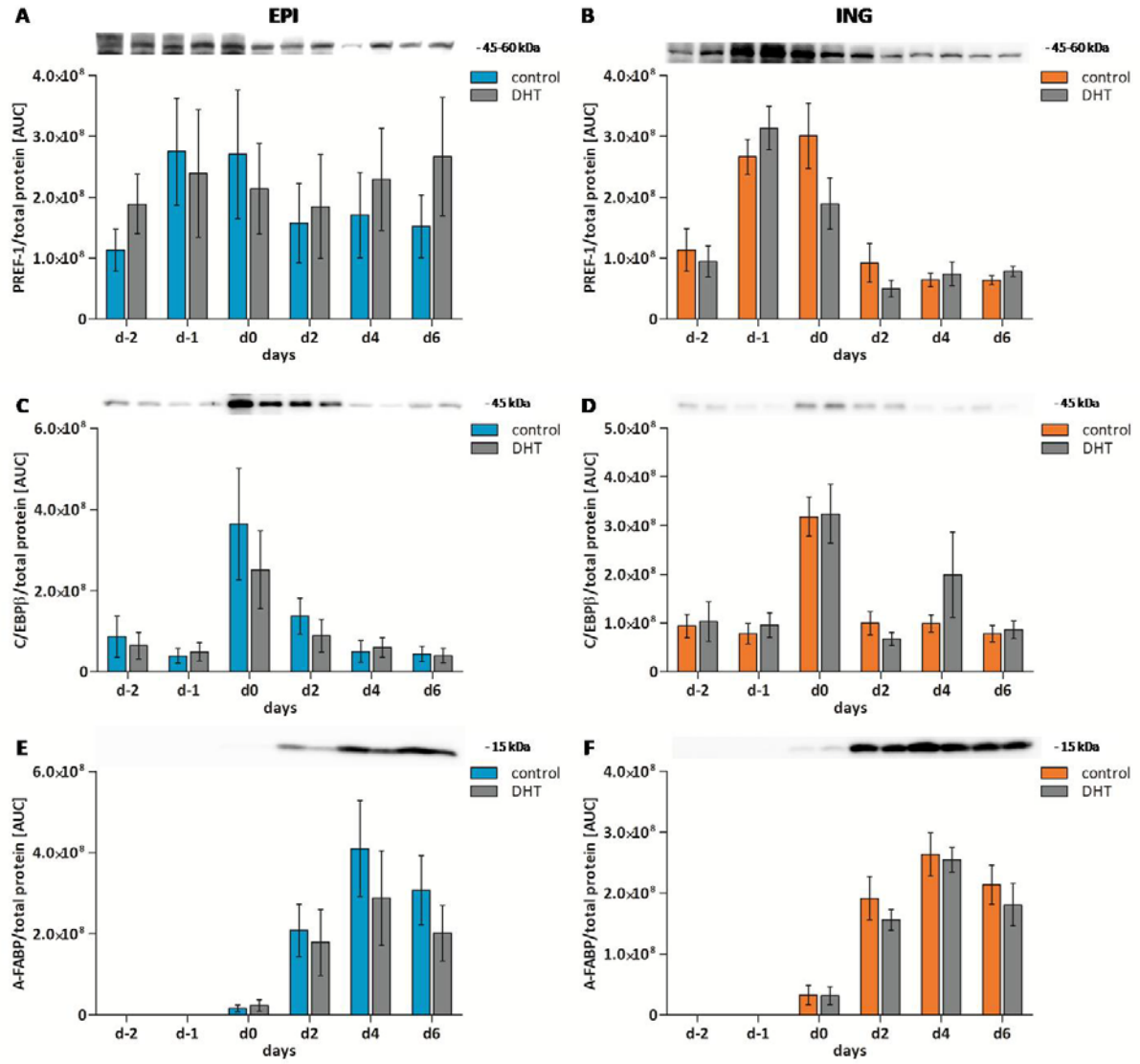

Figure 18 - Effects of chronic DHT stimulation on adipogenesis marker in EPI and ING adipocytes. Quantification and representative western blot for (A, B) PREF-1, (C, D) C/EBPβ and (E, F) A-FABP protein levels in chronically 10 nM DHT stimulated cells compared to controls in murine (A, C, E) EPI and (B, D, F) ING cell lines at days -2, -1, 0, 2, 4 and 6 of adipocyte differentiation, n=4-6/group. Total protein blots for normalization see supplementary Figure S2.

Results so far might suggest a fat depot-specific effect of DHT on EPI adipocyte differentiation. To identify a possible underlying mechanism the androgen receptor expression and localization upon DHT treatment in both adipose tissues were further analyzed.

4.7 Androgen receptor expression and localization

4.7.1 DHT effects on androgen receptor protein levels

Binding of androgens to the androgen receptor (AR) should lead to a stabilization of this transcription factor by preventing its degradation [279]. Hence, the DHT effects on AR expression and stabilization were studied in both adipose tissues by western blot.

In the EPI cells the AR expression peaked at day 2 of differentiation and was significantly elevated in the DHT treated cells at all time points of differentiation compared to control cells (Figure 19a), suggesting a response of these cells to the DHT treatment. In contrast, AR expression in ING cells was constantly increasing during differentiation and showed a significant increase only at days -2, 4 and 6 of adipocyte differentiation when treated with DHT (Figure 19b), leading to the assumption that the ING cells might not be able to respond as good as EPI cells to the DHT treatment.

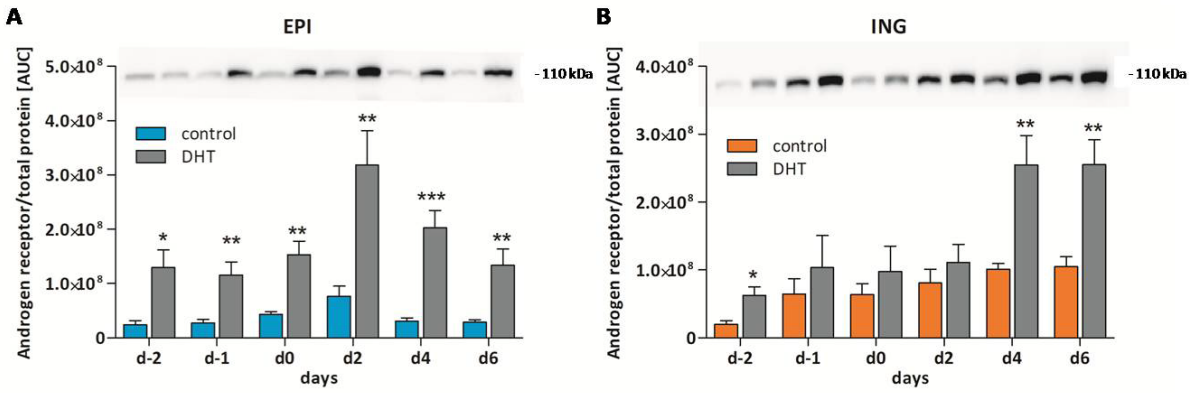

Figure 19 – Effects of chronic DHT stimulation on androgen receptor expression and stabilization in EPI and ING cells. Quantification and representative western blot for androgen receptor (AR) protein levels in chronically 10 nM DHT stimulated cells compared to controls in murine (A) EPI and (B) ING cell lines at days -2, -1, 0, 2, 4 and 6 of adipocyte differentiation, n=5/group. Total protein blots for normalization see supplementary Figure S3.

Thus, this analysis unveiled a different AR expression pattern between the both fat depots under control conditions and indicated a better response of EPI cells to DHT treatment.

Since the AR acts as a ligand-dependent transcription factor, the translocation to the nucleus upon DHT treatment was assessed in preadipocytes and mature adipocytes by immunocytochemistry in both fat depots.

4.7.2 DHT effects on the cellular androgen receptor localization

With immunocytochemical staining the sub-cellular (nucleus and/or cytoplasm) localization of a protein of interest within cells can be visualized by the formation of a brown colored product. Here, the AR localization and its conceivable translocation to the nucleus after 24 hours DHT stimulation should be visualized in preadipocytes and mature adipocytes in both fat depots.

The negative controls (without primary antibody) revealed, as expected, no brown staining of the cells in any sub-cellular compartment in all four tested conditions (preadipocytes (pre) and mature adipocytes (mat) in both fat depots EPI and ING) (Figure 20). The positive controls were stained against Lamin A, which is expected to be located in the nucleus of the cells (Figure 20). The positive staining in all four conditions showed that the permeabilization of the nucleus worked and that a conceivable translocation of the AR to the nucleus would be detectable.

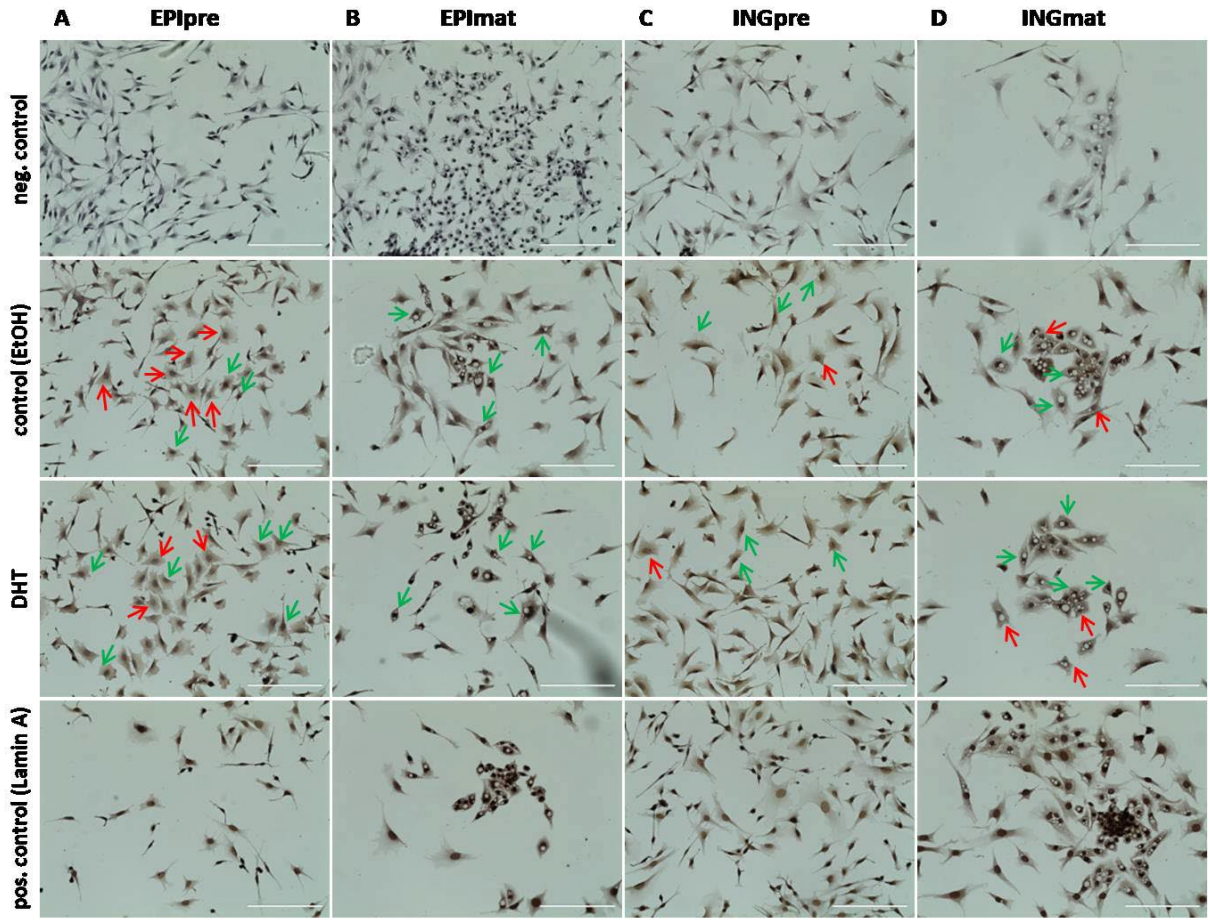

Figure 20 - Effects of DHT stimulation on androgen receptor localization in EPI and ING cells. Representative ICC staining of androgen receptor (AR) protein in 10 nM DHT stimulated cells compared to controls (EtOH) as well as negative control (neg. control; without primary antibody) and positive control (pos. control; stained to nucleus-located Lamin A) in murine (A) EPI preadipocytes (EPIpre), (B) EPI mature adipocytes (EPImat), (C) ING preadipocytes (INGpre) and (D) ING mature adipocytes (INGmat). Green arrow = nucleus positive staining; red arrow = nucleus negative staining; 20X magnification, white bar = 200 µm; n=6/group.

All analyzed conditions showed AR positive staining in the cytosolic fraction (Figure 20). Thus further analysis was concentrated on whether the nucleic compartment showed positive AR staining (nucleus positive) or not (nucleus negative).

Table 2 - Quantification of nucleic AR staining in cytosolic AR positive cells. (*) significantly different between EtOH controls and DHT treated cells.

AR ICC staining	Nucleus Negative	Nucleus Positive
EPIpre control	61%	39%
EPIpre DHT	28%	72% **(*)**
EPImat control	18%	82%
EPImat DHT	24%	76%
INGpre control	13%	87%
INGpre DHT	10%	90%
INGmat control	43%	57%
INGmat DHT	40%	60%

The ratio of AR nucleus positive to AR nucleus negative cells did not differ between the DHT treated cells and controls in EPI and ING mature adipocytes as well as in ING preadipocytes (Table 2). Only in EPI preadipocytes DHT treatment led to a significantly increased AR staining in the nucleus compared to controls, indicating a higher AR translocation to the nucleus upon DHT treatment.

In summary, DHT does not seem to affect proliferation in both depots but might negatively affect EPI differentiation. The response to DHT was higher in the EPI cells, as determined by AR stabilization. Also AR translocation upon DHT treatment only seems to occur in EPI preadipocytes but not in ING cells (see 4.6).

5 Discussion

The aim of the study was to identify new microRNAs that could be considered as species-independent general or as fat depot-specific regulators of adipocyte differentiation and by this shed more light onto the underlying mechanisms of adipogenesis. To achieve these aims an unsupervised microRNA array approach was used. The results were restricted to common microRNAs derived from primary mouse and human adipocytes from subcutaneous and visceral WAT depots. They were further functionally tested in fat depot-specific, immortalized mouse EPI and ING cell lines and in hMSC from a subcutaneous depot. Among the microRNAs characterized two novel microRNAs, miR-708-5p and miR-193a-3p, emerged as previously undescribed in adipocytes and potentially serving as regulators of adipocyte differentiation (see 4.1). Further functional characterization using an antagomir approach and direct tests of metabolic function revealed that miR-708-5p seems not to play an active role in adipocyte differentiation (see 4.2), lipid storage and mobilization as well as their endocrine function (see 4.4). However, miR-708-5p might be regulated by androgens (see 4.5). In contrast, miR-193a-3p was identified to serve as a novel inhibitory regulator of adipogenesis in EPI WAT (see 4.2).

5.1 MicroRNAs and regulation of adipogenesis

Several previous studies described a regulatory role of microRNAs in adipogenesis. Most of these studies focusing on single microRNAs with proposed pro- or anti-adipogenic properties. Among these, miR-103, miR-143, miR-221, miR-222, miR-378 and the miR-17-92 cluster are well established microRNAs described to promote adipogenesis whereas miR-130, miR-138, miR-155 and miR-27a/b are associated with an inhibitory role [228-231, 280-283]. Almost all of them are restricted either to cell culture (e.g. 3T3-L1, hMSCs) or *in vivo/ex vivo* models derived from a given animal species (e.g. mouse, rat, cattle, pig, human) or compare control vs. a diseased cohort in a human model. Generalization from these data is not easy because of the restriction to a single species or cell specific model. In contrast, the microRNA array approach in the present study attempts to overcome these restrictions. The present approach contrasts to that by combining different species and an *ex vivo* approach to fat depot-specific cell lines. The latter appears to be indispensable due to their ability to map a dynamic process like adipogenesis which can only incompletely be captured in a steady state situation like in

an *ex vivo*/*in vivo* approach. Another advantage of the present cell culture model is that it allows the fat depot-specific analysis of adipocyte function. This has not been studied in previous studies using the 3T3-L1 cell line as a fat cell model which does not allow to distinguish between inguinal and epididymal fat cells. In addition, inclusion of human adipocytes derived from human subcutaneously isolated MSCs helped to generalize at least for the subcutaneous human depot. It thus adds more confidence to the underlying approach to identify and verify potential microRNA candidates.

The single model approach used in most previous studies identified a higher number of candidate microRNAs. Indeed, this could be confirmed in the analysis of the present results taken from a given depot or a single species (mouse/human) which yielded many more microRNAs exceeding the preset threshold of a 2-fold positive or negative change when comparing preadipocytes and mature fat cells (see Table S1 – S4). When mouse and human primary adipocytes from healthy donors were compared and when additionally microRNA expression in the two WAT depots EPI and ING were included the number of candidate microRNAs expectedly dropped dramatically. But especially this may lead to important new, species-independent findings as discussed below. On the other side the approach highlights also potential limitations as demonstrated by the ambiguous results obtained for microRNAs miR-378a and miR-146b. At variance to the results of many other studies [255, 256, 258, 259, 268-270] miR-378 changes between preadipocytes and mature fat cells did not exceed the preset threshold. They were thus not formally included in the final array output because the threshold expression changes were only exceeded in the human primary adipocytes but not in the corresponding mouse data sets (see Table S1-S4). However, when mouse and human cell culture models were directly tested for the expression of miR-378a a significant increase during adipogenesis was detected (see Figure 5) supporting the importance of this microRNA in the present study. This finding is well comparing to previous data [268, 270]. Similarly, miR-146b has been described to promote adipogenesis in 3T3-L1 adipocytes [273] and the differentiation of human visceral preadipocytes [257]. In addition, Shi *et al.* showed that miR-146b was highly expressed in mature adipocytes and increased in response to TNF-α and IL-6 [274]. Furthermore, miR-146b was upregulated in visceral and subcutaneous adipose tissue from obese humans compared to lean controls [257] as well as in epididymal adipose tissue from high-fat diet induced obese mice [257, 275]. The suspected importance of miR-146b could be confirmed in the present experiments with an increased expression of miR-146b along the differentiation of adipocytes derived from the mouse EPI and ING fat depots (see Figure 5), supporting the validity of the underlying cell culture model. Hence, despite the

initial ambiguous results, these two microRNAs were considered to be corroborating microRNAs for the underlying cell culture system. Nevertheless, these microRNA array results were not formally included as they both violated the preset criteria aimed to minimize the impact of *in vitro* systems and to closely reflect the *in vivo* situation.

The large number of different source material and the limited access to human samples comprise additional limitations and the interpretation of the results must have been done carefully. The first selection was based on *ex vivo* isolated stroma-vascular cells (containing the preadipocytes) and their corresponding mature adipocytes to mimic the *in vivo* situation as close as possible. A potential setback of this technique is that the preadipocyte compartment was not further isolated from the stroma-vascular fraction of the *ex vivo* tissues. This may potentially include contaminations with other cell populations and thus may lead to the detection of candidate microRNAs not specific for preadipocyte. Another potential setback is due to the low number of replicates which increases the likelihood for false positive or negative results. To overcome these restrictions and ambiguities all identified microRNAs were further verified in cell lines derived from mouse EPI and ING fat depots as well as in hMSCs. By this strategy single model restrictions appear to be no longer relevant and the likelihood to define species independent, general microRNA regulators of adipogenesis is greatly increased.

MiR-142-3p and miR-223-3p were significantly higher expressed in preadipocytes compared to mature adipocytes in the microRNA array data set (see Figure 4). This finding was independent of the origin (mouse or human) or the WAT depot (EPI or ING). However, their expression could not be confirmed in the respective cell lines. The finding may be explained as a cell line-specific alteration induced potentially by interference between the expression of the respective microRNAs and the SV40 transfection used for immortalization of the cells. It could alternatively be viewed as a false positive result identified by the microRNA array. However, as previous studies described them in the context of adipose tissue, miR-142 is likely to play a role in adipocyte regulation. It appears to be regulated by dietary fatty acid composition in ovine adipose tissue samples [284] and by high-fat diet in mouse EPI fat depot [275]. Whether miR-142 has a direct impact on adipocyte differentiation is not known yet and still needs to be examined. MiR-223 has extensively been described to play a role in insulin resistance [285-287] in the context of obesity [288] and with this in the regulation of adipose tissue macrophage polarization from classic to alternative activation [287, 289, 290]. Thus, miR-223 might rather influence adipose tissue development under pathophysiological than

physiological conditions. That might be supported by the underlying results as only lean, metabolically healthy donors were used in this study here.

In summary, the strategy used here to identify new microRNAs revealed multiple advantages, especially by validating results via a cross-species approach but despite that suffers a number of limitations. Nevertheless, its potential to identify new general adipogenesis regulators indeed lead to several interesting microRNAs as a result of the current study.

5.2 MiR-708 and regulation of adipogenesis

Among the microRNAs identified by the multistep approach, miR-708 was of high potential because it is positively associated with adipocyte differentiation and was not previously described to be involved in adipogenesis. Furthermore, due to its initially very low expression in preadipocytes and its rapid increase following the induction of differentiation it fulfilled the criteria for a candidate microRNA generally governing mouse and human adipogenesis (see Figure 5). This idea is further supported by data suggesting a role of miR-708 to induce a switch between adipogenesis and osteogenesis. In osteogenesis miR-708 via SMAD-dependent signaling inhibits osteogenic differentiation of hMSCs, a process generally fitting to the present results in adipocytes [291].

Adipogenesis is divided in different phases. It starts with the commitment of mesenchymal stem cells to develop into preadipocytes and thereafter to differentiate to mature adipocytes with the characteristic adipose tissue phenotype and functions. As miR-708-5p is not expressed in preadipocytes and only increased after induction of differentiation (see Figure 5) the focus was led to the later stages of the differentiation process. An effective inhibition of miR-708-5p by using a specific miR-708-5p inhibitor (antagomir) did not change the differentiation process. Hence, these analyses revealed no obvious causal role of miR-708-5p for the progress of differentiation neither when judging differentiation by genetic markers nor phenotypically. With the protocol used the specific antagomir and its control are transfected 24 h before the induction of differentiation. Eearly markers of adipogenesis like PREF-1 are not expected to be altered within this time frame. PREF-1 physiologically drops quickly to undetectable levels within the first days following induction of differentiation. Hence, to evaluate the differentiation process, the current work concentrated on intermediate (e.g. C/EBPβ) and late (e.g. A-FABP) molecular markers of adipogenesis. The results of functional testing in this study using a specific miR-708-5p inhibitor argued against a role of

miR-708 in adipogenic differentiation. The significantly increased C/EBPβ protein level at day 2 and day 4 only in ING cells, compatible with altered adipogenesis, might be viewed as an important effect. However, as they are not paralleled by compatible alterations in A-FAPB protein expression in western blot analysis they were not regarded as relevant (see Figure 8). This was supported by the general results obtained by Oil Red O staining which showed no changes at any time point of differentiation (see Figure 7). Additionally, these changes on C/EBPβ or any changes in the differentiation process were not confirmed in EPI cells. Hence, given that the intermediate and late adipogenesis markers C/EBPβ and A-FABP are not consistently altered by miR-708-5p inhibition an exclusive role of miR-708-5p on adipocyte differentiation *per se* appears unlikely.

However, the parallelism of miR-708-5p expression with the maturation process of adipocytes still suggests a possible functional role of this microRNA in the mature adipocytes. Thus, the involvement of miR-708-5p in adipocyte key functions like lipolysis, glucose uptake and lipogenesis (see Figure 10 and 11) as well as in adipokine expression (adiponectin, leptin and IL-6; see Figure 12) was assessed in a loss-of-function approach employing the specific antagomir in comparison to a control transfection. The results indicate that none of these functions were altered by miR-708-5p inhibition in hMSCs and murine cell lines. As both, radioactive glucose uptake and lipogenesis methods were not yet established for mouse cell lines according to the hMSC protocol a further detailed analysis in these cell lines was waived because of time constraints. It remains therefore an open question whether miR-708-5p may have depot-specific effects, particularly on visceral fat depots where no human cell line was available. Thus, a role of miR-708-5p effects on glucose uptake and/or lipogenesis cannot be answered conclusively. In contrast, lipolysis was determined in human and murine cells. Isoprenaline, a synthetic catecholamine, was first choice to assess stimulated lipolysis, due to its selectivity to bind to β-adrenergic receptors important for the stimulation of lipolysis. In neither of the cell lines miR-708-5p inhibition revealed any effects on lipolysis under basal as well as isoprenaline stimulated conditions compared to control transfected cells also when tested over a wide concentration range (see Figure S4). This indicates that miR-708 does not target lipolysis in any of the tested cells. However, it cannot be ruled out that the physiological catecholaminergic stimulator, norepinephrine, might exert different effects under miR-708-5p inhibition because his action is mediated by α- and β-adrenergic receptor pathways [292]. Furthermore, the endocrine function assessed by adipokine expression was not directly altered by miR-708-5p inhibition as tested for adiponectin, leptin and IL-6. However, an indirect effect of miR-708-5p on adipokines e.g. on peripheral metabolism or

secretion cannot be excluded. In conclusion, a role for miR-708-5p in lipolysis, lipogenesis and glucose uptake as well as on the expression of important adipokines could not be revealed.

The interpretation of these findings may be hampered by a potential interaction of miR-708-5p with other microRNAs or its replacement by other microRNAs. It is well known that microRNAs may act synergistically to modulate a given output [208-210]. Also a compensatory role seems possible as mRNAs can be targeted by different microRNAs [205]. If miR-708-5p is only active in cooperation with another microRNA it will not necessarily be expected that a selective inhibition of miR-708-5p results in a clear alteration in adipose tissue development and function. This would also be the case if miR-708-5p loss was compensated by other microRNAs. One possible candidate microRNA that might act synergistically or compensatory could be miR-5579. MiR-5579 is transcribed from the same gene locus as miR-708 within the Tenm4 gene transcript [293];[I]. MiR-5579 was not under the microRNA array candidates arguing against a specific role for it in adipose tissue development. Nevertheless, for time constraints a formal test of any interaction with miR-708-5p or its compensation was not possible.

Finally, the question arises, whether miR-708-5p exerts a regulatory role in MSC lineage commitment or clonal expansion of preadipocytes. In previous studies, miR-708 was described to be regulated by dexamethasone, a component of the induction cocktail used to initiate differentiation. Thus, as miR-708-5p might be regulated by dexamethasone as it is in C2C12 [294], cancer cells [295] and hMSCs [291] and exerts a role in the inhibition of osteogenesis [291] it potentially may serve as a very early regulator in the osteogenic-adipogenic switch or in the clonal expansion of preadipocytes. Dexamethasone, a synthetic product selectively acting on the GR and used in pharmacological dose, is widely used *in vitro* to initiate and synchronize adipocyte differentiation. But as cells do not differentiate *in vitro* without dexamethasone in the induction cocktail a conclusive, dexamethasone-dependent role for miR-708-5p in adipocyte differentiation can hardly be determined and remains elusive. In addition, studies are inconsistent in the way dexamethasone regulated miR-708-5p expression. As in hMSCs [291] miR-708-5p was upregulated by dexamethasone but downregulated in C2C12 cells [294] making it difficult to define a clear mode of action between dexamethasone and miR-708-5p. In this sense, it might also be possible that the increased expression of miR-708-5p after induction of differentiation is only a byproduct of dexamethasone treatment but lacks physiological relation to adipocyte differentiation *per se*.

However, a regulatory role of miR-708-5p in clonal expansion could in part explain the large expression differences seen between preadipocytes and mature adipocytes in this study. Any putative mechanism underlying this and explaining dependence on dexamethasone, shown to be less important during mitotic expansion but rather to establish the postmitotic adipocytes [296], needs further detailed investigations which were not possible here due to time constraints. A role in lineage commitment of miR-708-5p as well remains elusive. But the underlying murine cell culture model used here is inappropriate to study lineage commitment as it is already primed to the adipogenic lineage and lost its stem cell properties.

5.3 Androgens, miR-708 and fat depot-specific regulation of adipogenesis

Under physiological, not pathophysiological conditions androgens may be more important for the regulation of adipogenesis as suggested by the well known, large gender differences [297-299]. Previous studies have already proposed that androgens may act on microRNA expression to regulate androgen dependent biological processes, including fat cell differentiation. This was shown by Kraus *et al.* who convincingly demonstrated that the androgen-regulated microRNA miR-375 inhibited adipogenic differentiation in human SGBS cells [300]. To test a comparable effect for miR-708-5p on adipogenesis it was elucidated whether the highly potent androgen, DHT, directly affects miR-708-5p expression or whether an indirect effect on adipocyte differentiation is present.

The results showed ambiguous results of androgens on miR-708-5p expression as well as on EPI and ING differentiation not fully in line with previous studies. This may allow different ways of interpretation depending on the prioritization of the different results.

Chronic DHT stimulation significantly decreased miR-708-5p expression following initiation of the differentiation process in both, EPI and ING cell lines (see Figure 14). This may be explained by a direct inhibitory effect of DHT on miR-708-5p expression. It would be supported by the results that DHT did not significantly altered EPI and ING differentiation as determined by Oil Red O staining and western blot analysis in both fat depots of the cell culture model (see Figure 17 and 18). Furthermore, proliferation of preadipocytes was not altered by a chronic DHT stimulation when compared to controls, further supporting a direct effect of DHT on miR-708-5p expression. These findings, however, contrast to previous studies indicating a regulatory role of androgens on adipogenesis [93-95, 159, 170-173]. These rather fit to an indirect effect of DHT on miR-708-5p expression simply due to an

attenuated adipogenesis paralleled by a delayed increase of miR-708-5p expression due to delayed differentiation of the cells. [232]. For this may further argue that an acute DHT stimulation did not alter miR-708-5p expression within the first 8 hours of treatment (see Figure 13). Moreover, the lack of a direct DHT effect on the transcriptome of EPI and ING cells within the first 24 hours of DHT stimulation augmented the assumption that DHT might not directly affect miR-708-5p expression (see Figure 16). However, this line of interpretation ignores that neither proliferation (see Figure 15) nor differentiation (see Figure 17 and 18) of EPI and ING cells were significantly altered by DHT stimulation in this study. In summary, the present data do not satisfyingly support either interpretation.

Currently no data are available on the dynamics of miR-708-5p expression and its turnover. Therefore, the time span of 8 hours may be too short and insufficient to judge any acute effect of DHT on miR-708-5p expression and might explain these discrepancies between the chronic and acute DHT stimulation results. However, prolongation of the time span up to 24 hours might not further reveal any effects as indicated in the transcriptome experiment which showed no differences between controls and DHT treated cells after 24 hours.

It needs to be considered, that the androgen response might further depend on the dose. However, a DHT concentration of 10 nM was used throughout all experiments to potentially achieve comparable results to other studies as they used this DHT concentration as well to test androgen effects on adipocytes [170, 300, 301].

As an important control the expected stabilization of the AR under chronic DHT treatment as well as its translocation to the nucleus by acute DHT treatment was investigated using western blot (see Figure 19) and immunocytochemistry (see Figure 20 and Table 2), respectively. Both cell lines showed a different response to chronic DHT stimulation. These findings support several studies proposing an inhibitory effect of DHT on adipogenic differentiation of hMSCs as well of human primary cells derived from abdominal subcutaneous, mesenteric and omental fat depots in males [170], of abdominal subcutaneous adipose-derived stem cells in women [171] and of abdominal subcutaneous and omental primary human cell cultures in both sexes [172]. They are further in line with data using 3T3-L1 [159] and C3H10T1/2 [173] cell lines showing an exerted inhibitory effect of DHT on adipocyte differentiation. From these studies it appears that androgens have a predominant effect on the epididymal/visceral fat depot compared to inguinal/subcutaneous cells [93-95]. This might be explained by a higher expression of the AR in these fat depots [302-306]. This is in line with the data shown in this study. The expression of the AR and its stabilization by

DHT differed between both fat depots. In ING cells AR expression increased with adipogenesis, whereas EPI cells rather showed a peak of AR expression in the intermediate phase of adipogenesis. This is supported by the study of Blouin *et al*. who detected a higher expression of AR during adipogenesis of abdominal subcutaneous but not omental primary fat cell of women [305]. This finding was contrasted by Dieudonne *et al*. who described a decreasing AR expression during adipogenesis. Nevertheless, the significant upregulation of AR by androgen stimulation, in particular in the EPI cells, can be confirmed by other studies as well [170, 303]. These results suggest a different ability of ING and EPI cells to respond to androgen stimulus due to a diverse AR expression during the differentiation process. Thus, androgens might be able to influence ING differentiation at later time points of differentiation as well compared to EPI cells where AR expression peaks at the intermediate phase. However, the AR expression in both cell lines might not be sufficient enough to induce DHT-mediated signaling as Hartig *et al.* showed that in 3T3-L1 cells inhibitory effects of androgens were only observed when AR was overexpressed in these cells [301]. The immunocytochemical analysis of AR localization in the nucleus upon DHT stimulation was only significantly increased in EPI preadipocytes but not in EPI mature adipocytes or ING cells. These findings indicate an AR response to DHT only in EPI preadipocytes. Together with the results of the transcriptome study these observations raise the question whether AR translocation to the nucleus, as seen in EPI preadipocytes, has any functional impact. But again, whether AR expression *per se* in EPI and ING cells is sufficient enough to respond to DHT and by this mediating an AR translocation to the nucleus still remains elusive. To shed more light on this, a luciferase reporter-gene assay for AR activation in the adipocytes was designed. But due to inappropriate transfection efficiencies the results of these experiments could not be considered. Within the time period of the project we were not able to establish a protocol for plasmid transfection for the underlying adipocyte cell culture model and thus missed to clarify this question.

As shown and discussed above, whether miR-708-5p expression changes were directly regulated by DHT treatment or were only a byproduct of an altered adipocyte differentiation is difficult to clarify in particular in the context of other previous studies. A clear role for miR-708-5p in the context of adipose tissue development and function could also not be confirmed here, although many possibilities were tested. Thus, in regard to the aim of the study to identify potent general or fat depot-specific regulators of adipogenesis, miR-708-5p first identified as a potential candidate, might be rather a byproduct of adipogenesis than an effector.

5.4 MiR-193a and fat depot-specific regulation of adipogenesis

In contrast to miR-708-5p microRNA miR-193a-3p appears to play a new, not previously described, inhibitory role on EPI adipocyte differentiation. MiR-193a-3p negatively modulates adipogenesis as its inhibition by a specific miR-193a-3p antagomir enhanced the differentiation of EPI cells. This was characterized by significant changes of differentiation markers like C/EBPβ and A-FABP (see Figure 8) as well as increased lipid content (see Figure 7). Interestingly and in line with this findings, the expression of miR-193a-3p was also down-regulated when human adipocyte derived stem cells were forced into osteogenesis [307], indicating that full differentiation in both cells depend on a low level of the microRNA. A similar role of miR-193a-3p in maintaining a proliferative potential of cells and inhibiting complete differentiation has been recently suggested in other studies not focusing on adipocytes. Wang *et al*. showed that miR-193 is important for maintaining the proliferative capacity of bone mesenchymal stem cells by targeting the inhibitor of growth protein 5 mRNA [308]. A comparable pro-proliferative role for miR-193a was described in human endothelia cells [309] as well as in various cancer models such as ovarian, lung cancer and myeloid leukemia cells [310-312].

The microRNA expression profiles for miR-193a-3p indicate a higher expression in the ING cells compared to EPI cells when semi-quantitatively compared in RT-qPCR experiments (see Figure 5). In contrast to the consequent expectation that ING differentiation might be more affected by miR-193a-3p, an exclusive regulatory role for miR-193a-3p in the EPI adipogenesis was identified. These results preliminary contra-intuitive not necessarily exclude each other since the transcriptome not always equals the proteome or functional output of a cell. This is also true when comparing mRNA expression analysis (e.g. by PCR) to the respective protein concentrations (e.g. by western blot). Changes in mRNA expression are not always reflected in the protein concentrations and *vice versa*. This might be the case for miR-193a-3p as well. Its functional impact on EPI adipogenesis does not necessarily requires higher miR-193a baseline expression in these cells compared to ING cells. Furthermore, it is well known that epididymal and subcutaneous adipose tissue, although similar in their basic functions, also exert different properties [85], e.g. lipid turnover, metabolic risk factor. In this sense, also the sensitivity and response to transcriptional and translational changes might be different between cells from different fat depots. In addition, the transcriptome analysis of EPI and ING preadipocytes in this study already identified differences in their transcriptome expression levels (see Figure 16). From this one could further speculate that they also differ in

their behavior or response to different stimuli which would support the findings of the microRNA expression profiles as well as the results for miR-193a-3p effects on EPI, but not ING, differentiation. This result is further supported by the findings of Chen *et al.* who showed that the expression of the miR-146b target KLF7 was only changed in human visceral obesity, although miR-146 expression increased in visceral and subcutaneous fat tissues when comparing obese to lean controls [257]. Thus, a fat depot-specific regulation independent of underlying expression profiles is not a unique occurrence of this study.

An *in silico* approach was applied to identify potential targets of miR-193a-3p. Target prediction analysis for miR-193a-3p with subsequently KEGG pathway enrichment analysis included the WNT signaling pathway within the top 10 predicted pathways (see Table 1). The WNT signaling pathway is known to play an important role in developmental processes and has a leading role in the determination of mesenchymal stem cells either to osteogenic or adipogenic lineage [122, 151-153]. Some of the predicted targets for miR-193a include proteins that are either directly part of the β-catenin destruction complex (e.g APC2, DKK2) or indirectly alter canonical WNT signaling by interaction with β-catenin degradation through ubiquitination pathway (e.g Fbxw11, SIAH1a, SIAH1b) [151-153]. Thus miR-193a-3p might regulate proliferation by targeting WNT pathway antagonists. Gokhale *et al.* showed that in medulloblastoma cell in which WNT signaling is activated due to a point-mutation of β-catenin, the miR-193a was overexpressed, This was associated to a robust overexpression of negative regulators of WNT signaling (WNT inhibitory factor 1, DKK, AXIN2, Naked cuticle 1 and 2) [313]. Target prediction is only helpful to generate ideas about a potential functional context but is never sufficient to draw conclusions. For the underlying target prediction here six algorithms were used for a more reliable prediction. Each one premises different properties among miRNA-mRNA targeting, e.g. complete complementarity, complete complementarity at least in the seed region, number of allowed mismatches, etc. Predicted mouse microRNA targets by at least four algorithms were used for pathway analysis. Here, only KEGG pathway prediction analysis was applied which might lead to an incomplete picture of involved pathways, suggesting that also other pathways than WNT might be prone to explain the miR-193a-3p effects on EPI differentiation.

6 Overview and Outlook

The unsupervised microRNA array approach applied here identified potential microRNAs that might serve as general regulators of adipogenesis, at least in comparison of mice and man. Nine candidate microRNAs were identified, from which two, previous undescribed, microRNAs (miR-193a-3p, miR-708-5p) were further analyzed regarding their potential to regulate adipogenesis.

MiR-708-5p suggested an important role as a general adipogenesis regulator due to its expression pattern in the cell culture models. Its role in adipose tissue function and development could not conclusively been answered in this study. However, its role could be narrowed down by excluding several key components. Loss-of-function experiments showed that miR-708-5p had no direct effect on adipocyte differentiation. Furthermore, lipolysis, glucose uptake and lipogenesis were not affected by miR-708-5p inhibition, suggesting no regulatory role for miR-708-5p characteristic lipid storage and lipid mobilization function of mature adipocytes. Additionally, adiponectin, leptin and Il-6 expression were not influenced by loss of miR-708-5p, indicating that also these endocrine functions of adipocytes are not altered. However, not all adipokines could be tested in this study, thus an impact of miR-708-5p on other adipokines expression as well as secretion cannot fully be excluded and needs further investigations. Finally, the results may suggest that miR-708-5p expression is regulated by androgens. For future studies on miR-708-5p it would be also interesting to further examine its role on the commitment and/or clonal expansion of adipocytes, since previous studies indicate such role for miR-708-5p [291, 294, 295]. In conclusion, the current work suggests a role for miR-708-5p in adipogenesis but only allows to exclude some distinct interactions without defining a clear target of action.

MiR-193a-3p was identified to be a negative regulator of epididymal adipogenesis under physiological conditions. Using target prediction WNT-mediated pathways may serve as potential targets but due to time constraints these hypothesis could not experimentally be verified [313]. Hence prospective studies might be able to unravel the mechanism underlying miR-193a adipogenesis regulation.

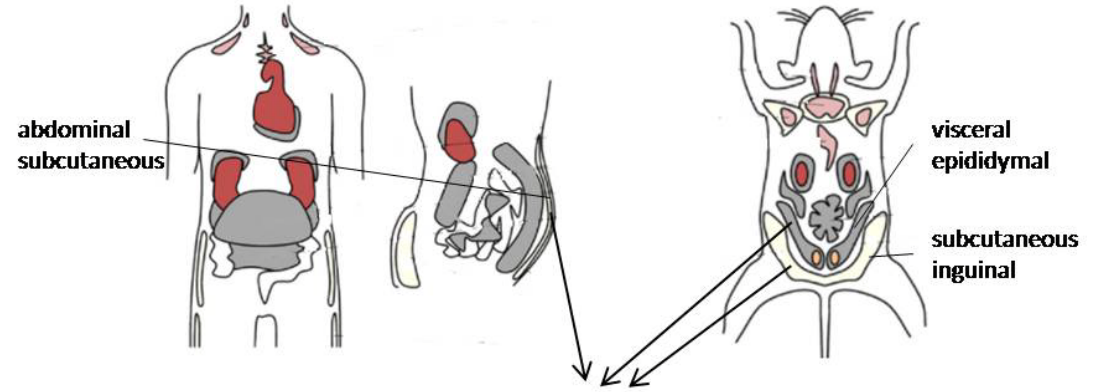

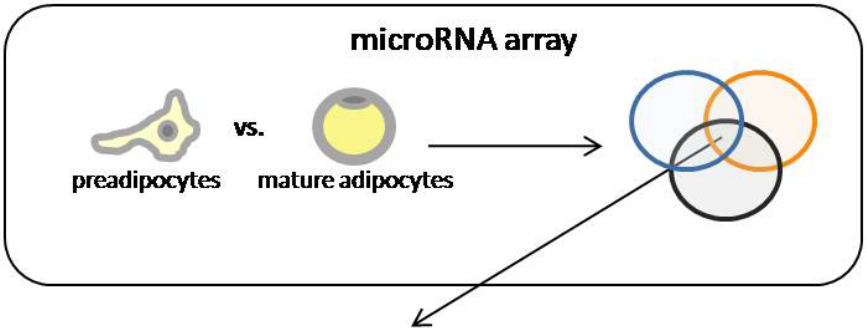

miR-	193a	199a -5p	199a -3p	652	142	223	146b	365a	708
Array	↑	↔	↔	↔	↓	↓	↓	↑	↑
Cell culture	↑	n.d.	n.d.	n.d.	↔	↔	↑	↑	↑
Literature	x	n.d.	n.d.	n.d.	(√)	(√)	√	√	x
analyzed	√	x	x	x	x	x	x	x	√

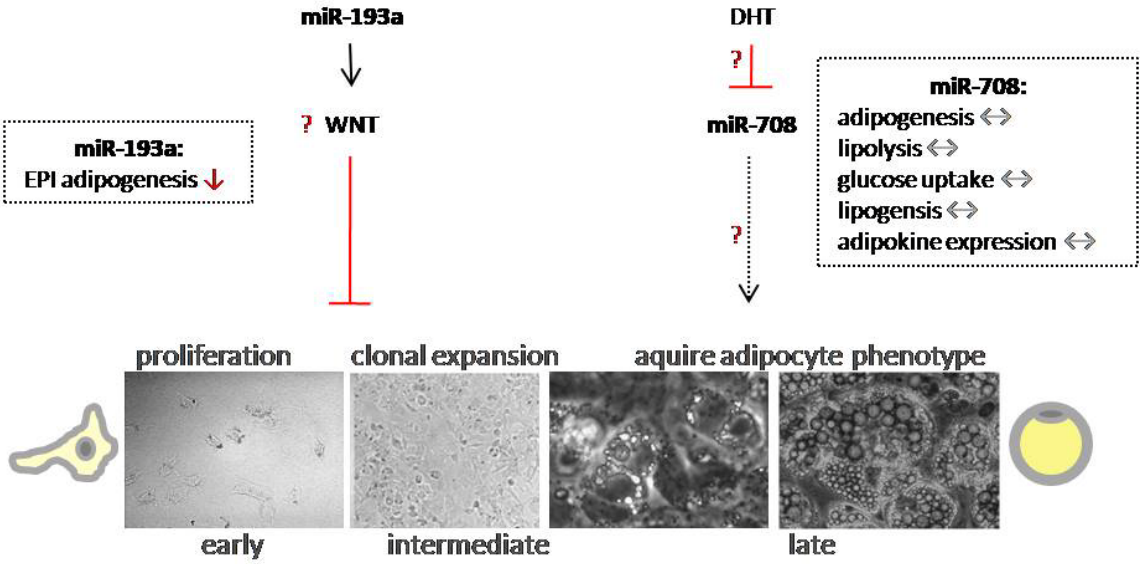

Figure 21 - Schematically depicted main results that answer the underlying question. ↓: downregulated in mature adipocytes or negative regulation; ↑: upregulated in mature adipocytes; ↔: no/controversial expression/regulation; √: yes; x: no/excluded; n.d.: not determined. Human and mouse fat distribution modified from Choe *et al.* 2016 [262].

7 Literature

1. Flegal, K.M., et al., *Association of all-cause mortality with overweight and obesity using standard body mass index categories: a systematic review and meta-analysis.* JAMA. **309**(1): p. 71-82.
2. Kitahara, C.M., et al., *Association between class III obesity (BMI of 40-59 kg/m2) and mortality: a pooled analysis of 20 prospective studies.* PLoS Med. **11**(7): p. e1001673.
3. Mensink, G.B., et al., *[Overweight and obesity in Germany: results of the German Health Interview and Examination Survey for Adults (DEGS1)]*. Bundesgesundheitsblatt Gesundheitsforschung Gesundheitsschutz. **56**(5-6): p. 786-94.
4. Abdalla, M.M., *Central and peripheral control of food intake.* Endocr Regul. **51**(1): p. 52-70.
5. Shimizu, H. and M. Mori, *The brain-adipose axis: a review of involvement of molecules.* Nutr Neurosci, 2005. **8**(1): p. 7-20.
6. Lutter, M. and E.J. Nestler, *Homeostatic and hedonic signals interact in the regulation of food intake.* J Nutr, 2009. **139**(3): p. 629-32.
7. Cowley, M.A., et al., *Leptin activates anorexigenic POMC neurons through a neural network in the arcuate nucleus.* Nature, 2001. **411**(6836): p. 480-4.
8. De Vriese, C. and C. Delporte, *Influence of ghrelin on food intake and energy homeostasis.* Curr Opin Clin Nutr Metab Care, 2007. **10**(5): p. 615-9.
9. Rodin, J., *Insulin levels, hunger, and food intake: an example of feedback loops in body weight regulation.* Health Psychol, 1985. **4**(1): p. 1-24.
10. Allen, Y.S., et al., *Neuropeptide Y distribution in the rat brain.* Science, 1983. **221**(4613): p. 877-9.
11. Hahn, T.M., et al., *Coexpression of Agrp and NPY in fasting-activated hypothalamic neurons.* Nat Neurosci, 1998. **1**(4): p. 271-2.
12. Haskell-Luevano, C., et al., *Characterization of the neuroanatomical distribution of agouti-related protein immunoreactivity in the rhesus monkey and the rat.* Endocrinology, 1999. **140**(3): p. 1408-15.
13. van den Top, M., et al., *Orexigen-sensitive NPY/AgRP pacemaker neurons in the hypothalamic arcuate nucleus.* Nat Neurosci, 2004. **7**(5): p. 493-4.
14. Kalra, S.P., et al., *Interacting appetite-regulating pathways in the hypothalamic regulation of body weight.* Endocr Rev, 1999. **20**(1): p. 68-100.
15. Woods, S.C., et al., *Signals that regulate food intake and energy homeostasis.* Science, 1998. **280**(5368): p. 1378-83.
16. Saltiel, A.R. and C.R. Kahn, *Insulin signalling and the regulation of glucose and lipid metabolism.* Nature, 2001. **414**(6865): p. 799-806.
17. Tilg, H. and A.R. Moschen, *Adipocytokines: mediators linking adipose tissue, inflammation and immunity.* Nat Rev Immunol, 2006. **6**(10): p. 772-83.
18. Zhang, Y., et al., *Positional cloning of the mouse obese gene and its human homologue.* Nature, 1994. **372**(6505): p. 425-32.

19. Kershaw, E.E. and J.S. Flier, *Adipose tissue as an endocrine organ.* J Clin Endocrinol Metab, 2004. **89**(6): p. 2548-56.

20. Virtanen, K.A., et al., *Functional brown adipose tissue in healthy adults.* N Engl J Med, 2009. **360**(15): p. 1518-25.

21. Cannon, B. and J. Nedergaard, *Brown adipose tissue: function and physiological significance.* Physiol Rev, 2004. **84**(1): p. 277-359.

22. van Marken Lichtenbelt, W.D., et al., *Cold-activated brown adipose tissue in healthy men.* N Engl J Med, 2009. **360**(15): p. 1500-8.

23. Bartelt, A., et al., *Brown adipose tissue activity controls triglyceride clearance.* Nat Med. **17**(2): p. 200-5.

24. Bartelt, A., et al., *Thermogenic adipocytes promote HDL turnover and reverse cholesterol transport.* Nat Commun. **8**: p. 15010.

25. Fruhbeck, G., et al., *The adipocyte: a model for integration of endocrine and metabolic signaling in energy metabolism regulation.* Am J Physiol Endocrinol Metab, 2001. **280**(6): p. E827-47.

26. Pittas, A.G., N.A. Joseph, and A.S. Greenberg, *Adipocytokines and insulin resistance.* J Clin Endocrinol Metab, 2004. **89**(2): p. 447-52.

27. Gammeltoft, S. and E. Van Obberghen, *Protein kinase activity of the insulin receptor.* Biochem J, 1986. **235**(1): p. 1-11.

28. Bryant, N.J., R. Govers, and D.E. James, *Regulated transport of the glucose transporter GLUT4.* Nat Rev Mol Cell Biol, 2002. **3**(4): p. 267-77.

29. Kohn, A.D., et al., *Expression of a constitutively active Akt Ser/Thr kinase in 3T3-L1 adipocytes stimulates glucose uptake and glucose transporter 4 translocation.* J Biol Chem, 1996. **271**(49): p. 31372-8.

30. Ng, Y., et al., *Rapid activation of Akt2 is sufficient to stimulate GLUT4 translocation in 3T3-L1 adipocytes.* Cell Metab, 2008. **7**(4): p. 348-56.

31. Leney, S.E. and J.M. Tavare, *The molecular basis of insulin-stimulated glucose uptake: signalling, trafficking and potential drug targets.* J Endocrinol, 2009. **203**(1): p. 1-18.

32. Rowland, A.F., D.J. Fazakerley, and D.E. James, *Mapping insulin/GLUT4 circuitry.* Traffic. **12**(6): p. 672-81.

33. Ahmadian, M., et al., *Triacylglycerol metabolism in adipose tissue.* Future Lipidol, 2007. **2**(2): p. 229-237.

34. Coleman, R.A. and D.P. Lee, *Enzymes of triacylglycerol synthesis and their regulation.* Prog Lipid Res, 2004. **43**(2): p. 134-76.

35. Wong, R.H. and H.S. Sul, *Insulin signaling in fatty acid and fat synthesis: a transcriptional perspective.* Curr Opin Pharmacol. **10**(6): p. 684-91.

36. Rutkowski, J.M., J.H. Stern, and P.E. Scherer, *The cell biology of fat expansion.* J Cell Biol. **208**(5): p. 501-12.

37. Villena, J.A., et al., *Desnutrin, an adipocyte gene encoding a novel patatin domain-containing protein, is induced by fasting and glucocorticoids: ectopic expression of desnutrin increases triglyceride hydrolysis.* J Biol Chem, 2004. **279**(45): p. 47066-75.

38. Zimmermann, R., et al., *Fat mobilization in adipose tissue is promoted by adipose triglyceride lipase.* Science, 2004. **306**(5700): p. 1383-6.

39. Giudicelli, H., N. Combes-Pastre, and J. Boyer, *Lipolytic activity of adipose tissue. IV. The diacylglycerol lipase activity of human adipose tissue.* Biochim Biophys Acta, 1974. **369**(1): p. 25-33.

40. Haemmerle, G., et al., *Hormone-sensitive lipase deficiency in mice causes diglyceride accumulation in adipose tissue, muscle, and testis.* J Biol Chem, 2002. **277**(7): p. 4806-15.

41. Yeaman, S.J., et al., *The multifunctional role of hormone-sensitive lipase in lipid metabolism.* Adv Enzyme Regul, 1994. **34**: p. 355-70.

42. Fredrikson, G., H. Tornqvist, and P. Belfrage, *Hormone-sensitive lipase and monoacylglycerol lipase are both required for complete degradation of adipocyte triacylglycerol.* Biochim Biophys Acta, 1986. **876**(2): p. 288-93.

43. Karlsson, M., et al., *cDNA cloning, tissue distribution, and identification of the catalytic triad of monoglyceride lipase. Evolutionary relationship to esterases, lysophospholipases, and haloperoxidases.* J Biol Chem, 1997. **272**(43): p. 27218-23.

44. Tornqvist, H. and P. Belfrage, *Purification and some properties of a monoacylglycerol-hydrolyzing enzyme of rat adipose tissue.* J Biol Chem, 1976. **251**(3): p. 813-9.

45. Vaughan, M., J.E. Berger, and D. Steinberg, *HORMONE-SENSITIVE LIPASE AND MONOGLYCERIDE LIPASE ACTIVITIES IN ADIPOSE TISSUE.* J Biol Chem, 1964. **239**: p. 401-9.

46. Coe, N.R., M.A. Simpson, and D.A. Bernlohr, *Targeted disruption of the adipocyte lipid-binding protein (aP2 protein) gene impairs fat cell lipolysis and increases cellular fatty acid levels.* J Lipid Res, 1999. **40**(5): p. 967-72.

47. Maeda, N., et al., *Adaptation to fasting by glycerol transport through aquaporin 7 in adipose tissue.* Proc Natl Acad Sci U S A, 2004. **101**(51): p. 17801-6.

48. Coelho, M., T. Oliveira, and R. Fernandes, *Biochemistry of adipose tissue: an endocrine organ.* Arch Med Sci. **9**(2): p. 191-200.

49. Fasshauer, M. and M. Bluher, *Adipokines in health and disease.* Trends Pharmacol Sci. **36**(7): p. 461-70.

50. Fischer-Posovszky, P., M. Wabitsch, and Z. Hochberg, *Endocrinology of adipose tissue - an update.* Horm Metab Res, 2007. **39**(5): p. 314-21.

51. Hauner, H., *Secretory factors from human adipose tissue and their functional role.* Proc Nutr Soc, 2005. **64**(2): p. 163-9.

52. Khan, M. and F. Joseph, *Adipose tissue and adipokines: the association with and application of adipokines in obesity.* Scientifica (Cairo). **2014**: p. 328592.

53. Zhang, F., et al., *Crystal structure of the obese protein leptin-E100.* Nature, 1997. **387**(6629): p. 206-9.

54. Fain, J.N., et al., *Comparison of the release of adipokines by adipose tissue, adipose tissue matrix, and adipocytes from visceral and subcutaneous abdominal adipose tissues of obese humans.* Endocrinology, 2004. **145**(5): p. 2273-82.

55. Elmquist, J.K., C.F. Elias, and C.B. Saper, *From lesions to leptin: hypothalamic control of food intake and body weight.* Neuron, 1999. **22**(2): p. 221-32.

56. Munzberg, H., J.S. Flier, and C. Bjorbaek, *Region-specific leptin resistance within the hypothalamus of diet-induced obese mice.* Endocrinology, 2004. **145**(11): p. 4880-9.

57. Khan, A., et al., *Long-term leptin treatment of ob/ob mice improves glucose-induced insulin secretion.* Int J Obes Relat Metab Disord, 2001. **25**(6): p. 816-21.

58. Koch, C., et al., *Leptin rapidly improves glucose homeostasis in obese mice by increasing hypothalamic insulin sensitivity.* J Neurosci. **30**(48): p. 16180-7.

59. Lee, J.W. and D.R. Romsos, *Leptin administration normalizes insulin secretion from islets of Lep(ob)/Lep(ob) mice by food intake-dependent and -independent mechanisms.* Exp Biol Med (Maywood), 2003. **228**(2): p. 183-7.

60. Considine, R.V., et al., *Serum immunoreactive-leptin concentrations in normal-weight and obese humans.* N Engl J Med, 1996. **334**(5): p. 292-5.

61. Farooqi, I.S., et al., *Beneficial effects of leptin on obesity, T cell hyporesponsiveness, and neuroendocrine/metabolic dysfunction of human congenital leptin deficiency.* J Clin Invest, 2002. **110**(8): p. 1093-103.

62. O'Rahilly, S., *Insights into obesity and insulin resistance from the study of extreme human phenotypes.* Eur J Endocrinol, 2002. **147**(4): p. 435-41.

63. Scherer, P.E., et al., *A novel serum protein similar to C1q, produced exclusively in adipocytes.* J Biol Chem, 1995. **270**(45): p. 26746-9.

64. Wang, Y., et al., *Hydroxylation and glycosylation of the four conserved lysine residues in the collagenous domain of adiponectin. Potential role in the modulation of its insulin-sensitizing activity.* J Biol Chem, 2002. **277**(22): p. 19521-9.

65. Arita, Y., et al., *Paradoxical decrease of an adipose-specific protein, adiponectin, in obesity. 1999.* Biochem Biophys Res Commun. **425**(3): p. 560-4.

66. Yamauchi, T., et al., *Cloning of adiponectin receptors that mediate antidiabetic metabolic effects.* Nature, 2003. **423**(6941): p. 762-9.

67. Pajvani, U.B., et al., *Structure-function studies of the adipocyte-secreted hormone Acrp30/adiponectin. Implications fpr metabolic regulation and bioactivity.* J Biol Chem, 2003. **278**(11): p. 9073-85.

68. Fruebis, J., et al., *Proteolytic cleavage product of 30-kDa adipocyte complement-related protein increases fatty acid oxidation in muscle and causes weight loss in mice.* Proc Natl Acad Sci U S A, 2001. **98**(4): p. 2005-10.

69. Weyer, C., et al., *Hypoadiponectinemia in obesity and type 2 diabetes: close association with insulin resistance and hyperinsulinemia.* J Clin Endocrinol Metab, 2001. **86**(5): p. 1930-5.

70. Yang, W.S., et al., *Weight reduction increases plasma levels of an adipose-derived anti-inflammatory protein, adiponectin.* J Clin Endocrinol Metab, 2001. **86**(8): p. 3815-9.

71. Berg, A.H., et al., *The adipocyte-secreted protein Acrp30 enhances hepatic insulin action.* Nat Med, 2001. **7**(8): p. 947-53.

72. Yamauchi, T., et al., *The fat-derived hormone adiponectin reverses insulin resistance associated with both lipoatrophy and obesity.* Nat Med, 2001. **7**(8): p. 941-6.

73. Maeda, N., et al., *Diet-induced insulin resistance in mice lacking adiponectin/ACRP30.* Nat Med, 2002. **8**(7): p. 731-7.

74. Ouchi, N., et al., *Adipocyte-derived plasma protein, adiponectin, suppresses lipid accumulation and class A scavenger receptor expression in human monocyte-derived macrophages.* Circulation, 2001. **103**(8): p. 1057-63.

75. Yamaguchi, N., et al., *Adiponectin inhibits Toll-like receptor family-induced signaling.* FEBS Lett, 2005. **579**(30): p. 6821-6.

76. Kern, P.A., et al., *Adipose tissue tumor necrosis factor and interleukin-6 expression in human obesity and insulin resistance.* Am J Physiol Endocrinol Metab, 2001. **280**(5): p. E745-51.

77. Tsigos, C., et al., *Dose-dependent effects of recombinant human interleukin-6 on glucose regulation.* J Clin Endocrinol Metab, 1997. **82**(12): p. 4167-70.

78. Vozarova, B., et al., *Circulating interleukin-6 in relation to adiposity, insulin action, and insulin secretion.* Obes Res, 2001. **9**(7): p. 414-7.

79. Pradhan, A.D., et al., *C-reactive protein, interleukin 6, and risk of developing type 2 diabetes mellitus.* JAMA, 2001. **286**(3): p. 327-34.

80. Senn, J.J., et al., *Suppressor of cytokine signaling-3 (SOCS-3), a potential mediator of interleukin-6-dependent insulin resistance in hepatocytes.* J Biol Chem, 2003. **278**(16): p. 13740-6.

81. Fasshauer, M., et al., *Adiponectin gene expression and secretion is inhibited by interleukin-6 in 3T3-L1 adipocytes.* Biochem Biophys Res Commun, 2003. **301**(4): p. 1045-50.

82. Bastard, J.P., et al., *Elevated levels of interleukin 6 are reduced in serum and subcutaneous adipose tissue of obese women after weight loss.* J Clin Endocrinol Metab, 2000. **85**(9): p. 3338-42.

83. Cleal, L., T. Aldea, and Y.Y. Chau, *Fifty shades of white: Understanding heterogeneity in white adipose stem cells.* Adipocyte. **6**(3): p. 205-216.

84. Tchkonia, T., et al., *Fat depot-specific characteristics are retained in strains derived from single human preadipocytes.* Diabetes, 2006. **55**(9): p. 2571-8.

85. Tchkonia, T., et al., *Abundance of two human preadipocyte subtypes with distinct capacities for replication, adipogenesis, and apoptosis varies among fat depots.* Am J Physiol Endocrinol Metab, 2005. **288**(1): p. E267-77.

86. Loh, N.Y., et al., *LRP5 regulates human body fat distribution by modulating adipose progenitor biology in a dose- and depot-specific fashion.* Cell Metab. **21**(2): p. 262-72.

87. Kleppe, R., et al., *The 14-3-3 proteins in regulation of cellular metabolism.* Semin Cell Dev Biol. **22**(7): p. 713-9.

88. Lim, G.E., et al., *14-3-3zeta coordinates adipogenesis of visceral fat.* Nat Commun. **6**: p. 7671.

89. Khaw, K.T. and E. Barrett-Connor, *Lower endogenous androgens predict central adiposity in men.* Ann Epidemiol, 1992. **2**(5): p. 675-82.

90. Pasquali, R., et al., *Effect of obesity and body fat distribution on sex hormones and insulin in men.* Metabolism, 1991. **40**(1): p. 101-4.

91. Evans, D.J., J.H. Barth, and C.W. Burke, *Body fat topography in women with androgen excess.* Int J Obes, 1988. **12**(2): p. 157-62.

92. Blouin, K., A. Boivin, and A. Tchernof, *Androgens and body fat distribution.* J Steroid Biochem Mol Biol, 2008. **108**(3-5): p. 272-80.

93. Dieudonne, M.N., et al., *Opposite effects of androgens and estrogens on adipogenesis in rat preadipocytes: evidence for sex and site-related specificities and possible involvement of insulin-like growth factor 1 receptor and peroxisome proliferator-activated receptor gamma2.* Endocrinology, 2000. **141**(2): p. 649-56.

94. Lacasa, D., et al., *Evidence for a regional-specific control of rat preadipocyte proliferation and differentiation by the androgenic status.* Endocrine, 1995. **3**(11): p. 789-93.

95. Marin, P., et al., *Assimilation of triglycerides in subcutaneous and intraabdominal adipose tissues in vivo in men: effects of testosterone.* J Clin Endocrinol Metab, 1996. **81**(3): p. 1018-22.

96. Joe, A.W., et al., *Depot-specific differences in adipogenic progenitor abundance and proliferative response to high-fat diet.* Stem Cells, 2009. **27**(10): p. 2563-70.

97. Wang, Q.A., et al., *Tracking adipogenesis during white adipose tissue development, expansion and regeneration.* Nat Med. **19**(10): p. 1338-44.

98. Cinti, S., et al., *Adipocyte death defines macrophage localization and function in adipose tissue of obese mice and humans.* J Lipid Res, 2005. **46**(11): p. 2347-55.

99. de Ferranti, S. and D. Mozaffarian, *The perfect storm: obesity, adipocyte dysfunction, and metabolic consequences.* Clin Chem, 2008. **54**(6): p. 945-55.

100. Faust, I.M., et al., *Diet-induced adipocyte number increase in adult rats: a new model of obesity.* Am J Physiol, 1978. **235**(3): p. E279-86.

101. Maumus, M., et al., *Evidence of in situ proliferation of adult adipose tissue-derived progenitor cells: influence of fat mass microenvironment and growth.* J Clin Endocrinol Metab, 2008. **93**(10): p. 4098-106.

102. Strissel, K.J., et al., *Adipocyte death, adipose tissue remodeling, and obesity complications.* Diabetes, 2007. **56**(12): p. 2910-8.

103. Arner, E., et al., *Adipocyte turnover: relevance to human adipose tissue morphology.* Diabetes. **59**(1): p. 105-9.

104. Arner, P., et al., *Variations in the size of the major omentum are primarily determined by fat cell number.* J Clin Endocrinol Metab. **98**(5): p. E897-901.

105. Arner, P. and K.L. Spalding, *Fat cell turnover in humans.* Biochem Biophys Res Commun. **396**(1): p. 101-4.

106. Heinonen, S., et al., *Adipocyte morphology and implications for metabolic derangements in acquired obesity.* Int J Obes (Lond). **38**(11): p. 1423-31.

107. Hoffstedt, J., et al., *Regional impact of adipose tissue morphology on the metabolic profile in morbid obesity.* Diabetologia. **53**(12): p. 2496-503.

108. Tchoukalova, Y.D., et al., *Regional differences in cellular mechanisms of adipose tissue gain with overfeeding.* Proc Natl Acad Sci U S A. **107**(42): p. 18226-31.

109. Lundgren, M., et al., *Fat cell enlargement is an independent marker of insulin resistance and 'hyperleptinaemia'.* Diabetologia, 2007. **50**(3): p. 625-33.

110. Guilherme, A., et al., *Adipocyte dysfunctions linking obesity to insulin resistance and type 2 diabetes.* Nat Rev Mol Cell Biol, 2008. **9**(5): p. 367-77.

111. Gregor, M.F. and G.S. Hotamisligil, *Inflammatory mechanisms in obesity.* Annu Rev Immunol. **29**: p. 415-45.

112. Boden, G., *Obesity and free fatty acids.* Endocrinol Metab Clin North Am, 2008. **37**(3): p. 635-46, viii-ix.

113. Shulman, G.I., *Ectopic fat in insulin resistance, dyslipidemia, and cardiometabolic disease.* N Engl J Med. **371**(12): p. 1131-41.

114. Gustafson, B. and U. Smith, *Regulation of white adipogenesis and its relation to ectopic fat accumulation and cardiovascular risk.* Atherosclerosis. **241**(1): p. 27-35.

115. Heilbronn, L., S.R. Smith, and E. Ravussin, *Failure of fat cell proliferation, mitochondrial function and fat oxidation results in ectopic fat storage, insulin resistance and type II diabetes mellitus.* Int J Obes Relat Metab Disord, 2004. **28 Suppl 4**: p. S12-21.

116. Primeau, V., et al., *Characterizing the profile of obese patients who are metabolically healthy.* Int J Obes (Lond). **35**(7): p. 971-81.

117. Fabbrini, E., et al., *Metabolically normal obese people are protected from adverse effects following weight gain.* J Clin Invest. **125**(2): p. 787-95.

118. Coutinho, T., et al., *Central obesity and survival in subjects with coronary artery disease: a systematic review of the literature and collaborative analysis with individual subject data.* J Am Coll Cardiol. **57**(19): p. 1877-86.

119. Westphal, S.A., *Obesity, abdominal obesity, and insulin resistance.* Clin Cornerstone, 2008. **9**(1): p. 23-29; discussion 30-1.

120. Covas, D.T., et al., *Multipotent mesenchymal stromal cells obtained from diverse human tissues share functional properties and gene-expression profile with CD146+ perivascular cells and fibroblasts.* Exp Hematol, 2008. **36**(5): p. 642-54.

121. Young, H.E., et al., *Mesenchymal stem cells reside within the connective tissues of many organs.* Dev Dyn, 1995. **202**(2): p. 137-44.

122. Tang, Q.Q. and M.D. Lane, *Adipogenesis: from stem cell to adipocyte.* Annu Rev Biochem. **81**: p. 715-36.

123. Smas, C.M. and H.S. Sul, *Pref-1, a protein containing EGF-like repeats, inhibits adipocyte differentiation.* Cell, 1993. **73**(4): p. 725-34.

124. Smas, C.M., D. Green, and H.S. Sul, *Structural characterization and alternate splicing of the gene encoding the preadipocyte EGF-like protein pref-1.* Biochemistry, 1994. **33**(31): p. 9257-65.

125. Mei, B., et al., *Only the large soluble form of preadipocyte factor-1 (Pref-1), but not the small soluble and membrane forms, inhibits adipocyte differentiation: role of alternative splicing.* Biochem J, 2002. **364**(Pt 1): p. 137-44.

126. Smas, C.M., L. Chen, and H.S. Sul, *Cleavage of membrane-associated pref-1 generates a soluble inhibitor of adipocyte differentiation.* Mol Cell Biol, 1997. **17**(2): p. 977-88.

127. Villena, J.A., K.H. Kim, and H.S. Sul, *Pref-1 and ADSF/resistin: two secreted factors inhibiting adipose tissue development.* Horm Metab Res, 2002. **34**(11-12): p. 664-70.

128. Wang, Y., et al., *Pref-1, a preadipocyte secreted factor that inhibits adipogenesis.* J Nutr, 2006. **136**(12): p. 2953-6.

129. Moon, Y.S., et al., *Mice lacking paternally expressed Pref-1/Dlk1 display growth retardation and accelerated adiposity.* Mol Cell Biol, 2002. **22**(15): p. 5585-92.

130. Lee, K., et al., *Inhibition of adipogenesis and development of glucose intolerance by soluble preadipocyte factor-1 (Pref-1).* J Clin Invest, 2003. **111**(4): p. 453-61.

131. Yeh, W.C., et al., *Cascade regulation of terminal adipocyte differentiation by three members of the C/EBP family of leucine zipper proteins.* Genes Dev, 1995. **9**(2): p. 168-81.

132. Tanaka, T., et al., *Defective adipocyte differentiation in mice lacking the C/EBPbeta and/or C/EBPdelta gene.* EMBO J, 1997. **16**(24): p. 7432-43.

133. Christy, R.J., et al., *CCAAT/enhancer binding protein gene promoter: binding of nuclear factors during differentiation of 3T3-L1 preadipocytes.* Proc Natl Acad Sci U S A, 1991. **88**(6): p. 2593-7.

134. Clarke, S.L., C.E. Robinson, and J.M. Gimble, *CAAT/enhancer binding proteins directly modulate transcription from the peroxisome proliferator-activated receptor gamma 2 promoter.* Biochem Biophys Res Commun, 1997. **240**(1): p. 99-103.

135. Flodby, P., et al., *Increased hepatic cell proliferation and lung abnormalities in mice deficient in CCAAT/enhancer binding protein alpha.* J Biol Chem, 1996. **271**(40): p. 24753-60.

136. Wang, N.D., et al., *Impaired energy homeostasis in C/EBP alpha knockout mice.* Science, 1995. **269**(5227): p. 1108-12.

137. Freytag, S.O., D.L. Paielli, and J.D. Gilbert, *Ectopic expression of the CCAAT/enhancer-binding protein alpha promotes the adipogenic program in a variety of mouse fibroblastic cells.* Genes Dev, 1994. **8**(14): p. 1654-63.

138. Lin, F.T. and M.D. Lane, *Antisense CCAAT/enhancer-binding protein RNA suppresses coordinate gene expression and triglyceride accumulation during differentiation of 3T3-L1 preadipocytes.* Genes Dev, 1992. **6**(4): p. 533-44.

139. Rosen, E.D., et al., *C/EBPalpha induces adipogenesis through PPARgamma: a unified pathway.* Genes Dev, 2002. **16**(1): p. 22-6.

140. Jiang, M.S., et al., *Derepression of the C/EBPalpha gene during adipogenesis: identification of AP-2alpha as a repressor.* Proc Natl Acad Sci U S A, 1998. **95**(7): p. 3467-71.

141. Tang, Q.Q., M.S. Jiang, and M.D. Lane, *Repression of transcription mediated by dual elements in the CCAAT/enhancer binding protein alpha gene.* Proc Natl Acad Sci U S A, 1997. **94**(25): p. 13571-5.

142. Ron, D. and J.F. Habener, *CHOP, a novel developmentally regulated nuclear protein that dimerizes with transcription factors C/EBP and LAP and functions as a dominant-negative inhibitor of gene transcription.* Genes Dev, 1992. **6**(3): p. 439-53.

143. Darlington, G.J., S.E. Ross, and O.A. MacDougald, *The role of C/EBP genes in adipocyte differentiation.* J Biol Chem, 1998. **273**(46): p. 30057-60.

144. Fajas, L., J.C. Fruchart, and J. Auwerx, *PPARgamma3 mRNA: a distinct PPARgamma mRNA subtype transcribed from an independent promoter.* FEBS Lett, 1998. **438**(1-2): p. 55-60.

145. Zhu, Y., et al., *Structural organization of mouse peroxisome proliferator-activated receptor gamma (mPPAR gamma) gene: alternative promoter use and different splicing yield two mPPAR gamma isoforms.* Proc Natl Acad Sci U S A, 1995. **92**(17): p. 7921-5.

146. Kliewer, S.A., et al., *Convergence of 9-cis retinoic acid and peroxisome proliferator signalling pathways through heterodimer formation of their receptors.* Nature, 1992. **358**(6389): p. 771-4.

147. Imai, T., et al., *Peroxisome proliferator-activated receptor gamma is required in mature white and brown adipocytes for their survival in the mouse.* Proc Natl Acad Sci U S A, 2004. **101**(13): p. 4543-7.

148. Bhanot, P., et al., *A new member of the frizzled family from Drosophila functions as a Wingless receptor.* Nature, 1996. **382**(6588): p. 225-30.

149. Pinson, K.I., et al., *An LDL-receptor-related protein mediates Wnt signalling in mice.* Nature, 2000. **407**(6803): p. 535-8.

150. Tamai, K., et al., *LDL-receptor-related proteins in Wnt signal transduction.* Nature, 2000. **407**(6803): p. 530-5.

151. Christodoulides, C., et al., *Adipogenesis and WNT signalling.* Trends Endocrinol Metab, 2009. **20**(1): p. 16-24.

152. James, A.W., *Review of Signaling Pathways Governing MSC Osteogenic and Adipogenic Differentiation.* Scientifica (Cairo). **2013**: p. 684736.

153. Takada, I., A.P. Kouzmenko, and S. Kato, *Wnt and PPARgamma signaling in osteoblastogenesis and adipogenesis.* Nat Rev Rheumatol, 2009. **5**(8): p. 442-7.

154. Logan, C.Y. and R. Nusse, *The Wnt signaling pathway in development and disease.* Annu Rev Cell Dev Biol, 2004. **20**: p. 781-810.

155. Ross, S.E., et al., *Inhibition of adipogenesis by Wnt signaling.* Science, 2000. **289**(5481): p. 950-3.

156. Bennett, C.N., et al., *Regulation of osteoblastogenesis and bone mass by Wnt10b.* Proc Natl Acad Sci U S A, 2005. **102**(9): p. 3324-9.

157. Bowers, R.R. and M.D. Lane, *Wnt signaling and adipocyte lineage commitment.* Cell Cycle, 2008. **7**(9): p. 1191-6.

158. Kang, S., et al., *Wnt signaling stimulates osteoblastogenesis of mesenchymal precursors by suppressing CCAAT/enhancer-binding protein alpha and peroxisome proliferator-activated receptor gamma.* J Biol Chem, 2007. **282**(19): p. 14515-24.

159. Singh, R., et al., *Testosterone inhibits adipogenic differentiation in 3T3-L1 cells: nuclear translocation of androgen receptor complex with beta-catenin and T-cell factor 4 may bypass canonical Wnt signaling to down-regulate adipogenic transcription factors.* Endocrinology, 2006. **147**(1): p. 141-54.

160. Tomlinson, J.J., et al., *Modulation of early human preadipocyte differentiation by glucocorticoids.* Endocrinology, 2006. **147**(11): p. 5284-93.

161. Wiper-Bergeron, N., et al., *Glucocorticoid-stimulated preadipocyte differentiation is mediated through acetylation of C/EBPbeta by GCN5.* Proc Natl Acad Sci U S A, 2007. **104**(8): p. 2703-8.

162. Wu, Z., N.L. Bucher, and S.R. Farmer, *Induction of peroxisome proliferator-activated receptor gamma during the conversion of 3T3 fibroblasts into adipocytes is mediated by C/EBPbeta, C/EBPdelta, and glucocorticoids.* Mol Cell Biol, 1996. **16**(8): p. 4128-36.

163. Zhang, Y.Y., et al., *Down-regulation of type I Runx2 mediated by dexamethasone is required for 3T3-L1 adipogenesis.* Mol Endocrinol. **26**(5): p. 798-808.

164. Chapman, A.B., D.M. Knight, and G.M. Ringold, *Glucocorticoid regulation of adipocyte differentiation: hormonal triggering of the developmental program and induction of a differentiation-dependent gene.* J Cell Biol, 1985. **101**(4): p. 1227-35.

165. Smas, C.M., et al., *Transcriptional repression of pref-1 by glucocorticoids promotes 3T3-L1 adipocyte differentiation.* J Biol Chem, 1999. **274**(18): p. 12632-41.

166. Lee, M.J., et al., *Pathways regulated by glucocorticoids in omental and subcutaneous human adipose tissues: a microarray study.* Am J Physiol Endocrinol Metab. **300**(3): p. E571-80.

167. Yu, C.Y., et al., *Genome-wide analysis of glucocorticoid receptor binding regions in adipocytes reveal gene network involved in triglyceride homeostasis.* PLoS One. **5**(12): p. e15188.

168. Lee, M.J., et al., *Deconstructing the roles of glucocorticoids in adipose tissue biology and the development of central obesity.* Biochim Biophys Acta. **1842**(3): p. 473-81.

169. Rockall, A.G., et al., *Computed tomography assessment of fat distribution in male and female patients with Cushing's syndrome.* Eur J Endocrinol, 2003. **149**(6): p. 561-7.

170. Gupta, V., et al., *Effects of dihydrotestosterone on differentiation and proliferation of human mesenchymal stem cells and preadipocytes.* Mol Cell Endocrinol, 2008. **296**(1-2): p. 32-40.

171. Chazenbalk, G., et al., *Androgens inhibit adipogenesis during human adipose stem cell commitment to preadipocyte formation.* Steroids. **78**(9): p. 920-6.

172. Blouin, K., et al., *Effects of androgens on adipocyte differentiation and adipose tissue explant metabolism in men and women.* Clin Endocrinol (Oxf). **72**(2): p. 176-88.

173. Singh, R., et al., *Androgens stimulate myogenic differentiation and inhibit adipogenesis in C3H 10T1/2 pluripotent cells through an androgen receptor-mediated pathway.* Endocrinology, 2003. **144**(11): p. 5081-8.

174. Lee, R.C., R.L. Feinbaum, and V. Ambros, *The C. elegans heterochronic gene lin-4 encodes small RNAs with antisense complementarity to lin-14.* Cell, 1993. **75**(5): p. 843-54.

175. Wightman, B., I. Ha, and G. Ruvkun, *Posttranscriptional regulation of the heterochronic gene lin-14 by lin-4 mediates temporal pattern formation in C. elegans.* Cell, 1993. **75**(5): p. 855-62.

176. Bartel, D.P., *MicroRNAs: genomics, biogenesis, mechanism, and function.* Cell, 2004. **116**(2): p. 281-97.

177. Guo, H., et al., *Mammalian microRNAs predominantly act to decrease target mRNA levels.* Nature. **466**(7308): p. 835-40.

178. Lee, Y., et al., *MicroRNA maturation: stepwise processing and subcellular localization.* EMBO J, 2002. **21**(17): p. 4663-70.

179. Cai, X., C.H. Hagedorn, and B.R. Cullen, *Human microRNAs are processed from capped, polyadenylated transcripts that can also function as mRNAs.* RNA, 2004. **10**(12): p. 1957-66.

180. Lee, Y., et al., *MicroRNA genes are transcribed by RNA polymerase II.* EMBO J, 2004. **23**(20): p. 4051-60.

181. Borchert, G.M., W. Lanier, and B.L. Davidson, *RNA polymerase III transcribes human microRNAs.* Nat Struct Mol Biol, 2006. **13**(12): p. 1097-101.

182. Lagos-Quintana, M., et al., *Identification of novel genes coding for small expressed RNAs.* Science, 2001. **294**(5543): p. 853-8.

183. Lau, N.C., et al., *An abundant class of tiny RNAs with probable regulatory roles in Caenorhabditis elegans.* Science, 2001. **294**(5543): p. 858-62.

184. Rodriguez, A., et al., *Identification of mammalian microRNA host genes and transcription units.* Genome Res, 2004. **14**(10A): p. 1902-10.

185. Zeng, Y. and B.R. Cullen, *Sequence requirements for micro RNA processing and function in human cells.* RNA, 2003. **9**(1): p. 112-23.

186. Basyuk, E., et al., *Human let-7 stem-loop precursors harbor features of RNase III cleavage products.* Nucleic Acids Res, 2003. **31**(22): p. 6593-7.

187. Lee, Y., et al., *The nuclear RNase III Drosha initiates microRNA processing.* Nature, 2003. **425**(6956): p. 415-9.

188. Lund, E., et al., *Nuclear export of microRNA precursors.* Science, 2004. **303**(5654): p. 95-8.

189. Yi, R., et al., *Exportin-5 mediates the nuclear export of pre-microRNAs and short hairpin RNAs.* Genes Dev, 2003. **17**(24): p. 3011-6.

190. Bernstein, E., et al., *Role for a bidentate ribonuclease in the initiation step of RNA interference.* Nature, 2001. **409**(6818): p. 363-6.

191. Grishok, A., et al., *Genes and mechanisms related to RNA interference regulate expression of the small temporal RNAs that control C. elegans developmental timing.* Cell, 2001. **106**(1): p. 23-34.

192. Hutvagner, G., et al., *A cellular function for the RNA-interference enzyme Dicer in the maturation of the let-7 small temporal RNA.* Science, 2001. **293**(5531): p. 834-8.

193. Ketting, R.F., et al., *Dicer functions in RNA interference and in synthesis of small RNA involved in developmental timing in C. elegans.* Genes Dev, 2001. **15**(20): p. 2654-9.

194. Knight, S.W. and B.L. Bass, *A role for the RNase III enzyme DCR-1 in RNA interference and germ line development in Caenorhabditis elegans.* Science, 2001. **293**(5538): p. 2269-71.

195. Khvorova, A., A. Reynolds, and S.D. Jayasena, *Functional siRNAs and miRNAs exhibit strand bias.* Cell, 2003. **115**(2): p. 209-16.

196. Schwarz, D.S., et al., *Asymmetry in the assembly of the RNAi enzyme complex.* Cell, 2003. **115**(2): p. 199-208.

197. Song, J.J., et al., *The crystal structure of the Argonaute2 PAZ domain reveals an RNA binding motif in RNAi effector complexes.* Nat Struct Biol, 2003. **10**(12): p. 1026-32.

198. Lewis, B.P., et al., *Prediction of mammalian microRNA targets.* Cell, 2003. **115**(7): p. 787-98.

199. Rhoades, M.W., et al., *Prediction of plant microRNA targets.* Cell, 2002. **110**(4): p. 513-20.

200. Humphreys, D.T., et al., *MicroRNAs control translation initiation by inhibiting eukaryotic initiation factor 4E/cap and poly(A) tail function.* Proc Natl Acad Sci U S A, 2005. **102**(47): p. 16961-6.

201. Petersen, C.P., et al., *Short RNAs repress translation after initiation in mammalian cells.* Mol Cell, 2006. **21**(4): p. 533-42.

202. Pillai, R.S., et al., *Inhibition of translational initiation by Let-7 MicroRNA in human cells.* Science, 2005. **309**(5740): p. 1573-6.

203. Pillai, R.S., S.N. Bhattacharyya, and W. Filipowicz, *Repression of protein synthesis by miRNAs: how many mechanisms?* Trends Cell Biol, 2007. **17**(3): p. 118-26.

204. Wu, L., J. Fan, and J.G. Belasco, *MicroRNAs direct rapid deadenylation of mRNA.* Proc Natl Acad Sci U S A, 2006. **103**(11): p. 4034-9.

205. Lim, L.P., et al., *Microarray analysis shows that some microRNAs downregulate large numbers of target mRNAs.* Nature, 2005. **433**(7027): p. 769-73.

206. Chen, J., et al., *The role of miRNAs in the differentiation of adipose-derived stem cells.* Curr Stem Cell Res Ther. **9**(3): p. 268-79.

207. Tsang, J., J. Zhu, and A. van Oudenaarden, *MicroRNA-mediated feedback and feedforward loops are recurrent network motifs in mammals.* Mol Cell, 2007. **26**(5): p. 753-67.

208. Gennarino, V.A., et al., *Identification of microRNA-regulated gene networks by expression analysis of target genes.* Genome Res. **22**(6): p. 1163-72.

209. Tsang, J.S., M.S. Ebert, and A. van Oudenaarden, *Genome-wide dissection of microRNA functions and cotargeting networks using gene set signatures.* Mol Cell. **38**(1): p. 140-53.

210. Kulyte, A., et al., *Additive effects of microRNAs and transcription factors on CCL2 production in human white adipose tissue.* Diabetes. **63**(4): p. 1248-58.

211. Huang, X., et al., *Characterization of human plasma-derived exosomal RNAs by deep sequencing.* BMC Genomics. **14**: p. 319.

212. Turchinovich, A., et al., *Characterization of extracellular circulating microRNA.* Nucleic Acids Res. **39**(16): p. 7223-33.

213. Thomou, T., et al., *Adipose-derived circulating miRNAs regulate gene expression in other tissues.* Nature. **542**(7642): p. 450-455.

214. Ortega, F.J., et al., *Targeting the circulating microRNA signature of obesity.* Clin Chem. **59**(5): p. 781-92.

215. Prats-Puig, A., et al., *Changes in circulating microRNAs are associated with childhood obesity.* J Clin Endocrinol Metab. **98**(10): p. E1655-60.

216. Ortega, F.J., et al., *Profiling of circulating microRNAs reveals common microRNAs linked to type 2 diabetes that change with insulin sensitization.* Diabetes Care. **37**(5): p. 1375-83.

217. Rome, S., *Are extracellular microRNAs involved in type 2 diabetes and related pathologies?* Clin Biochem. **46**(10-11): p. 937-45.

218. Karolina, D.S., et al., *Circulating miRNA profiles in patients with metabolic syndrome.* J Clin Endocrinol Metab. **97**(12): p. E2271-6.

219. Wang, Y.T., et al., *Circulating microRNAs have a sex-specific association with metabolic syndrome.* J Biomed Sci. **20**: p. 72.

220. Blondal, T., et al., *Assessing sample and miRNA profile quality in serum and plasma or other biofluids.* Methods. **59**(1): p. S1-6.

221. Williams, Z., et al., *Comprehensive profiling of circulating microRNA via small RNA sequencing of cDNA libraries reveals biomarker potential and limitations.* Proc Natl Acad Sci U S A. **110**(11): p. 4255-60.

222. Guay, C. and R. Regazzi, *Circulating microRNAs as novel biomarkers for diabetes mellitus.* Nat Rev Endocrinol. **9**(9): p. 513-21.

223. Elmen, J., et al., *LNA-mediated microRNA silencing in non-human primates.* Nature, 2008. **452**(7189): p. 896-9.

224. Krutzfeldt, J., et al., *Silencing of microRNAs in vivo with 'antagomirs'.* Nature, 2005. **438**(7068): p. 685-9.

225. Li, Z. and T.M. Rana, *Therapeutic targeting of microRNAs: current status and future challenges.* Nat Rev Drug Discov. **13**(8): p. 622-38.

226. van Rooij, E., A.L. Purcell, and A.A. Levin, *Developing microRNA therapeutics.* Circ Res. **110**(3): p. 496-507.

227. Romao, J.M., et al., *MicroRNAs in bovine adipogenesis: genomic context, expression and function.* BMC Genomics, 2014. **15**: p. 137.

228. Brandao, B.B., B.A. Guerra, and M.A. Mori, *Shortcuts to a functional adipose tissue: The role of small non-coding RNAs.* Redox biology, 2017. **12**: p. 82-102.

229. Arner, P. and A. Kulyte, *MicroRNA regulatory networks in human adipose tissue and obesity.* Nature reviews. Endocrinology, 2015. **11**(5): p. 276-88.

230. Shi, C., et al., *Adipogenic miRNA and meta-signature miRNAs involved in human adipocyte differentiation and obesity.* Oncotarget, 2016. **7**(26): p. 40830-40845.

231. Hamam, D., et al., *microRNAs as regulators of adipogenic differentiation of mesenchymal stem cells.* Stem cells and development, 2014. **24**(4): p. 417-25.

232. O'Reilly, M.W., P.J. House, and J.W. Tomlinson, *Understanding androgen action in adipose tissue.* J Steroid Biochem Mol Biol. **143**: p. 277-84.

233. Peng, Y., et al., *MicroRNAs: emerging roles in adipogenesis and obesity.* Cell Signal, 2014. **26**(9): p. 1888-96.

234. Hilton, C., M.J. Neville, and F. Karpe, *MicroRNAs in adipose tissue: their role in adipogenesis and obesity.* International journal of obesity, 2012. **37**(3): p. 325-32.

235. Oskowitz, A.Z., et al., *Human multipotent stromal cells from bone marrow and microRNA: regulation of differentiation and leukemia inhibitory factor expression.* Proc Natl Acad Sci U S A, 2008. **105**(47): p. 18372-7.

236. Li, H., et al., *miR-17-5p and miR-106a are involved in the balance between osteogenic and adipogenic differentiation of adipose-derived mesenchymal stem cells.* Stem Cell Res. **10**(3): p. 313-24.

237. Huang, J., et al., *MicroRNA-204 regulates Runx2 protein expression and mesenchymal progenitor cell differentiation.* Stem Cells. **28**(2): p. 357-64.

238. Gu, C., et al., *miR-27a attenuates adipogenesis and promotes osteogenesis in steroid-induced rat BMSCs by targeting PPARgamma and GREM1.* Scientific reports, 2016. **6**: p. 38491.

239. Wang, Q., et al., *miR-17-92 cluster accelerates adipocyte differentiation by negatively regulating tumor-suppressor Rb2/p130.* Proc Natl Acad Sci U S A, 2008. **105**(8): p. 2889-94.

240. Chen, L., et al., *A novel negative regulator of adipogenesis: microRNA-363.* Stem Cells. **32**(2): p. 510-20.

241. Sun, F., et al., *Characterization of function and regulation of miR-24-1 and miR-31.* Biochem Biophys Res Commun, 2009. **380**(3): p. 660-5.

242. Tang, Y.F., et al., *Expression of miR-31, miR-125b-5p, and miR-326 in the adipogenic differentiation process of adipose-derived stem cells.* OMICS, 2009. **13**(4): p. 331-6.

243. Karbiener, M., et al., *microRNA miR-27b impairs human adipocyte differentiation and targets PPARgamma.* Biochem Biophys Res Commun, 2009. **390**(2): p. 247-51.

244. Kim, S.Y., et al., *miR-27a is a negative regulator of adipocyte differentiation via suppressing PPARgamma expression.* Biochem Biophys Res Commun. **392**(3): p. 323-8.

245. Lin, Q., et al., *A role of miR-27 in the regulation of adipogenesis.* FEBS J, 2009. **276**(8): p. 2348-58.

246. Lee, E.K., et al., *miR-130 suppresses adipogenesis by inhibiting peroxisome proliferator-activated receptor gamma expression.* Mol Cell Biol. **31**(4): p. 626-38.

247. Liu, S., Y. Yang, and J. Wu, *TNFalpha-induced up-regulation of miR-155 inhibits adipogenesis by down-regulating early adipogenic transcription factors.* Biochem Biophys Res Commun. **414**(3): p. 618-24.

248. Ling, H.Y., et al., *MicroRNA-375 promotes 3T3-L1 adipocyte differentiation through modulation of extracellular signal-regulated kinase signalling.* Clin Exp Pharmacol Physiol. **38**(4): p. 239-46.

249. Kim, Y.J., et al., *MiR-21 regulates adipogenic differentiation through the modulation of TGF-beta signaling in mesenchymal stem cells derived from human adipose tissue.* Stem Cells, 2009. **27**(12): p. 3093-102.

250. Peng, Y., et al., *MiR-224 impairs adipocyte early differentiation and regulates fatty acid metabolism.* Int J Biochem Cell Biol. **45**(8): p. 1585-93.

251. Bork, S., et al., *Adipogenic differentiation of human mesenchymal stromal cells is down-regulated by microRNA-369-5p and up-regulated by microRNA-371.* J Cell Physiol. **226**(9): p. 2226-34.

252. Guo, Y., et al., *Up-regulated miR-145 expression inhibits porcine preadipocytes differentiation by targeting IRS1.* Int J Biol Sci. **8**(10): p. 1408-17.

253. He, A., et al., *Overexpression of micro ribonucleic acid 29, highly up-regulated in diabetic rats, leads to insulin resistance in 3T3-L1 adipocytes.* Mol Endocrinol, 2007. **21**(11): p. 2785-94.

254. Trajkovski, M., et al., *MicroRNAs 103 and 107 regulate insulin sensitivity.* Nature. **474**(7353): p. 649-53.

255. Kulyte, A., et al., *MicroRNA profiling links miR-378 to enhanced adipocyte lipolysis in human cancer cachexia.* American journal of physiology. Endocrinology and metabolism. **306**(3): p. E267-74.

256. Gerin, I., et al., *Roles for miRNA-378/378* in adipocyte gene expression and lipogenesis.* American journal of physiology. Endocrinology and metabolism. **299**(2): p. E198-206.

257. Chen, L., et al., *MiR-146b is a regulator of human visceral preadipocyte proliferation and differentiation and its expression is altered in human obesity.* Molecular and cellular endocrinology. **393**(1-2): p. 65-74.

258. Kim, J., et al., *Eicosapentaenoic Acid Potentiates Brown Thermogenesis through FFAR4-dependent Up-regulation of miR-30b and miR-378.* The Journal of biological chemistry. **291**(39): p. 20551-62.

259. Pan, D., et al., *MicroRNA-378 controls classical brown fat expansion to counteract obesity.* Nature communications. **5**: p. 4725.

260. Mori, M.A., et al., *Altered miRNA processing disrupts brown/white adipocyte determination and associates with lipodystrophy.* The Journal of clinical investigation. **124**(8): p. 3339-51.

261. Sun, L., et al., *Mir193b-365 is essential for brown fat differentiation.* Nature cell biology. **13**(8): p. 958-65.

262. Choe, S.S., et al., *Adipose Tissue Remodeling: Its Role in Energy Metabolism and Metabolic Disorders.* Front Endocrinol (Lausanne). **7**: p. 30.

263. Ritchie, M.E., et al., *A comparison of background correction methods for two-colour microarrays.* Bioinformatics, 2007. **23**(20): p. 2700-7.

264. Klein, J., et al., *Insulin and the beta3-adrenoceptor differentially regulate uncoupling protein-1 expression.* Molecular endocrinology, 2000. **14**(6): p. 764-73.

265. Rodriguez, A.M., et al., *Transplantation of a multipotent cell population from human adipose tissue induces dystrophin expression in the immunocompetent mdx mouse.* J Exp Med, 2005. **201**(9): p. 1397-405.

266. Lietzow, J., et al., *3,5-T2 alters murine genes relevant for xenobiotic, steroid, and thyroid hormone metabolism.* J Mol Endocrinol. **56**(4): p. 311-23.

267. Chomczynski, P. and N. Sacchi, *Single-step method of RNA isolation by acid guanidinium thiocyanate-phenol-chloroform extraction.* Anal Biochem, 1987. **162**(1): p. 156-9.

268. Huang, N., et al., *MiR-378a-3p enhances adipogenesis by targeting mitogen-activated protein kinase 1.* Biochemical and biophysical research communications. **457**(1): p. 37-42.

269. Ishida, M., et al., *MicroRNA-378 regulates adiponectin expression in adipose tissue: a new plausible mechanism.* PLoS One. **9**(11): p. e111537.

270. Liu, S.Y., et al., *MiR-378 Plays an Important Role in the Differentiation of Bovine Preadipocytes.* Cellular physiology and biochemistry. **36**(4): p. 1552-62.

271. Xu, L.L., et al., *TNF-alpha, IL-6, and leptin increase the expression of miR-378, an adipogenesis-related microRNA in human adipocytes.* Cell biochemistry and biophysics. **70**(2): p. 771-6.

272. Yu, J., et al., *Expression profiling of PPARgamma-regulated microRNAs in human subcutaneous and visceral adipogenesis in both genders.* Endocrinology. **155**(6): p. 2155-65.

273. Ahn, J., et al., *MicroRNA-146b promotes adipogenesis by suppressing the SIRT1-FOXO1 cascade.* EMBO molecular medicine. **5**(10): p. 1602-12.

274. Shi, C., et al., *IL-6 and TNF-alpha induced obesity-related inflammatory response through transcriptional regulation of miR-146b.* Journal of interferon & cytokine research. **34**(5): p. 342-8.

275. Chartoumpekis, D.V., et al., *Differential expression of microRNAs in adipose tissue after long-term high-fat diet-induced obesity in mice.* PLoS One. **7**(4): p. e34872.

276. Bouhaddioui, W., P.R. Provost, and Y. Tremblay, *Expression profile of androgen-modulated microRNAs in the fetal murine lung.* Biol Sex Differ. **7**: p. 20.

277. Ahram, M., et al., *Differential expression and androgen regulation of microRNAs and metalloprotease 13 in breast cancer cells.* Cell Biol Int.

278. Ruegger, S. and H. Grosshans, *MicroRNA turnover: when, how, and why.* Trends Biochem Sci. **37**(10): p. 436-46.

279. Zhou, Z.X., et al., *Specificity of ligand-dependent androgen receptor stabilization: receptor domain interactions influence ligand dissociation and receptor stability.* Mol Endocrinol, 1995. **9**(2): p. 208-18.

280. McGregor, R.A. and M.S. Choi, *microRNAs in the regulation of adipogenesis and obesity.* Current molecular medicine, 2011. **11**(4): p. 304-16.

281. Son, Y.H., et al., *Regulation of Adipocyte Differentiation via MicroRNAs.* Endocrinology and metabolism (Seoul, Korea) 2014. **29**(2): p. 122-35.

282. Romao, J.M., et al., *MicroRNA regulation in mammalian adipogenesis.* Experimental biology and medicine (Maywood, N.J.). **236**(9): p. 997-1004.

283. Martin, E.C., et al., *MicroRNA regulation of stem cell differentiation and diseases of the bone and adipose tissue: Perspectives on miRNA biogenesis and cellular transcriptome.* Biochimie. **124**: p. 98-111.

284. Meale, S.J., et al., *Effect of diet on microRNA expression in ovine subcutaneous and visceral adipose tissues.* Asian-Australasian journal of animal sciences. **92**(8): p. 3328-37.

285. Chuang, T.Y., et al., *MicroRNA-223 Expression is Upregulated in Insulin Resistant Human Adipose Tissue.* Journal of diabetes research. **2015**: p. 943659.

286. Deiuliis, J.A., et al., *Visceral Adipose MicroRNA 223 Is Upregulated in Human and Murine Obesity and Modulates the Inflammatory Phenotype of Macrophages.* PLoS One. **11**(11): p. e0165962.

287. Zhuang, G., et al., *A novel regulator of macrophage activation: miR-223 in obesity-associated adipose tissue inflammation.* Circulation. **125**(23): p. 2892-903.

288. Kilic, I.D., et al., *MicroRNA -143 and -223 in obesity.* Gene. **560**(2): p. 140-2.

289. Ying, W., et al., *MicroRNA-223 is a crucial mediator of PPARgamma-regulated alternative macrophage activation.* The Journal of clinical investigation. **125**(11): p. 4149-59.

290. Deiuliis, J.A., *MicroRNAs as regulators of metabolic disease: pathophysiologic significance and emerging role as biomarkers and therapeutics.* International journal of obesity (2005). **40**(1): p. 88-101.

291. Hao, C., et al., *MiR-708 promotes steroid-induced osteonecrosis of femoral head, suppresses osteogenic differentiation by targeting SMAD3.* Scientific reports. **6**: p. 22599.

292. Lafontan, M. and M. Berlan, *Fat cell adrenergic receptors and the control of white and brown fat cell function.* J Lipid Res, 1993. **34**(7): p. 1057-91.

293. Fiorentino, A., et al., *Genetic variation in the miR-708 gene and its binding targets in bipolar disorder.* Bipolar Disord. **18**(8): p. 650-656.

294. Shen, H., et al., *Identification of microRNAs involved in dexamethasone-induced muscle atrophy.* Mol Cell Biochem. **381**(1-2): p. 105-13.

295. Lin, K.T., et al., *Glucocorticoids mediate induction of microRNA-708 to suppress ovarian cancer metastasis through targeting Rap1B.* Nature communications. **6**: p. 5917.

296. Shugart, E.C. and R.M. Umek, *Dexamethasone signaling is required to establish the postmitotic state of adipocyte development.* Cell Growth Differ, 1997. **8**(10): p. 1091-8.

297. Kuk, J.L., et al., *Waist circumference and abdominal adipose tissue distribution: influence of age and sex.* Am J Clin Nutr, 2005. **81**(6): p. 1330-4.

298. Lemieux, S., et al., *Sex differences in the relation of visceral adipose tissue accumulation to total body fatness.* Am J Clin Nutr, 1993. **58**(4): p. 463-7.

299. Ross, R., et al., *Sex differences in lean and adipose tissue distribution by magnetic resonance imaging: anthropometric relationships.* Am J Clin Nutr, 1994. **59**(6): p. 1277-85.

300. Kraus, M., et al., *Inhibition of adipogenic differentiation of human SGBS preadipocytes by androgen-regulated microRNA miR-375.* Mol Cell Endocrinol. **414**: p. 177-85.

301. Hartig, S.M., et al., *Feed-forward inhibition of androgen receptor activity by glucocorticoid action in human adipocytes.* Chem Biol. **19**(9): p. 1126-41.

302. Rodriguez-Cuenca, S., et al., *Depot differences in steroid receptor expression in adipose tissue: possible role of the local steroid milieu.* Am J Physiol Endocrinol Metab, 2005. **288**(1): p. E200-7.

303. Dieudonne, M.N., et al., *Androgen receptors in human preadipocytes and adipocytes: regional specificities and regulation by sex steroids.* Am J Physiol, 1998. **274**(6 Pt 1): p. C1645-52.

304. Joyner, J., L. Hutley, and D. Cameron, *Intrinsic regional differences in androgen receptors and dihydrotestosterone metabolism in human preadipocytes.* Horm Metab Res, 2002. **34**(5): p. 223-8.

305. Blouin, K., et al., *Pathways of adipose tissue androgen metabolism in women: depot differences and modulation by adipogenesis.* Am J Physiol Endocrinol Metab, 2009. **296**(2): p. E244-55.

306. Mayes, J.S. and G.H. Watson, *Direct effects of sex steroid hormones on adipose tissues and obesity.* Obes Rev, 2004. **5**(4): p. 197-216.

307. Zhang, Z.J., et al., *miRNA expression profile during osteogenic differentiation of human adipose-derived stem cells.* Journal of cellular biochemistry. **113**(3): p. 888-98.

308. Wang, J., et al., *MicroRNA-193 pro-proliferation effects for bone mesenchymal stem cells after low-level laser irradiation treatment through inhibitor of growth family, member 5.* Stem Cells Dev. **21**(13): p. 2508-19.

309. Khoo, C.P., et al., *miR-193a-3p interaction with HMGB1 downregulates human endothelial cell proliferation and migration.* Scientific reports. **7**: p. 44137.

310. Liang, H., et al., *miR-193a-3p functions as a tumor suppressor in lung cancer by down-regulating ERBB4.* J Biol Chem. **290**(2): p. 926-40.

311. Nakano, H., et al., *Gain-of-function microRNA screens identify miR-193a regulating proliferation and apoptosis in epithelial ovarian cancer cells.* Int J Oncol. **42**(6): p. 1875-82.

312. Williams, M., et al., *miR-193a-3p is a potential tumor suppressor in malignant pleural mesothelioma.* Oncotarget. **6**(27): p. 23480-95.

313. Gokhale, A., et al., *Distinctive microRNA signature of medulloblastomas associated with the WNT signaling pathway.* J Cancer Res Ther. **6**(4): p. 521-9.

I. https://www.ncbi.nlm.nih.gov/gene/100126333 (08.03.2018)

8 Supplementary Information

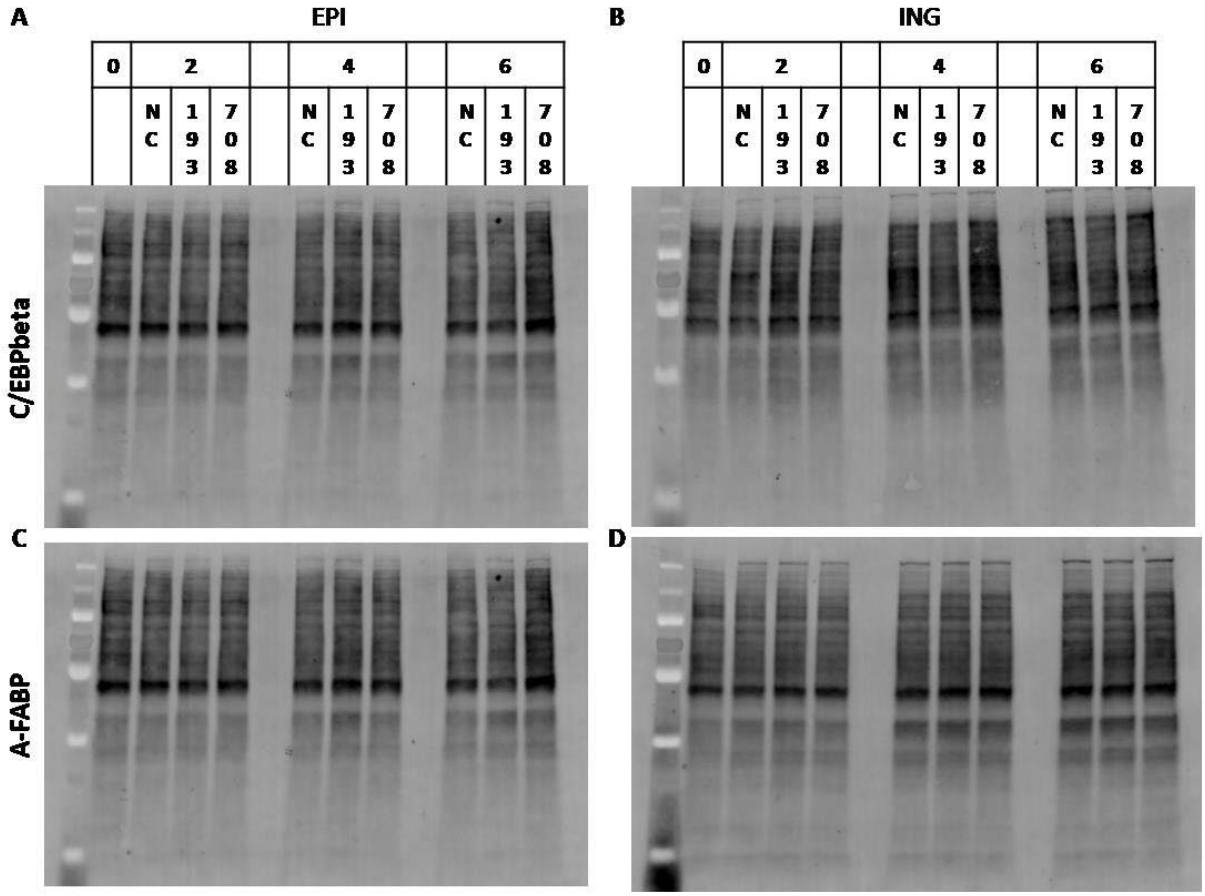

Figure S1 - Effects of miR-193a-3p and miR-708-5p inhibition on adipogenesis markers in EPI and ING cells. Total protein blots of represented western blots in Figure 8 (A, B) C/EBPβ, (C, D) A-FABP protein levels in negative controls (NC), anti-193a (193) and anti-708 (708) inhibitor transfected cells in murine (A, C) EPI and (B, D) ING cell lines at days 0, 2, 4 and 6 of adipocyte differentiation.

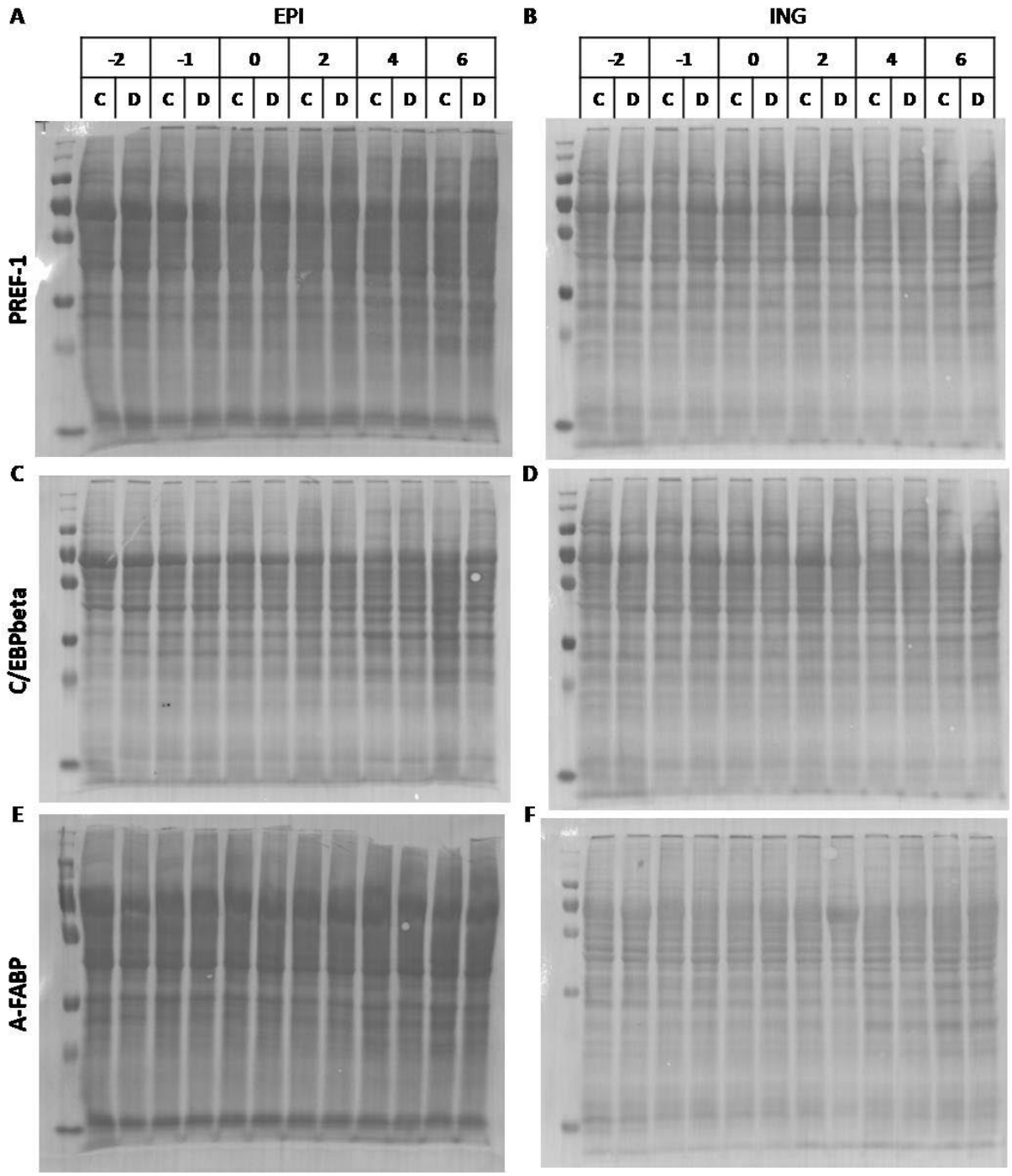

Figure S2 - Effects of chronic DHT stimulation on adipogenesis marker in EPI and ING adipocytes. Total protein blots of represented western blots in Figure 18 (A, B) PREF-1, (C, D) C/EBPβ and (E, F) A-FABP protein levels in chronically 10 nM DHT stimulated cells ("D") compared to controls ("C") in murine (A, C, E) EPI and (B, D, F) ING cell lines at days -2, -1, 0, 2, 4 and 6 of adipocyte differentiation.

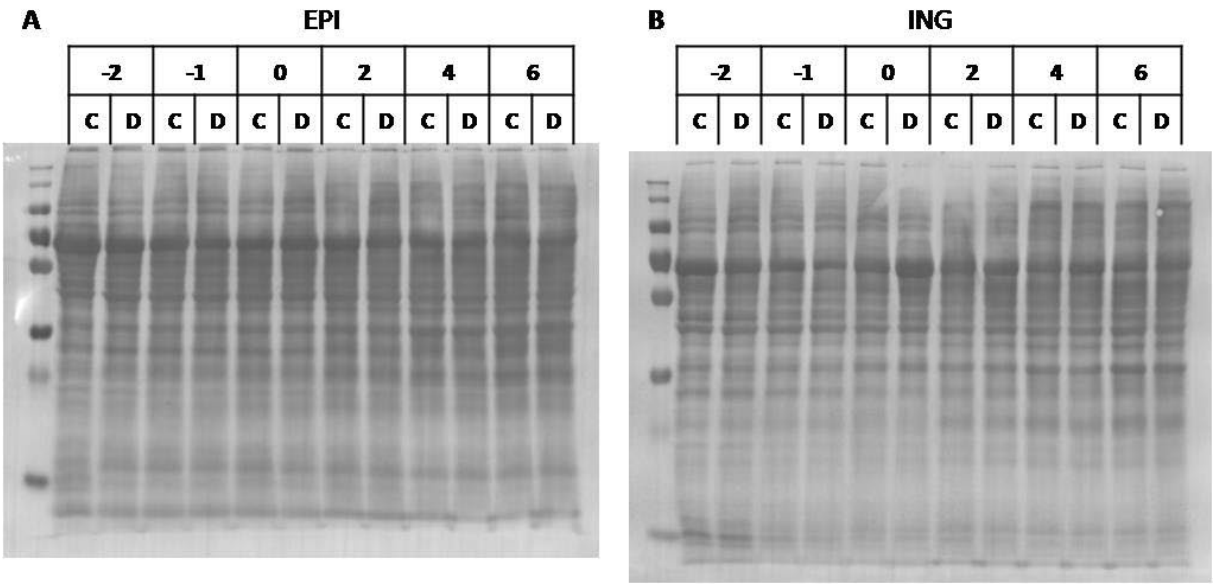

Figure S3 – Effects of chronic DHT stimulation on androgen receptor expression and stabilization in EPI and ING cells. Total protein blots of represented western blots in Figure 19 for androgen receptor (AR) protein levels in chronically 10 nM DHT ("D") stimulated cells compared to controls ("C") in murine (A) EPI and (B) ING cell lines at days -2, -1, 0, 2, 4 and 6 of adipocyte differentiation.

Table S1 – MicroRNA array analysis for mouse ING *ex vivo* white adipose tissue. Differently expressed microRNAs between preadipocytes (pre) and their corresponding mature adipocytes (mat) with logarithmic fold change (logFC) ≥ ±1 and fold change (FC) ≥ ±2, respectively. ProbeID was defined by Exiqon.

ProbeID	Annotation	ING pre	ING mat	logFC	FC
42530	mmu-let-7a-2-3p	-1,057	-0,017	1,040	2,05645
46438	mmu-let-7g-5p	0,966	-0,228	-1,195	2,28869
9938	mmu-let-7i-5p	1,192	-0,198	-1,391	2,62221
31026	mmu-miR-101a-3p	0,653	-0,355	-1,008	2,0117
42851	mmu-miR-105	-0,068	0,964	1,031	2,04385
19599	mmu-miR-106a-5p	1,431	-0,393	-1,824	3,54076
19582	mmu-miR-106b-5p	1,470	-0,354	-1,825	3,54215
145977	mmu-miR-1247-5p	-0,442	0,604	1,046	2,0644
42630	mmu-miR-140-3p	1,518	-0,255	-1,772	3,41628
4700	mmu-miR-140-5p	1,425	0,109	-1,316	2,48912
10946	mmu-miR-141-3p	0,900	-0,957	-1,857	3,62297
10947	mmu-miR-142-3p	2,475	-2,006	-4,481	22,3264
145798	mmu-miR-142-5p	2,678	-1,109	-3,787	13,8026
13177	mmu-miR-143-3p	0,750	-0,334	-1,083	2,119
10952	mmu-miR-146a-5p	1,970	-0,386	-2,356	5,11957
10306	mmu-miR-146b-5p	1,765	-0,408	-2,172	4,50704

10955	mmu-miR-148a-3p	-0,261	0,775	1,036	2,05039
145678	mmu-miR-150-5p	0,959	-0,315	-1,274	2,41756
27558	mmu-miR-155-5p	2,249	0,090	-2,158	4,46332
27720	mmu-miR-15a-5p	1,100	-0,500	-1,600	3,03148
17280	mmu-miR-15b-5p	2,018	-0,739	-2,757	6,75868
10967	mmu-miR-16-5p	1,749	-0,458	-2,207	4,6178
169336	mmu-miR-17-5p	1,602	-0,695	-2,297	4,91365
42865	mmu-miR-181a-5p	1,284	0,033	-1,251	2,38024
17953	mmu-miR-183-3p	-0,859	0,459	1,318	2,49238
169394	mmu-miR-1843a-5p	1,174	-0,043	-1,217	2,32533
168876	mmu-miR-1843b-5p	0,849	-0,276	-1,125	2,18133
146172	mmu-miR-1892	-0,129	1,263	1,392	2,62403
145994	mmu-miR-1900	-0,105	0,911	1,016	2,02197
10985	mmu-miR-191-5p	2,033	0,364	-1,669	3,17992
10986	mmu-miR-193a-3p	-2,077	0,444	2,521	5,73861
146012	mmu-miR-1949	1,541	0,017	-1,524	2,87652
13148	mmu-miR-195a-5p	0,855	-0,170	-1,025	2,03507
10995	mmu-miR-199a-3p/mmu-miR-199b-3p	1,144	-0,168	-1,312	2,48266
29562	mmu-miR-199a-5p	1,154	-0,157	-1,312	2,48217
11205	mmu-miR-199b-5p	1,024	-0,306	-1,330	2,51363
10997	mmu-miR-19a-3p	1,430	-0,526	-1,957	3,88163
10998	mmu-miR-19b-3p	1,540	-0,389	-1,930	3,80964
168819	mmu-miR-200a-3p	1,045	-0,841	-1,886	3,69618
147186	mmu-miR-200b-3p	0,447	-0,666	-1,113	2,16362
17427	mmu-miR-200c-3p	0,101	-1,047	-1,148	2,21616
11004	mmu-miR-203-3p	1,395	0,231	-1,164	2,24028
46917	mmu-miR-205-5p	1,433	-0,023	-1,456	2,74319
145845	mmu-miR-20a-5p	1,681	-0,484	-2,165	4,484
42640	mmu-miR-20b-5p	1,575	-0,665	-2,240	4,72294
147506	mmu-miR-21a-5p	1,156	0,096	-1,060	2,08532
11024	mmu-miR-223-3p	0,902	-0,601	-1,503	2,83458
42744	mmu-miR-23a-3p	0,665	-0,416	-1,081	2,11566
169330	mmu-miR-23b-3p	0,825	-0,422	-1,247	2,3736
17506	mmu-miR-24-3p	0,722	-0,482	-1,204	2,30342
42682	mmu-miR-25-3p	1,397	0,046	-1,350	2,54971
46483	mmu-miR-27a-3p	0,719	-0,369	-1,088	2,12591
147199	mmu-miR-27b-3p	0,926	-0,360	-1,286	2,43932
148632	mmu-miR-2861	-0,111	0,979	1,090	2,12898
168687	mmu-miR-29a-3p	1,299	-0,059	-1,358	2,56282
11040	mmu-miR-29b-3p	1,041	-0,231	-1,272	2,41513
148391	mmu-miR-3068-5p	1,132	0,054	-1,078	2,11174
148035	mmu-miR-3084-5p	0,819	-0,458	-1,276	2,42204
148199	mmu-miR-3102-3p	0,074	1,091	1,017	2,0233
11053	mmu-miR-32-5p	0,975	-0,265	-1,241	2,36289
145859	mmu-miR-33-5p	1,605	-0,836	-2,442	5,43292

42592	mmu-miR-338-3p	1,681	-0,146	-1,827	3,54738
32884	mmu-miR-342-3p	2,031	-0,870	-2,901	7,46933
148653	mmu-miR-3474	-0,132	1,170	1,302	2,46609
148579	mmu-miR-3544-3p	-0,025	1,080	1,105	2,15088
11078	mmu-miR-365-3p	-1,092	1,001	2,092	4,2647
168859	mmu-miR-3962	1,093	-0,132	-1,225	2,3379
168762	mmu-miR-3964	1,623	-0,514	-2,137	4,39739
169277	mmu-miR-3970	0,912	-0,474	-1,386	2,61349
17608	mmu-miR-425-5p	1,272	0,025	-1,247	2,37326
42518	mmu-miR-465b-5p	0,196	-0,847	-1,042	2,05943
168880	mmu-miR-489-5p	1,645	-0,579	-2,224	4,67206
169268	mmu-miR-5112	-0,367	0,990	1,357	2,56146
169153	mmu-miR-5116	-0,632	0,506	1,138	2,20033
168715	mmu-miR-5119	1,024	-0,235	-1,259	2,39344
168630	mmu-miR-5121	1,777	0,014	-1,764	3,39548
169291	mmu-miR-5126	-0,189	1,031	1,219	2,32807
168738	mmu-miR-5127	-0,640	0,385	1,025	2,03537
168706	mmu-miR-5129-5p	-0,488	1,245	1,733	3,32493
42811	mmu-miR-542-5p	0,634	1,757	1,123	2,17867
168835	mmu-miR-5621-5p	-1,037	0,023	1,060	2,0847
168752	mmu-miR-5627-3p	0,233	1,265	1,031	2,04398
42827	mmu-miR-652-3p	1,187	-0,227	-1,414	2,66524
17669	mmu-miR-690	0,992	-0,719	-1,711	3,27338
17495	mmu-miR-697	0,513	-0,544	-1,057	2,08114
29190	mmu-miR-708-5p	-1,079	0,842	1,921	3,78573
27575	mmu-miR-711	0,164	1,236	1,072	2,1024
27855	mmu-miR-763	-0,541	0,714	1,256	2,3875
42817	mmu-miR-770-5p	1,226	0,062	-1,164	2,24117
42888	mmu-miR-875-3p	0,774	-0,436	-1,209	2,31213
42687	mmu-miR-883b-5p	-0,235	0,767	1,002	2,00275
169075	mmu-miR-92a-3p	1,745	-0,296	-2,041	4,1141
30687	mmu-miR-93-5p	1,291	0,114	-1,177	2,26042

Table S2 - MicroRNA array analysis for mouse EPI *ex vivo* white adipose tissue. Differently expressed microRNAs between preadipocytes (pre) and their corresponding mature adipocytes (mat) with logarithmic fold change (logFC) ≥ ±1 and fold change (FC) ≥ ±2, respectively. ProbeID was defined by Exiqon.

ProbeID	**Annotation**	**EPI mat**	**EPI pre**	**logFC**	**FC**
13485	mmu-miR-10a-5p	-0,219	1,040	-1,259	2,393581
10925	mmu-miR-10b-5p	-0,018	1,105	-1,123	2,178487
30787	mmu-miR-125b-5p	0,110	1,237	-1,127	2,184244
42839	mmu-miR-135a-5p	0,109	1,894	-1,785	3,44679

42630	mmu-miR-140-3p	-0,657	0,349	-1,007	2,009139
10946	mmu-miR-141-3p	-1,262	2,154	-3,417	10,67842
10947	mmu-miR-142-3p	-3,014	-0,733	-2,281	4,860201
145798	mmu-miR-142-5p	-2,426	-0,729	-1,697	3,24225
42641	mmu-miR-145a-5p/mmu-miR-145b	0,022	1,038	-1,016	2,02243
10952	mmu-miR-146a-5p	-0,632	0,844	-1,476	2,781197
10306	mmu-miR-146b-5p	-0,638	0,798	-1,437	2,707108
17280	mmu-miR-15b-5p	-1,208	0,153	-1,361	2,568832
10967	mmu-miR-16-5p	-0,426	0,655	-1,082	2,116451
27536	mmu-miR-190a-5p	0,600	1,786	-1,187	2,276112
10986	mmu-miR-193a-3p	1,311	-1,808	3,119	8,687716
10995	mmu-miR-199a-3p/mmu-miR-199b-3p	-1,002	1,125	-2,127	4,366903
29562	mmu-miR-199a-5p	-0,809	1,135	-1,944	3,847293
11205	mmu-miR-199b-5p	-0,944	1,097	-2,041	4,113984
10916	mmu-miR-1a-3p	-0,597	0,551	-1,147	2,214807
168819	mmu-miR-200a-3p	-1,653	1,746	-3,399	10,55081
147186	mmu-miR-200b-3p	-0,571	1,220	-1,791	3,460495
17427	mmu-miR-200c-3p	-1,338	1,651	-2,989	7,938236
11005	mmu-miR-204-5p	0,150	1,303	-1,153	2,223203
46917	mmu-miR-205-5p	-1,381	1,663	-3,043	8,243148
42640	mmu-miR-20b-5p	-1,042	-0,040	-1,003	2,003865
11022	mmu-miR-221-3p	-0,132	1,363	-1,494	2,81714
11023	mmu-miR-222-3p	-0,508	1,359	-1,868	3,649008
11024	mmu-miR-223-3p	-0,182	1,323	-1,504	2,836554
42744	mmu-miR-23a-3p	-0,310	0,758	-1,068	2,096698
169330	mmu-miR-23b-3p	-0,329	0,826	-1,155	2,227501
17506	mmu-miR-24-3p	-0,207	0,957	-1,164	2,241436
148020	mmu-miR-3078-3p	-0,092	-1,111	1,019	2,027201
148045	mmu-miR-3094-3p	0,754	-1,039	1,792	3,464105
32884	mmu-miR-342-3p	-1,341	0,119	-1,461	2,75205
29153	mmu-miR-34b-5p	-0,472	1,680	-2,153	4,446409
11074	mmu-miR-34c-5p	-0,085	1,006	-1,091	2,130507
11235	mmu-miR-351-5p	0,532	-1,000	1,532	2,89087
11078	mmu-miR-365-3p	1,017	-0,955	1,972	3,923329
11105	mmu-miR-378a-3p/mmu-miR-378b/mmu-miR-378c	-0,430	-1,747	1,317	2,49186
169277	mmu-miR-3970	-0,446	0,576	-1,022	2,031036
17822	mmu-miR-490-5p	0,452	-0,587	1,039	2,054959
147701	mmu-miR-491-3p	0,126	-1,072	1,198	2,294465
42670	mmu-miR-500-3p	-0,368	0,677	-1,045	2,06276
169104	mmu-miR-5099	-0,580	0,517	-1,097	2,139357
168835	mmu-miR-5621-5p	0,791	-0,525	1,316	2,489772
169373	mmu-miR-5626-5p	0,979	-0,792	1,771	3,413996
42827	mmu-miR-652-3p	-0,378	1,088	-1,466	2,762415
17669	mmu-miR-690	-0,393	0,694	-1,087	2,124657
29190	mmu-miR-708-5p	1,512	-1,051	2,563	5,910697

Table S3 - MicroRNA array analysis for male human subcutaneous (SUB) *ex vivo* white adipose tissue. Differently expressed microRNAs between preadipocytes (pre) and their corresponding mature adipocytes (mat) with logarithmic fold change (logFC) ≥ ±1 and fold change (FC) ≥ ±2, respectively. ProbeID was defined by Exiqon.

ProbeID	Annotation	SUB mat ♂	SUB pre ♂	logFC	FC
147165	hsa-let-7b-5p	0,562	-0,469	1,031	2,044
17752	hsa-let-7f-5p	0,694	-0,310	1,004	2,006
145943	hsa-miR-100-5p	1,023	-0,560	1,583	2,996
31026	hsa-miR-101-3p	1,140	-0,379	1,519	2,865
10925	hsa-miR-10b-5p	-0,450	0,638	-1,088	2,125
46258	hsa-miR-1184	-0,797	0,762	-1,559	2,946
46695	hsa-miR-1228-3p	1,194	-0,622	1,816	3,522
168870	hsa-miR-1246	-0,953	0,680	-1,633	3,101
46924	hsa-miR-1252-5p	-0,545	0,570	-1,115	2,166
169412	hsa-miR-1260a	0,527	-0,885	1,412	2,660
168619	hsa-miR-1260b	0,686	-0,723	1,409	2,656
4610	hsa-miR-126-3p	-3,636	1,339	-4,975	31,453
46732	hsa-miR-1264	0,548	-0,821	1,370	2,584
33596	hsa-miR-126-5p	-1,889	1,444	-3,333	10,076
46623	hsa-miR-1273a	-1,142	0,053	-1,195	2,289
168846	hsa-miR-1273f	-1,200	0,167	-1,368	2,580
169082	hsa-miR-1275	-0,375	0,717	-1,091	2,131
46642	hsa-miR-1276	1,115	-1,187	2,302	4,933
168568	hsa-miR-1290	-1,056	0,625	-1,681	3,207
42571	hsa-miR-129-1-3p	0,959	-0,607	1,566	2,960
46479	hsa-miR-1304-5p	-1,295	-0,066	-1,230	2,345
148316	hsa-miR-134-3p	0,486	-0,621	1,107	2,154
148278	hsa-miR-138-2-3p	0,735	-1,100	1,835	3,568
145972	hsa-miR-141-5p	0,405	-2,525	2,930	7,621
10947	hsa-miR-142-3p	-2,205	1,423	-3,628	12,366
13177	hsa-miR-143-3p	0,886	-0,799	1,685	3,215
46467	hsa-miR-143-5p	0,872	-1,074	1,946	3,854
31867	hsa-miR-145-3p	0,926	-0,375	1,301	2,465
42641	hsa-miR-145-5p	0,685	-0,335	1,020	2,028
10306	hsa-miR-146b-5p	-0,526	1,291	-1,817	3,523
10955	hsa-miR-148a-3p	1,477	-0,903	2,380	5,205
19585	hsa-miR-148b-3p	1,169	-0,061	1,230	2,346
17676	hsa-miR-152-3p	1,257	-0,554	1,811	3,509
10964	hsa-miR-155-5p	-0,526	1,105	-1,631	3,096
46810	hsa-miR-1827	-1,239	-0,229	-1,010	2,014
148687	hsa-miR-1908-5p	-0,587	0,570	-1,157	2,230
27536	hsa-miR-190a-5p	1,403	-1,154	2,557	5,886
10986	hsa-miR-193a-3p	0,973	-2,722	3,695	12,953
46443	hsa-miR-193a-5p	1,114	-1,905	3,019	8,106

10987	hsa-miR-193b-3p	1,612	-0,898	2,510	5,697
10990	hsa-miR-196a-5p	1,477	-0,203	1,679	3,203
145889	hsa-miR-196b-5p	1,293	0,024	1,269	2,410
19591	hsa-miR-199b-5p	-1,219	1,414	-2,633	6,204
42502	hsa-miR-204-3p	-0,624	0,533	-1,156	2,229
146161	hsa-miR-2115-3p	0,436	-0,699	1,135	2,197
42509	hsa-miR-219a-5p	1,331	-1,031	2,361	5,138
11022	hsa-miR-221-3p	-0,491	0,933	-1,423	2,682
11023	hsa-miR-222-3p	-1,471	0,763	-2,234	4,704
11024	hsa-miR-223-3p	-3,253	1,835	-5,088	34,016
11020	hsa-miR-22-3p	1,025	-1,371	2,397	5,267
146163	hsa-miR-224-3p	0,731	-0,613	1,344	2,539
42532	hsa-miR-22-5p	0,948	-1,165	2,114	4,328
169245	hsa-miR-2467-3p	-1,322	-0,105	-1,217	2,325
11040	hsa-miR-29b-3p	1,102	-1,449	2,550	5,857
11041	hsa-miR-29c-3p	1,235	-1,106	2,341	5,066
14300	hsa-miR-29c-5p	1,111	-0,747	1,858	3,625
45764	hsa-miR-302e	0,267	-0,977	1,244	2,369
146086	hsa-miR-30a-5p	0,747	-0,418	1,165	2,243
145676	hsa-miR-30e-3p	0,893	-0,280	1,173	2,255
56873	hsa-miR-3124-5p	-0,259	0,757	-1,016	2,022
147820	hsa-miR-3133	0,434	-1,276	1,709	3,270
169198	hsa-miR-3145-5p	0,103	-0,965	1,068	2,096
147823	hsa-miR-3146	-0,819	0,401	-1,220	2,330
147806	hsa-miR-3149	-1,250	-0,248	-1,003	2,003
147667	hsa-miR-3182	1,214	-2,978	4,192	18,279
148000	hsa-miR-3195	-0,333	0,677	-1,010	2,014
147817	hsa-miR-3196	-0,722	0,496	-1,218	2,326
29575	hsa-miR-32-3p	-1,317	-0,262	-1,055	2,077
42887	hsa-miR-331-3p	0,981	-0,431	1,412	2,662
11065	hsa-miR-335-5p	1,394	-3,014	4,407	21,218
42592	hsa-miR-338-3p	-0,069	0,971	-1,040	2,056
145859	hsa-miR-33a-5p	0,904	-0,397	1,301	2,464
148465	hsa-miR-3611	-1,122	-0,088	-1,034	2,048
168689	hsa-miR-361-3p	1,274	-0,242	1,516	2,861
27544	hsa-miR-363-5p	0,482	-0,624	1,106	2,152
148377	hsa-miR-3653	-0,629	0,812	-1,441	2,715
148228	hsa-miR-3656	-0,630	1,121	-1,751	3,366
11078	hsa-miR-365a-3p/hsa-miR-365b-3p	1,343	-2,327	3,670	12,728
148038	hsa-miR-3679-3p	1,588	0,418	1,170	2,250
148599	hsa-miR-3680-5p	0,305	-0,854	1,159	2,232
148085	hsa-miR-3687	-0,975	0,720	-1,696	3,239
168978	hsa-miR-371b-5p	-0,366	0,780	-1,146	2,212
145844	hsa-miR-374a-5p	1,486	-0,509	1,995	3,986
148098	hsa-miR-374b-5p	1,291	-0,009	1,300	2,462

148430	hsa-miR-374c-5p	1,090	-0,090	1,180	2,266
148668	hsa-miR-378a-3p	0,948	-1,229	2,177	4,523
147530	hsa-miR-378b	0,509	-1,151	1,660	3,160
147755	hsa-miR-378c	1,199	-1,777	2,976	7,870
169266	hsa-miR-378d	1,116	-2,375	3,491	11,244
168635	hsa-miR-378e	1,048	-2,366	3,414	10,661
169132	hsa-miR-382-3p	0,097	-1,174	1,271	2,413
148495	hsa-miR-3915	-1,012	-0,008	-1,004	2,006
168637	hsa-miR-3940-5p	-0,532	0,563	-1,095	2,136
169024	hsa-miR-3960	-0,811	1,113	-1,924	3,795
169316	hsa-miR-3976	-0,996	0,030	-1,026	2,037
11104	hsa-miR-422a	1,059	-0,978	2,037	4,103
27565	hsa-miR-423-5p	-0,714	0,338	-1,052	2,073
42965	hsa-miR-424-5p	-0,775	0,872	-1,647	3,131
147743	hsa-miR-4275	0,483	-1,238	1,720	3,296
169129	hsa-miR-4284	0,408	-0,913	1,321	2,499
147604	hsa-miR-4285	-0,436	0,608	-1,044	2,062
169409	hsa-miR-4286	0,944	-0,566	1,510	2,848
147588	hsa-miR-4288	-0,830	0,267	-1,097	2,140
169282	hsa-miR-4290	-0,568	0,582	-1,149	2,218
169407	hsa-miR-4301	0,695	-0,812	1,507	2,842
147722	hsa-miR-4306	-0,938	0,074	-1,012	2,016
147832	hsa-miR-4326	0,108	-0,991	1,099	2,142
147771	hsa-miR-4328	0,518	-0,600	1,118	2,171
168971	hsa-miR-4449	-0,703	0,936	-1,639	3,114
169305	hsa-miR-4455	-1,114	0,075	-1,189	2,279
168919	hsa-miR-4456	0,437	-0,727	1,164	2,241
169143	hsa-miR-4459	-0,842	0,577	-1,419	2,673
168814	hsa-miR-4463	0,426	-0,718	1,144	2,210
169285	hsa-miR-4467	-0,727	0,728	-1,455	2,742
168967	hsa-miR-4476	-1,007	0,057	-1,065	2,092
168815	hsa-miR-4488	-0,288	0,893	-1,180	2,266
169110	hsa-miR-4497	-0,351	0,897	-1,248	2,375
168998	hsa-miR-4508	-0,589	0,489	-1,078	2,111
168917	hsa-miR-4511	-2,203	0,941	-3,144	8,841
168802	hsa-miR-4516	-0,397	0,983	-1,380	2,602
42866	hsa-miR-451a	-0,163	1,339	-1,502	2,833
169326	hsa-miR-451b	0,387	-0,730	1,117	2,168
29379	hsa-miR-452-5p	1,145	-1,438	2,583	5,993
168639	hsa-miR-4533	-1,027	-0,012	-1,015	2,021
168942	hsa-miR-4636	-1,361	0,647	-2,008	4,022
169183	hsa-miR-4644	-1,261	0,304	-1,565	2,960
169200	hsa-miR-4677-5p	-0,005	-1,033	1,028	2,039
169026	hsa-miR-4679	-1,076	0,115	-1,190	2,282
169070	hsa-miR-4695-3p	0,596	-0,699	1,295	2,453

169302	hsa-miR-4695-5p	-0,735	0,396	-1,131	2,191
168944	hsa-miR-4707-5p	-0,698	0,993	-1,691	3,229
169028	hsa-miR-4708-3p	-0,594	0,891	-1,485	2,798
169012	hsa-miR-4711-3p	-0,117	-1,257	1,140	2,204
169023	hsa-miR-4712-3p	-0,978	0,072	-1,049	2,070
169295	hsa-miR-4725-3p	-0,249	0,817	-1,066	2,093
169399	hsa-miR-4750-5p	-0,589	0,841	-1,430	2,695
169130	hsa-miR-4764-3p	0,314	-0,820	1,134	2,195
169050	hsa-miR-4787-5p	-0,466	0,917	-1,383	2,608
169116	hsa-miR-4788	-0,576	0,783	-1,359	2,566
169022	hsa-miR-4797-5p	0,574	-1,315	1,889	3,703
169313	hsa-miR-4800-3p	-0,377	1,074	-1,450	2,732
169390	hsa-miR-4800-5p	-0,852	0,244	-1,097	2,139
148682	hsa-miR-483-3p	-0,703	0,382	-1,085	2,121
42654	hsa-miR-483-5p	-0,832	0,275	-1,107	2,155
14285	hsa-miR-487b-3p	0,345	-1,105	1,449	2,731
147701	hsa-miR-491-3p	0,820	-0,918	1,739	3,337
148059	hsa-miR-493-5p	0,760	-0,557	1,317	2,492
42847	hsa-miR-497-5p	1,116	-0,013	1,129	2,187
42442	hsa-miR-498	-0,679	0,328	-1,007	2,010
168598	hsa-miR-5007-3p	0,338	-1,136	1,474	2,779
168878	hsa-miR-5100	0,201	-0,824	1,025	2,035
42811	hsa-miR-542-5p	-0,110	1,117	-1,227	2,342
169009	hsa-miR-548ap-5p/hsa-miR-548j-5p	-0,470	0,877	-1,347	2,544
168951	hsa-miR-548as-3p	0,478	-0,967	1,445	2,722
148644	hsa-miR-551b-3p	1,333	-1,457	2,790	6,914
17668	hsa-miR-552-3p	-0,533	0,528	-1,061	2,086
168834	hsa-miR-5571-5p	0,607	-0,717	1,324	2,503
168558	hsa-miR-5585-3p	-0,974	0,096	-1,070	2,100
169376	hsa-miR-5701	-0,560	0,761	-1,321	2,498
17546	hsa-miR-585-3p	-0,218	0,819	-1,037	2,051
42542	hsa-miR-589-5p	0,622	-1,210	1,833	3,562
145833	hsa-miR-596	0,843	-0,298	1,140	2,204
42818	hsa-miR-597-5p	0,702	-0,902	1,604	3,040
17377	hsa-miR-600	0,854	-0,656	1,510	2,848
17566	hsa-miR-629-3p	0,843	-0,400	1,243	2,367
42832	hsa-miR-638	-0,620	0,930	-1,550	2,927
168642	hsa-miR-642b-3p	0,674	-1,257	1,930	3,812
42827	hsa-miR-652-3p	1,294	-1,040	2,335	5,045
168963	hsa-miR-664b-5p	-0,820	0,574	-1,394	2,628
145768	hsa-miR-665	0,133	-0,891	1,024	2,034
42761	hsa-miR-675-5p	0,885	-0,606	1,491	2,811
146196	hsa-miR-711	-0,415	0,660	-1,076	2,108
42514	hsa-miR-937-3p	0,399	-1,131	1,529	2,886
42696	hsa-miR-943	-0,213	0,991	-1,204	2,304

11182	hsa-miR-98-5p	0,659	-0,348	1,007	2,010
42708	hsa-miR-99a-5p	0,928	-0,095	1,023	2,033
28302	hsa-miRPlus-A1015	-0,590	0,487	-1,077	2,110

Table S4 - MicroRNA array analysis for female human subcutaneous (SUB) *ex vivo* white adipose tissue. Differently expressed microRNAs between preadipocytes (pre) and their corresponding mature adipocytes (mat) with logarithmic fold change (logFC) ≥ ±1 and fold change (FC) ≥ ±2, respectively. ProbeID was defined by Exiqon.

ProbeID	Annotation	SUB mat ♀	SUB pre ♀	logFC	FC
147162	hsa-let-7a-5p	0,549	-0,986	1,535	2,897
145820	hsa-let-7c-5p	0,470	-0,854	1,324	2,504
145968	hsa-let-7d-5p	0,347	-0,849	1,196	2,291
17752	hsa-let-7f-5p	0,657	-1,431	2,088	4,252
46438	hsa-let-7g-5p	0,455	-1,198	1,653	3,145
9938	hsa-let-7i-5p	0,511	-0,789	1,300	2,462
145943	hsa-miR-100-5p	1,012	-1,824	2,836	7,141
31026	hsa-miR-101-3p	0,874	-2,365	3,239	9,440
46801	hsa-miR-106a-5p	0,518	-0,621	1,140	2,203
46806	hsa-miR-1227-3p	1,086	0,010	1,075	2,107
168870	hsa-miR-1246	-1,367	0,391	-1,758	3,382
46427	hsa-miR-1248	-0,403	0,720	-1,123	2,178
46924	hsa-miR-1252-5p	-0,581	0,419	-1,000	2,000
30787	hsa-miR-125b-5p	0,806	-1,315	2,122	4,352
169412	hsa-miR-1260a	0,628	-2,220	2,848	7,201
168619	hsa-miR-1260b	0,754	-1,864	2,618	6,139
4610	hsa-miR-126-3p	-3,986	0,377	-4,363	20,572
46732	hsa-miR-1264	0,786	-1,225	2,011	4,031
33596	hsa-miR-126-5p	-2,148	-0,046	-2,102	4,293
168973	hsa-miR-1268b	0,606	-0,674	1,280	2,428
46623	hsa-miR-1273a	-1,017	0,722	-1,739	3,338
148263	hsa-miR-1273e	-0,560	0,459	-1,019	2,027
168846	hsa-miR-1273f	-1,164	0,500	-1,664	3,168
168925	hsa-miR-1273g-3p	0,578	-0,777	1,355	2,558
145981	hsa-miR-1285-3p	-0,514	0,592	-1,106	2,152
168568	hsa-miR-1290	-1,794	0,091	-1,885	3,694
42571	hsa-miR-129-1-3p	0,847	-0,841	1,688	3,223
46944	hsa-miR-1297	0,479	-0,855	1,334	2,521
46788	hsa-miR-1299	-0,554	0,937	-1,491	2,811
46479	hsa-miR-1304-5p	-1,150	0,695	-1,845	3,592
46866	hsa-miR-1321	-0,577	0,613	-1,190	2,281
148316	hsa-miR-134-3p	0,549	-0,638	1,187	2,277
148278	hsa-miR-138-2-3p	0,728	-2,253	2,981	7,894

4700	hsa-miR-140-5p	0,856	-0,542	1,398	2,635
145972	hsa-miR-141-5p	1,514	-1,342	2,856	7,239
13177	hsa-miR-143-3p	0,942	-1,571	2,514	5,710
46467	hsa-miR-143-5p	1,100	-1,425	2,525	5,755
42641	hsa-miR-145-5p	0,738	-0,438	1,176	2,260
19585	hsa-miR-148b-3p	1,053	-0,818	1,872	3,660
169408	hsa-miR-181d-5p	0,679	-0,451	1,130	2,189
46810	hsa-miR-1827	-0,820	0,799	-1,618	3,070
17953	hsa-miR-183-3p	1,024	-0,009	1,033	2,047
18739	hsa-miR-186-5p	0,816	-0,884	1,700	3,249
27536	hsa-miR-190a-5p	1,759	-1,646	3,405	10,592
146103	hsa-miR-1913	1,195	-0,062	1,257	2,390
10985	hsa-miR-191-5p	0,893	-0,342	1,236	2,355
10986	hsa-miR-193a-3p	1,073	-4,155	5,227	37,462
46443	hsa-miR-193a-5p	1,197	-2,132	3,330	10,054
10987	hsa-miR-193b-3p	1,405	-1,571	2,976	7,870
13148	hsa-miR-195-5p	0,411	-0,876	1,287	2,440
10990	hsa-miR-196a-5p	0,751	-0,896	1,647	3,131
146165	hsa-miR-1973	0,547	-0,841	1,388	2,617
10995	hsa-miR-199a-3p/hsa-miR-199b-3p	0,448	-1,391	1,839	3,577
29562	hsa-miR-199a-5p	0,866	-1,123	1,989	3,970
10997	hsa-miR-19a-3p	0,343	-1,109	1,452	2,736
10998	hsa-miR-19b-3p	0,136	-0,878	1,014	2,019
42502	hsa-miR-204-3p	-1,111	-0,106	-1,005	2,007
169411	hsa-miR-205-3p	-0,635	0,534	-1,169	2,248
146074	hsa-miR-2114-5p	-0,533	0,545	-1,078	2,111
146161	hsa-miR-2115-3p	0,644	-0,529	1,173	2,254
42627	hsa-miR-212-3p	0,983	-0,112	1,095	2,136
147506	hsa-miR-21-5p	0,612	-1,560	2,172	4,506
11022	hsa-miR-221-3p	-0,740	0,373	-1,113	2,163
11023	hsa-miR-222-3p	-1,696	0,383	-2,080	4,227
11020	hsa-miR-22-3p	0,980	-2,225	3,205	9,222
146163	hsa-miR-224-3p	0,812	-0,619	1,432	2,698
42532	hsa-miR-22-5p	1,141	-1,009	2,150	4,438
148247	hsa-miR-2355-3p	-0,832	0,471	-1,304	2,468
169245	hsa-miR-2467-3p	-1,215	0,393	-1,608	3,047
46483	hsa-miR-27a-3p	0,404	-1,452	1,856	3,621
147199	hsa-miR-27b-3p	0,486	-1,081	1,568	2,964
168687	hsa-miR-29a-3p	0,063	-1,080	1,144	2,209
11040	hsa-miR-29b-3p	0,987	-3,349	4,336	20,191
11041	hsa-miR-29c-3p	1,033	-2,925	3,958	15,539
45764	hsa-miR-302e	1,192	-0,310	1,502	2,833
45745	hsa-miR-302f	1,052	0,051	1,001	2,001
146086	hsa-miR-30a-5p	0,860	-1,365	2,225	4,675
146112	hsa-miR-30b-5p	0,916	-0,960	1,876	3,670

42923	hsa-miR-30c-5p	0,597	-0,902	1,499	2,827
19596	hsa-miR-30d-5p	0,451	-1,133	1,584	2,998
145676	hsa-miR-30e-3p	1,004	-1,341	2,345	5,079
28191	hsa-miR-30e-5p	0,813	-1,635	2,448	5,457
168650	hsa-miR-3121-5p	-0,514	0,574	-1,088	2,126
169380	hsa-miR-3124-3p	-0,845	0,479	-1,324	2,504
147820	hsa-miR-3133	0,301	-0,952	1,253	2,383
147823	hsa-miR-3146	-1,008	0,286	-1,294	2,453
147904	hsa-miR-3148	-0,751	0,777	-1,527	2,882
147806	hsa-miR-3149	-0,775	0,944	-1,719	3,293
147667	hsa-miR-3182	0,967	-4,173	5,140	35,266
147851	hsa-miR-3201	-0,613	0,554	-1,167	2,245
29575	hsa-miR-32-3p	-0,855	1,002	-1,857	3,621
42887	hsa-miR-331-3p	0,741	-0,737	1,478	2,785
11065	hsa-miR-335-5p	1,247	-4,905	6,152	71,111
169368	hsa-miR-3529-3p	1,375	-1,519	2,894	7,434
148465	hsa-miR-3611	-0,820	0,618	-1,439	2,711
168689	hsa-miR-361-3p	1,251	-0,786	2,037	4,104
11078	hsa-miR-365a-3p/hsa-miR-365b-3p	1,242	-3,085	4,327	20,066
168796	hsa-miR-3664-3p	-0,652	0,579	-1,231	2,347
148214	hsa-miR-3675-3p	0,074	-1,062	1,136	2,197
148038	hsa-miR-3679-3p	1,692	-0,067	1,759	3,384
148156	hsa-miR-3686	-0,804	0,670	-1,474	2,778
148085	hsa-miR-3687	-1,697	0,321	-2,018	4,051
168692	hsa-miR-3688-5p	-0,629	0,553	-1,183	2,270
145844	hsa-miR-374a-5p	1,170	-2,087	3,257	9,559
148098	hsa-miR-374b-5p	0,951	-1,090	2,041	4,115
148430	hsa-miR-374c-5p	0,807	-1,298	2,106	4,304
146009	hsa-miR-376a-3p	1,409	-0,503	1,912	3,762
148668	hsa-miR-378a-3p	0,690	-1,088	1,779	3,431
147530	hsa-miR-378b	0,437	-0,696	1,133	2,193
147755	hsa-miR-378c	1,144	-2,564	3,708	13,068
169266	hsa-miR-378d	1,033	-3,120	4,153	17,794
168635	hsa-miR-378e	1,009	-2,900	3,908	15,015
169132	hsa-miR-382-3p	0,179	-1,131	1,310	2,480
148495	hsa-miR-3915	-0,934	0,533	-1,467	2,764
148064	hsa-miR-3926	-0,591	0,541	-1,132	2,191
169024	hsa-miR-3960	-1,271	0,009	-1,281	2,430
169316	hsa-miR-3976	-0,971	0,600	-1,571	2,971
11104	hsa-miR-422a	0,702	-0,801	1,503	2,835
147706	hsa-miR-4255	-0,527	0,834	-1,361	2,568
147631	hsa-miR-4258	1,178	-0,171	1,349	2,547
147942	hsa-miR-4268	-0,817	0,446	-1,264	2,401
147743	hsa-miR-4275	0,434	-1,429	1,864	3,640
147767	hsa-miR-4279	-0,675	0,428	-1,103	2,148

169129	hsa-miR-4284	0,644	-0,941	1,585	3,000
169409	hsa-miR-4286	0,960	-1,733	2,693	6,469
147588	hsa-miR-4288	-0,943	0,230	-1,172	2,254
147735	hsa-miR-4289	0,633	-0,977	1,610	3,053
169282	hsa-miR-4290	-0,939	0,394	-1,332	2,518
147600	hsa-miR-4292	0,303	-0,869	1,172	2,254
147632	hsa-miR-4297	-0,536	0,638	-1,174	2,256
169407	hsa-miR-4301	0,908	-1,094	2,002	4,005
147722	hsa-miR-4306	-0,778	0,470	-1,248	2,375
147608	hsa-miR-4307	-0,458	0,615	-1,073	2,104
147664	hsa-miR-4311	-0,579	0,570	-1,149	2,217
168980	hsa-miR-4324	0,414	-1,095	1,509	2,845
147832	hsa-miR-4326	1,185	-0,278	1,463	2,758
147771	hsa-miR-4328	0,634	-0,641	1,275	2,420
11245	hsa-miR-433-5p	0,052	-1,060	1,112	2,161
169381	hsa-miR-4421	-0,595	0,451	-1,046	2,065
168768	hsa-miR-4423-5p	-0,788	0,612	-1,400	2,638
168792	hsa-miR-4434	-0,762	0,440	-1,202	2,301
169260	hsa-miR-4436b-3p	-0,817	0,380	-1,197	2,293
168863	hsa-miR-4441	-0,933	0,418	-1,351	2,552
169188	hsa-miR-4443	0,506	-0,981	1,487	2,803
169360	hsa-miR-4445-5p	-0,663	0,423	-1,086	2,122
168964	hsa-miR-4450	-0,511	0,491	-1,002	2,003
169015	hsa-miR-4454	0,050	-1,674	1,725	3,305
169305	hsa-miR-4455	-1,018	0,707	-1,726	3,307
168919	hsa-miR-4456	0,550	-0,869	1,419	2,674
169270	hsa-miR-4458	-0,760	0,479	-1,238	2,359
169143	hsa-miR-4459	-1,073	0,179	-1,252	2,381
168814	hsa-miR-4463	0,643	-1,666	2,309	4,956
169285	hsa-miR-4467	-1,078	-0,045	-1,032	2,045
168904	hsa-miR-4473	-0,986	0,182	-1,169	2,248
168967	hsa-miR-4476	-0,997	0,425	-1,422	2,679
168917	hsa-miR-4511	-3,008	-1,202	-1,806	3,498
168948	hsa-miR-4514	-0,927	0,658	-1,585	2,999
29379	hsa-miR-452-5p	1,065	-1,389	2,454	5,478
168639	hsa-miR-4533	-0,852	0,609	-1,461	2,754
168702	hsa-miR-4540	-0,538	0,496	-1,035	2,049
168606	hsa-miR-4633-5p	0,227	-1,126	1,353	2,555
169183	hsa-miR-4644	-1,198	0,576	-1,775	3,421
168750	hsa-miR-4645-5p	-0,626	0,598	-1,224	2,336
169045	hsa-miR-4651	0,369	-1,018	1,388	2,617
168986	hsa-miR-4677-3p	-0,657	0,563	-1,221	2,331
169200	hsa-miR-4677-5p	0,716	-0,496	1,212	2,317
169026	hsa-miR-4679	-0,943	0,171	-1,115	2,165
169070	hsa-miR-4695-3p	0,580	-1,931	2,510	5,697

169228	hsa-miR-4698	-0,742	0,399	-1,141	2,205
169204	hsa-miR-4709-3p	-0,623	0,456	-1,079	2,112
169023	hsa-miR-4712-3p	-0,874	0,356	-1,229	2,345
169311	hsa-miR-4714-5p	0,129	-1,065	1,194	2,288
168703	hsa-miR-4716-3p	-1,165	0,323	-1,488	2,805
168668	hsa-miR-4732-3p	-0,838	0,365	-1,203	2,302
169239	hsa-miR-4732-5p	-0,997	0,037	-1,034	2,047
168722	hsa-miR-4742-3p	-0,772	0,726	-1,498	2,825
168852	hsa-miR-4764-5p	-0,782	0,655	-1,436	2,707
168557	hsa-miR-4777-5p	-0,792	0,536	-1,328	2,511
169064	hsa-miR-4778-3p	-0,450	0,590	-1,040	2,056
168959	hsa-miR-4778-5p	-0,815	0,259	-1,074	2,105
169271	hsa-miR-4784	-0,645	0,526	-1,171	2,251
168776	hsa-miR-4795-3p	-0,797	0,391	-1,187	2,277
169022	hsa-miR-4797-5p	0,612	-2,233	2,845	7,185
169313	hsa-miR-4800-3p	-1,579	-0,043	-1,536	2,901
169390	hsa-miR-4800-5p	-0,889	0,257	-1,146	2,213
148682	hsa-miR-483-3p	-0,812	0,384	-1,196	2,291
42654	hsa-miR-483-5p	-0,961	0,234	-1,194	2,288
145753	hsa-miR-484	0,706	-0,334	1,039	2,055
42694	hsa-miR-485-3p	-0,887	0,275	-1,161	2,237
14285	hsa-miR-487b-3p	0,364	-2,116	2,480	5,581
147701	hsa-miR-491-3p	0,295	-1,608	1,903	3,741
148059	hsa-miR-493-5p	0,401	-1,137	1,537	2,902
42847	hsa-miR-497-5p	0,706	-0,892	1,598	3,026
169136	hsa-miR-5006-3p	-0,555	0,671	-1,226	2,339
168598	hsa-miR-5007-3p	0,326	-0,890	1,215	2,322
42490	hsa-miR-505-5p	-0,687	0,573	-1,260	2,395
168704	hsa-miR-506-5p	-0,743	0,563	-1,306	2,472
169203	hsa-miR-5095	-0,794	0,640	-1,434	2,703
168878	hsa-miR-5100	0,556	-1,779	2,336	5,048
42581	hsa-miR-513a-5p	-0,790	0,964	-1,754	3,373
169185	hsa-miR-5187-3p	-1,365	0,037	-1,402	2,642
169181	hsa-miR-5191	-0,822	0,441	-1,262	2,399
148644	hsa-miR-551b-3p	1,236	-1,847	3,083	8,473
168922	hsa-miR-5584-3p	-0,664	0,600	-1,264	2,402
168558	hsa-miR-5585-3p	-0,745	0,675	-1,419	2,675
169169	hsa-miR-5684	0,453	-0,913	1,365	2,577
168597	hsa-miR-5699-3p	-0,569	0,568	-1,137	2,199
27740	hsa-miR-574-5p	-0,443	0,863	-1,306	2,473
42542	hsa-miR-589-5p	0,732	-1,517	2,249	4,753
17377	hsa-miR-600	0,553	-0,941	1,494	2,817
17566	hsa-miR-629-3p	0,876	-0,813	1,688	3,223
17327	hsa-miR-630	-0,862	0,414	-1,276	2,421
42749	hsa-miR-659-3p	0,810	-0,347	1,157	2,229

169375	hsa-miR-660-3p	-0,949	0,430	-1,379	2,601
145768	hsa-miR-665	0,760	-0,388	1,147	2,215
42761	hsa-miR-675-5p	-0,436	-2,092	1,656	3,152
29190	hsa-miR-708-5p	1,338	-0,886	2,225	4,674
148068	hsa-miR-758-5p	-0,618	0,462	-1,079	2,113
148504	hsa-miR-874-5p	0,675	-0,601	1,276	2,421
148621	hsa-miR-892a	-0,351	0,717	-1,068	2,097
30687	hsa-miR-93-5p	0,606	-0,685	1,291	2,447
42514	hsa-miR-937-3p	0,579	-1,637	2,216	4,646
11182	hsa-miR-98-5p	0,682	-1,034	1,716	3,284
42708	hsa-miR-99a-5p	1,104	-1,784	2,888	7,405
11184	hsa-miR-99b-5p	0,516	-0,955	1,472	2,773
147986	hsa-miRPlus-K1303*	0,083	-1,258	1,341	2,534

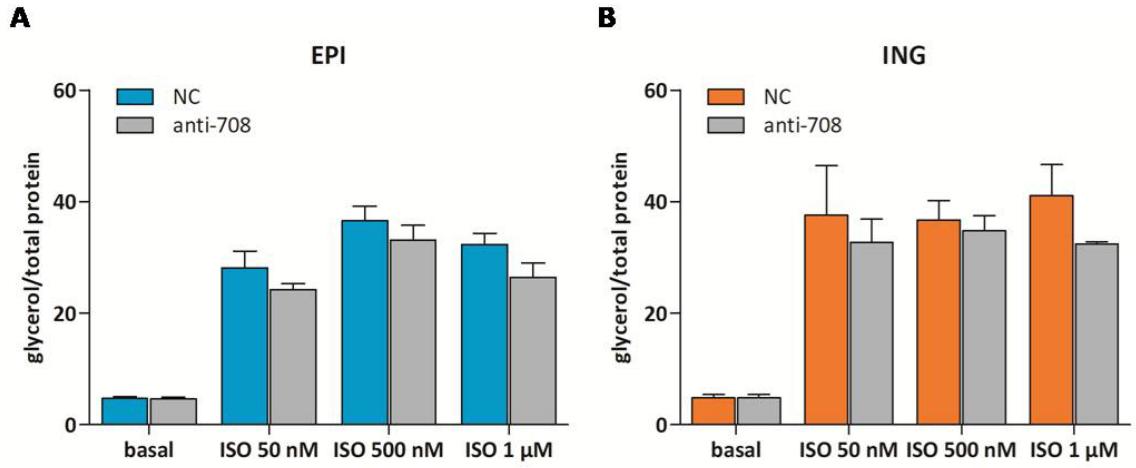

Figure S4 – Lipolysis: Isoprenaline dose response in miR-708-5p and control transfected EPI and ING cells. Glycerol release in anti-708 transfected cells compared to controls (NC) under basal and stimulated lipolysis conditions with 50 nM, 500 nM and 1 µM isoprenaline in (A) EPI and (B) ING murine cell lines, n=2-7/group.

IV Acknowledgment/Danksagung

Prof. Dr. G. Brabant gilt mein besonderer Dank. Mit seinem Forschungsdrang und seinem Ideenreichtum war er stets eine große Inspiration für mich. Ich danke ihm für die anregenden Diskussionen, sein großes Vertrauen sowie seine hilfreiche Unterstützung in allen Angelegenheiten meiner Arbeit. Ich weiß seinen Einsatz sehr zu schätzen.

Dr. Nina Perwitz möchte ich für ihre Betreuung und Hilfsbereitschaft in allen Laborangelegenheiten großen Dank aussprechen. Ihre kritische Betrachtungsweise von Ergebnissen schätze und bewundere ich sehr. Darin ist sie mir ein großes Vorbild.

Prof. Jörg Heeren möchte ich dafür danken, dass er in mir die Faszination und Leidenschaft für die „Fett-Forschung“ geweckt hat.

Prof. Mikael Rydén und **Prof. Peter Arner** bin ich zu großem Dank verpflichtet, da sie mich herzlich im „lipid lab“ am Karolinska Institut in Stockholm für 3 Monate aufgenommen haben und mich sehr im Weiterkommen meiner Arbeit unterstützt haben.

Dr. Agné Kulyté danke ich sehr für ihre Betreuung im „lipid lab“ und dafür, dass ich mich dort nicht als Gast, sondern als Kollegin gefühlt habe. Ich denke gern an diese besondere Zeit zurück.

Für eine manchmal turbulente aber vor allem lustige Zeit im Labor möchte ich von Herzen **Julia Resch**, **Rose Kohlie** und **Sebastian Nock** danken. Ich hatte viel Spaß mit euch. **Julia** gilt nochmal ein besonderer Dank für ihre großartige und unermüdliche Unterstützung im Labor.

Meinen GRK-Kolleginnen **Eva Frevel** und **Isa Kolbe** möchte ich für eine tolle Zeit danken, für die vielen Mittagspausen, für die kleinen und großen Kaffeepausen und für die kurzen und manchmal auch etwas längeren Gespräche zwischendurch, die einen die anstrengende Zeit auch mal haben vergessen lassen. Ihr ward mir eine große Unterstützung und Motivation!

Meiner **Familie** und meinen **Freunden** danke ich für ihre Unterstützung und ihr Verständnis, vor allem dann, wenn ich mal wieder mit den Augen gerollt habe, bei der Frage „Was genau ich nochmal mache und wie lange es denn noch dauern wird“. Danke, danke, danke!

Ein letzter und ganz besonderer Dank gilt meinen Ehemann **Adil**, ohne dessen Unterstützung, Geduld, Verständnis, Rücksichtnahme und richtigen Worte zur richtigen Zeit ich es nicht geschafft hätte. Möge Allah dich reich belohnen.